12-2001

# Relationships between Oceanographic Satellite Data and Alexandrium Distributions in the Gulf of Maine

Remy Martin Luerssen

# RELATIONSHIPS BETWEEN OCEANOGRAPHIC SATELLITE DATA AND *ALEXANDRIUM* DISTRIBUTIONS IN THE GULF OF MAINE

By

Remy Martin Luerssen

B.S. James Madison University, 1999

A THESIS

Submitted in Partial Fulfillment of the

Requirements for the Degree of

Master of Science

(in Oceanography)

The Graduate School

The University of Maine

December, 2001

Advisory Committee:

Andrew Thomas, Associate Professor of Oceanography, Advisor

David Townsend, Professor of Oceanography

Neal Pettigrew, Associate Professor of Oceanography

# RELATIONSHIPS BETWEEN OCEANOGRAPHIC SATELLITE DATA AND *ALEXANDRIUM* DISTRIBUTIONS IN THE GULF OF MAINE

By Remy Luerssen

Thesis Advisor: Dr. Andrew Thomas

An Abstract of the Thesis Presented
in Partial Fulfillment of the Requirements for the
Degree of Master of Science
(in Oceanography)
December, 2001

An examination is made of the qualitative and quantitative relationships between satellite derived sea-surface temperature (SST) and chlorophyll patterns and the distribution of *Alexandrium*, the toxic dinoflagellate species responsible for HABs in the GOM. Daily images coincident with five ECOHAB survey cruises in 1998 and 2000 are composited over each cruise period to create mean patterns for each sample period. Contours of surface *Alexandrium* cell concentrations are superimposed on the images as well as images showing the strength and location of SST frontal zones to examine qualitative relationships. Results indicate that high concentrations of *Alexandrium* are located primarily in the eastern Maine coastal current (EMCC) and that frontal zones in this region generally act as boundaries to their surface distributions. Linear regressions are used to explore quantitative relationships between location-specific satellite data extracted from the composites and *in situ* parameters important to the ecology of *Alexandrium*.

The most consistent results of these analyses were a linear relationship between satellite SST and *Alexandrium* that was used in a simple model to extrapolate/interpolate the distribution of *Alexandrium* based on satellite data. The regression results also suggest a seasonally shifting optimal temperature range for maximum *Alexandrium* concentrations. No qualitative or quantitative relationships between the SeaWiFS chlorophyll data and *Alexandrium* distributions in the GOM were found.

Relationships between satellite-measured SST patterns and toxicity in the western GOM were examined during a paralytic shellfish poisoning (PSP) closure in western GOM in May 2000 to test the hypothesis that toxicity events in the western GOM require a transport mechanism for *Alexandrium* cells in the EMCC to get into the western GOM and inshore. Thermal patterns evident in the satellite SST data at the time of the May 2000 closure were consistent with enhanced connectivity and advection from the EMCC to western GOM.

Ten years (1990-1999) of retrospective toxicity data from five sites along the coast of Maine and coincident AVHRR SST data are used to test the temporal stability of the observed May 2000 relationship between toxicity events in the western GOM and satellite-measured SST patterns. Results show that the occurrence of strong thermal gradients between eastern and western GOM, indicative of reduced alongshore connectivity, plays a key role in the occurrence and timing of toxicity event in the western GOM.

The results of this work indicate the utility of satellite derived SST data in defining hydrographic patterns associated with elevated *Alexandrium* cell concentrations

and in the detection and monitoring of oceanographic features that are conducive of toxicity events along the coast of western Maine.

Future work making use of the optical and biological information in SeaWiFS data, wind data and other SST products will likely improve the utility of satellite data in understanding the ecology of *Alexandrium* in the GOM demonstrated here.

## ACKNOWLEDGEMENTS

I would like to thank Laurie Bean and John Hurst at Maine DMR for all their help with the toxicity data and information about the May 2000 closure. Also, thanks to Jim Churchill of WHOI who supplied the drifter data for the May 2000 closure. The Townsend lab at the University Of Maine is greatly appreciated for their processing of the *in situ* data from all of the survey cruises in the GOM in 1998 and 2000. In addition, I would like to acknowledge Peter Cornillon at the University of Rhode Island for access to Pathfinder AVHRR data for the toxicity analysis.

I would also like to extend a special thanks to Jennifer Bosch and Ryan Weatherbee for all their help and support, Neal Pettigrew and Dave Townsend for agreeing to be on my committee and, especially, Andrew Thomas for advising me and guiding me through this project.

Funding for this project was provided by NASA grant #NAG5-6558 and NOAA ECOHAB grant #NA66RG0495.

## TABLE OF CONTENTS

## LIST OF TABLES

## LIST OF FIGURES

# Chapter 1

# JUSTIFICATION AND OBJECTIVES

## 1.1. Background Research

Harmful algal blooms (HABs) attract public attention in the Gulf of Maine (GOM) because of their health and economic implications (Blaxter and Southward, 1997). After ingesting toxic phytoplankton, filter feeding bivalves bioaccumulate toxins in their tissue creating health problems when humans ingest them. In the GOM the toxin associated with HABs causes paralytic shellfish poisoning (PSP). Ailments in humans associated with PSP range from slight numbness, nausea, and diarrhea, to death through respiratory paralysis in severe cases (Hallegraeff, 1995). HABs, therefore, pose a threat to human health, recreation and commercial interests in the GOM.

Maine's PSP monitoring program is one of the best in the United States. To ensure safe products on the market, the Maine Department of Marine Resources monitors toxin levels in shellfish. The toxins responsible for PSP in the GOM can be fatal to humans in doses as small as 500 μg/100 g tissue (Hallegraeff, 1995). If the toxin level, detected via mouse assay, approaches or exceeds 80 μg toxin/100 g shellfish meat, the shellfish beds are closed to further harvesting (Bean, personal communication, January 2001).

In 1992, commercial fisheries contributed a total of $1.1 billion to the Maine economy. In 1993 commercial fish landings alone in Maine (fish and shellfish) were valued at $255 million (MEPP, 1996). There is no good way to estimate economic losses

resulting from shellfish closures due to the numerous variables involved, but the cost of closures in Casco Bay alone was estimated at $1.6 to $1.7 million in 1994 (MEPP, 1996). When harvesting beds are closed, the price of shellfish rises. Restaurants may then decide to import their shellfish rather than pay the high Maine prices, further effecting the state's economy. Closures may also have a negative effect on tourism. According to the Maine Department of Environmental Protection (MEPP, 1996) 46% of tourists enjoy fishing, boating, or some other water activities while vacationing in Maine and knowledge of a closure may deter them from pursuing these activities.

HABs are considered toxic if they are composed of predominantly toxic phytoplankton (Blaxter and Southward, 1997), but only about 40 identified phytoplankton species have the ability to produce toxins (Hallegraeff, 1995). Nontoxic HABs can still be detrimental due to shading, nutrient depletion, and the reduction of oxygen concentration in the water column through bacterial degradation. These anoxic conditions stress fish, making them more vulnerable to disease (Hallegraeff, 1995).

Since monitoring began in 1972, there has been an increase in the number of annual PSP events recorded in the GOM. It has been argued that this increase is caused by excessive nutrient input, resulting in eutrophication (Blaxter and Southward, 1997). Anderson (1989) found a strong correlation between the number of HAB occurrences and increases in coastal pollution. Nutrient-rich wastewater discharged into coastal waters alters nutrient ratios, potentially favoring dinoflagellates (including the toxic phytoplankton in the GOM) over diatoms (Hallegraeff, 1995). It has also been proposed that increases in humic substances in the water, resulting from changes in land-use patterns such as deforestation, could be responsible for shifts in phytoplankton species

composition (Hallegraeff, 1995). Definitive statements quantifying and defining causes of the increase in frequency of HABs are difficult, due to an increase in monitoring frequency over the past few decades (Blaxter and Southward, 1997). Prior to 1972, no monitoring program was in place in Maine, consequently, PSP events were not documented. Since 1972 PSP events have been recorded every year. Thus, the lack of PSP events recorded prior to 1972 may simply be a result of the absence of monitoring, not the lack of toxic phytoplankton species.

The oceanographic ecology of the toxic dinoflagellate responsible for PSP, *Alexandrium,* in the GOM is poorly understood at present. Recently, research into this ecology has become the focus of a major multi-institution research collaborative. As part of this collaborative, the overall goal of this thesis project is to examine the extent to which available satellite data can contribute to our understanding of the distribution of *Alexandrium* in the GOM. More specifically, I will look at the qualitative and quantitative relationships of satellite data to *in situ* surface *Alexandrium* concentrations and to toxic events in the GOM. Satellite images provide a synoptic view of the study area, allowing repetitive measurements at smaller spatial and temporal scales and over larger areas than a traditional ship sampling grid. The satellite data that are used in this study are sea surface temperature (SST) measured by the advanced very high-resolution radiometer (AVHRR) and chlorophyll concentration measured via the Sea-viewing Wide Field of view Sensor (SeaWiFS). SST data are the most frequently measured ocean parameter from space, enabling the study of surface temperature patterns that are suggestive of physical processes (currents, vertical mixing, water-mass boundaries, etc.) in the GOM. These processes may play a direct role in the ecology of *Alexandrium*

and/or the single advective distribution of *Alexandrium*, making an understanding of the general circulation of the GOM important to this study.

### 1.1.1. Gulf of Maine Circulation

The GOM system contains features of widely varying dynamics such as river plumes, thermohaline influences, strong coastal currents and tides, wind-driven flows and gyres which create meso-scale circulation features and a complex coastal circulation system (Xue et al., 2000). Bathymetrically, the GOM is a partially isolated marginal sea with sufficient freshwater input to be classified as estuarine-like in its overall circulation. Freshwater inputs to the GOM include the St. John, Kennebec, Penobscot, and Androscoggin Rivers as well as St. Lawrence River water that enters the GOM from the Scotian Shelf (Pettigrew et al., 1998). A schematic of residual circulation and bathymetry of the GOM are shown in Figure 1.1.

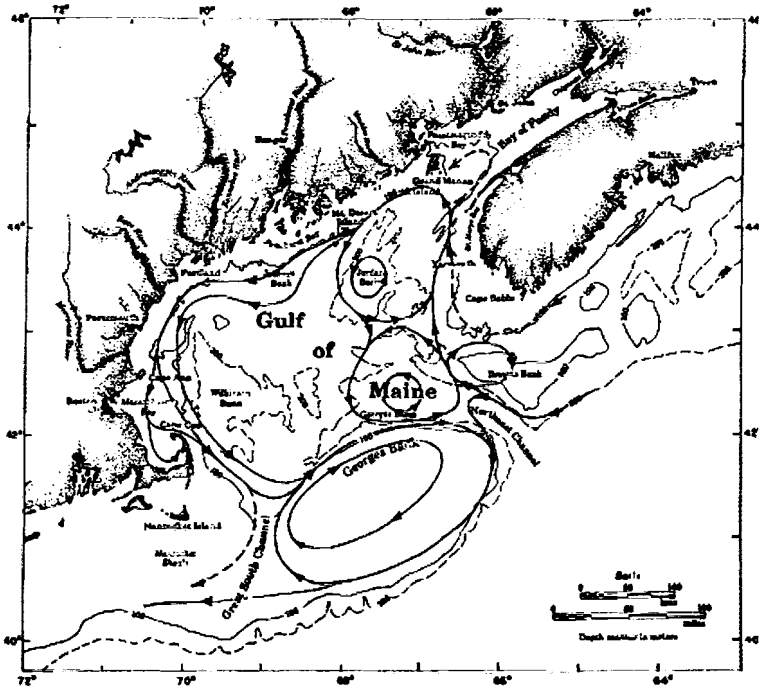


**Figure 1.1.** Circulation and Bathymetry of the Gulf of Maine (Xue et al., 2000)

Residual circulation in the GOM is counterclockwise, driven by buoyancy, with freshwater entering the system from the Scotian Shelf overlying the more dense, saline waters that enter through the Northeast Channel. Some surface and intermediate waters exit the GOM circulation via the Great South Channel, located southwest of the Northeast Channel and the rest exit through the Northeast Channel (Pettigrew et al., 1998).

Inflow from the Scotian Shelf continues along the Maine coast, creating the GOM coastal current that has two major legs; the eastern Maine coastal current (EMCC) and the western Maine coastal current (WMCC). A mix of St. Lawrence River and Labrador Current water enter the GOM and EMCC from the Scotian Shelf, which extends from the mouth of the Bay of Fundy southwestward along the coast to the vicinity of Penobscot Bay. Extensive tidal mixing keeps surface waters of the EMCC relatively cold and nutrient-rich all year long. This feature is considered the dominant hydrographic feature in the eastern GOM (Brooks and Townsend, 1989). In the vicinity of Penobscot Bay, the EMCC turns offshore. At this point, portions of the EMCC contribute either to the gyre over Jordan Basin or feed into the WMCC. Brooks and Townsend (1989) examined the variability of the turnoff point of the EMCC showing that in August of 1987 the turnoff point moved 50 kilometers to the west over a three week period. The mechanisms of this turnoff are not well understood. Brooks (1994) found that the front associated with the Penobscot River plume might partly block and redirect the EMCC. Lynch et al. (1997) agree that the effects of the Penobscot River plume are the main mechanism for steering the coastal current offshore. The EMCC, however, is likely present before the spring runoff period and can turn offshore east of Penobscot Bay (Pettigrew et al., 1998). It has

also been argued that the offshore turning point of the EMCC is closely related to the distribution of slope water in Jordan Basin. Hydrographic surveys support this hypothesis (Brooks and Townsend, 1989).

The WMCC begins immediately west of Penobscot Bay and continues southwestward along the coast of Maine and New Hampshire to Massachusetts Bay (Brooks, 1985). The WMCC has cyclonic turning points east of Massachusetts Bay and near the Great South Channel where it moves offshore. At the latter branch point, it contributes to the anti-cyclonic circulation around Georges Bank and the Nantucket Shoals (Xue et al., 2000). Freshwater input is a major physical feature of the WMCC. River runoff entering the western GOM produces plumes that extend along-shore from the mouth of the river to Massachusetts Bay in some instances (Franks and Anderson, 1992).

### 1.1.2. Phytoplankton Ecology

The general physiology and ecology of dinoflagellates underlies an understanding of the distribution of *Alexandrium*, a dinoflagellate, in the GOM. Dinoflagellates are mixotrophic (Broekhuizen, 1999), unicellular organisms classified as either plant or animal as not all species contain chlorophyll. Dinoflagellates are divided into two general groups, armored (Peridinales) and naked (Gymnodinales) (Charton and Tietjen, 1988). Both groups have two flagella (Figure 1.2.) that enable them to be motile. One flagellum is transverse, located in the horizontal groove that divides the cell into its anterior and posterior parts, making the cell spin. The other flagellum is longitudinal,

anchored in a shallow groove with the flagella itself trailing, allowing for vertical and horizontal movement (Raymont, 1963).

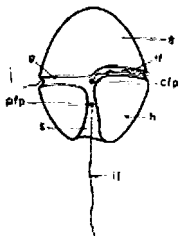

**Figure 1.2.** General Physiology of the Dinoflagellate (Raymont, 1963)

Dinoflagellates reproduce asexually via binary fission. Unarmored dinoflagellates typically produce two identical daughter cells of smaller size. In armored cells there are many patterns of division due to differences in how the theca splits. Both rate and occurrence of division are dependant on environmental conditions. Dinoflagellates divide only at certain times of the day causing differences in photosynthetic rates that vary with species. Marine dinoflagellates are generally said to divide late at night or in the early morning. Dinoflagellates only divide when cells are at optimum physiological states under suitable light, temperature, nutrient and salinity conditions. This can result in what Hastings and Sweeney (1964) termed "phased cell division," with some cells being physiologically ready to divide when the conditions are right and others having to wait for the next cycle. Environmental conditions also affect growth rate. Under unsuitable conditions, dinoflagellates may form a resting stage, thus halting any growth and allowing the cell to survive until conditions become suitable again (Walker, 1984).

Dinoflagellates also have a sexual reproductive phase. This is less common in marine dinoflagellates, but is observed in an increasing number of species every year. Marine species may lack a sexual phase or may have a shortened sexual phase lacking a hypnozygote. In the sexual phase, gametes are produced under optimal conditions and fuse to form a diploid planozygote. The planozygote is characterized by having two longitudinal flagella and the cell usually swells and becomes darker than the original vegetative cell. At this point the planozygote can either undergo meiosis or, more commonly, develop into a resting cyst called a hypnozygote (Walker, 1984). The stages of reproduction for dinoflagellates are illustrated in Figure 1.3 below.

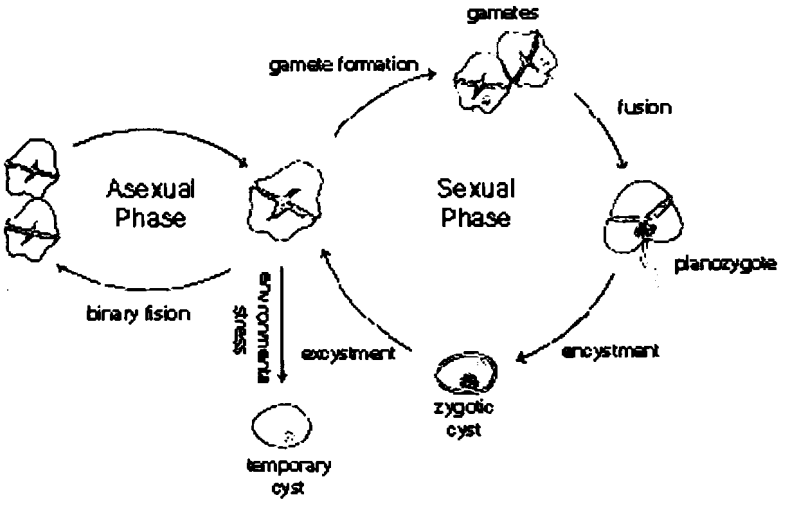


**Figure 1.3.** Dinoflagellate Reproductive Cycle (Walker, 1984)

The planozygote sheds its outer layer and its cell walls thicken, developing three layers to form the hypnozygote (cyst). It has been suggested that cysts may be the primary source of elevated summer concentrations of *Alexandrium* in the GOM (Anderson, 1997). These cysts are resistant to bacterial degradation, extreme temperatures and salinities as well as anoxic conditions and some degree of dessication

(Walker, 1984). The amount of time that a cyst can remain dormant varies on the order of years. Anderson (1980) found that cooler waters produced cysts with longer dormancy periods. Suitable, but poorly quantified environmental conditions are required for cyst germination. Changes in temperature, light, or other environmental parameters all can trigger excystment (Walker, 1984). Meiosis can occur within the cyst or after excystment in order to restore the vegetative haploid condition.

Dinoflagellates compete for light and nutrients with diatoms in the GOM throughout the year. Each have differing optimal light and nutrient requirements with maximum photosynthetic rates ($P_{max}$) and light intensity at half of $P_{max}$ ($I_k$) varying from species to species (Ryther, 1965). Saturation light intensities differ between species, suggesting that there are differences in environmental preferences, providing competitive advantage. Diatoms which have a lower $I_k$ value and a higher initial low photosynthesis slope, tolerate lower light levels than dinoflagellates and tend to dominate in spring. Under increasing light levels, dinoflagellates tend to dominate. Nutrient half saturation constants ($K_s$) also vary with species (Lalli and Parsons, 1993). In general, dinoflagellates have a lower $K_s$ than diatoms, enabling them to dominate during times of nutrient limitation (Holligan, 1985). Thus, dinoflagellates tend to dominate the population in surface waters at the end of spring and into the summer under stratified conditions of low nutrient concentrations and increased irradiance.

Dinoflagellates may also be the sole component of the fall phytoplankton bloom if one does occur (Eppley et al., 1969; Sieracki et al., 1993). Conditions more suitable for dinoflagellates than diatoms are created when vertical upwelling velocities are not strong enough for nutrient-rich subsurface waters to reach the surface. Motile dinoflagellates

are able to utilize both surface light and subsurface nutrients. Conditions of silica limitation in the water column can also lead to a dinoflagellate dominated population (Blasco, 1975).

### 1.1.3. *Alexandrium* in the GOM

*Alexandrium*, the genus of dinoflagellate in the GOM responsible for HABs, produces a saxitoxin that is dangerous to humans. In 1997, Anderson identified two species of *Alexandrium* in the North Atlantic; *Alexandrium fundyense* and *Alexandrium tamarense*. Anderson (1997) stated that within the GOM, only *A. tamarense* has been identified, but both species were present in waters further south. Deitz and Townsend (personal communication, March 2001) identified a possible third species of *Alexandrium* in the GOM, *Alexandrium ostenfeldii*, which was generally wide spread in April and May 2001 and present in high concentrations just north of Casco Bay. Together, their data suggest that *Alexandrium* species coexist, although *A. tamarense* is the dominant species in the GOM. In this thesis I do not distinguish species. The genus name *Alexandrium* will be used to refer to the combined grouping of all identified *Alexandrium* species.

Until very recently, the distribution of *Alexandrium* in the GOM was poorly understood and based primarily on observations close to shore. Townsend et al. (2001), however, observed large *Alexandrium* cell densities in offshore waters in the GOM during the summer months in 1998, spatially continuous with distributions in the Bay of Fundy (Martin and White, 1988). Within the Bay of Fundy, highest cell densities are found in the southeastern part of the Bay near the coast of Nova Scotia (Martin and White, 1988). *Alexandrium* cells have also been found to accumulate at frontal zones

(Seliger et al., 1981) where a combination of high nutrients and a shallow mixed layer, creates optimal conditions for increased phytoplankton growth (Pingree,1975). Townsend et al. (2001) also observed that *Alexandrium* cells tend to accumulate on the seaward side of high chlorophyll areas. These authors noted that the location of highest cell concentrations (ca. $5.5X10^3$ cells/liter) were coincident with the cold, nutrient-rich core of the EMCC possibly due to increased light penetration and elevated nutrient concentrations in surface waters. In the stratified and nutrient depleted surface waters of the western GOM the cell densities are uniform and low (ca. <50 cells/liter) suggesting less than optimal growth conditions. Subsurface data suggest that populations of *Alexandrium* are advected beneath the warmer, more stratified waters of the western GOM (Townsend et al., 2001).

The limited data available to date on overall distributions in the GOM (research cruises in 1998 and 2000) suggest that general temporal and spatial variability of *Alexandrium* is similar from year to year. Highest concentrations are found during the early summer (June) primarily in the EMCC. These concentrations decrease and recede to the eastern GOM and Bay of Fundy as the summer progresses (Townsend et al., 2001). Townsend et al. (2001) argue that as there are vegetative *Alexandrium* cells in the water column year round and these cells could provide the seed population for bloom initiation the following spring.

Anderson (1997) suggests that because of cyclonic offshore branching of the EMCC in the vicinity of Penobscot Bay it is highly unlikely that the cells present in the western GOM are transported there from eastern Maine. This would necessitate an independent population of *Alexandrium* in the western GOM, having its own source of

cells to initiate blooms and separate transport pathways (Anderson, 1997). Townsend et al. (2001) argue that *Alexandrium* in the EMCC can be transported into the western GOM meaning that a single *Alexandrium* population, possibly originating in the Bay of Fundy, could affect the entire GOM. The degree of connection between eastern and western GOM is highly variable (Townsend et al., 2001), however, and it is hard to generalize the nature of the connection between high offshore cell densities and toxicity of inshore shellfish beds (Pettigrew et al., 1998).

Toxicity in shellfish beds is found in both the eastern and western GOM, but there is a coastal area at the downstream end of the EMCC, in the vicinity of Penobscot Bay that is toxin-free. Shumway et al. (1988) coined the phrase the "PSP Sandwich," referring to this region. One possible explanation for this toxin-free area is an interaction of *Alexandrium* concentrations with offshore circulation patterns. The "PSP Sandwich" is located near the point where the EMCC most commonly turns cyclonically offshore. If the EMCC is a pathway along which *Alexandrium* are transported, such dynamics could leave the Penobscot Bay region toxin free. Interestingly, no *Alexandrium* cysts were found in Penobscot Bay (Lewis et al., 1979) eliminating this area as a site of local bloom initiation.

In the WMCC, Franks and Anderson (1992) found that *Alexandrium* cells tend to be most abundant in the buoyant freshwater plume from the Kennebec River, usually as subsurface populations. They hypothesize that coastal toxicity events in the western GOM are a function of the interaction of river plume dynamics and alongshore wind stress. This "plume advection hypothesis" suggests that the buoyant plume of freshwater originating from the Androscogin and Kennebec Rivers acts as a source of cells and

becomes coastally trapped, transporting *Alexandrium* cells to the southwest. Winds from the southeast induce offshore Ekman transport and move the plume (and toxic cells) offshore. Northeast winds have the opposite effect and may enhance coastal toxicity. In years of high freshwater runoff, increased surface velocities might overcome any effects of sustained upwelling winds and decrease the transit time of toxicity along the coast. In years of low runoff, wind-forcing could dominate plume dynamics and upwelling-favorable winds may slow down the alongshore transport of toxicity.

The distribution of *Alexandrium* cysts within the GOM differs from that of the vegetative cells. Keafer and Anderson (1985) found high concentrations of cysts in the deep basins of the GOM where clays and fine particles settle. White and Lewis (1982) found the highest concentration of cysts in the winter in offshore waters north and east of Grand Manan Island. This region is coincident with the location of an area of active sediment deposition, confirming what Keafer and Anderson (1985) found in the western GOM. High vegetative cell concentrations in the Bay of Fundy indicate that these cysts could be a major source for summer bloom initiation (Martin and White, 1988).

### 1.1.4. Satellite Oceanography

Satellite remote sensing provides a synoptic view of the ocean impossible to obtain through conventional ship sampling (Stewart, 1985, Njoku and Brown, 1993). Over the last two decades, as data and technology have become increasingly available, satellite remote sensing has been applied to many aspects of oceanographic research (Minnett, 1995). Two satellite data parameters commonly used in oceanographic research are sea surface temperature (SST), calculated from infrared measurements, and

chlorophyll concentrations, calculated from ocean color measurements. Because of the role of temperature in density, SST measurements provide direct insight into physical processes. Chlorophyll measurements provide an estimate of biological spatial patterns and can also act as a Lagrangian tracer of flow dynamics.

The literature contains numerous examples of satellite SST and chlorophyll data used to document and/or quantify the spatial distribution of phytoplankton, surface hydrography and their interaction. Two examples suggest that both SST and chlorophyll data contribute to an improved understanding of phytoplankton distributions. Satsuki et al. (1989) used Coastal Zone Color Scanner (CZCS) data to map phytoplankton pigment concentrations resulting from mixing patterns at large frontal eddies around Japan. They also used the channel six infrared data from the CZCS to determine sea surface temperature, examining the temperature and chlorophyll profiles of a frontal eddy. Differences between SST patterns and pigment patterns forced them to conclude that coincident analysis of temperature and chlorophyll are needed to isolate mechanisms for chlorophyll production. Holligan et al. (1983) used hydrographic cruise data from a two and a half month time period in 1981, along with coincident CZCS chlorophyll data and AVHRR sea surface temperature data to look at the spatial distribution of surface phytoplankton in the western English Channel. They found that satellites effectively monitor blooms and the CZCS data provided the basis for the first complete description of the spatial and temporal distribution of a *Gyrodinium aureolum* Hulburt bloom. They reported that if the chlorophyll images could be processed within hours the data could greatly aid in the process of choosing station locations.

Satellite data have previously been used in studies of harmful algal blooms to monitor their short time scales and large spatial scales (Yentsch, 1989). Blooms of the toxic dinoflagellate *Gymnodinium breve* along the Florida coast are associated with the transport of cells onshore by the Gulf Loop current. In February 1996 this association was demonstrated when toxic cells transported within the surface waters killed manatees in coastal waters (Landsberg and Steidinger, 1998). Similar thermal patterns could be identified in AVHRR SST imagery, making satellite data useful as a monitoring tool for *G. breve* blooms in Florida.

In the early 1990's a bloom of *G. breve* off the coast of North Carolina and Florida resulted from transport of toxic cells in the Gulf Stream to the shore waters (Tester et al., 1991). About a month after the bloom was identified, AVHRR SST images revealed a surface temperature feature that implied shoreward movement of a filament of Gulf Stream water onto the shelf near Cape Hatteras and Cape Lookout, North Carolina. This feature is the proposed source of the toxic cells (Tester and Stumpf, 1998), illustrating the use of satellite data in managing HABs.

Keafer and Anderson (1993) showed that satellite sea surface temperature data were helpful in studying *Alexandrium* bloom dynamics in the western Gulf of Maine, locating and tracking physical features such as fronts and specific water masses. They found a buoyant plume of water associated with the transport of *Alexandrium* and concluded that remote sensing gives an improved understanding of the short-term oceanographic processes responsible for the development and behavior of *Alexandrium*.

## 1.2. Goals and Objectives

ECOHAB is a national program funded by the National Science Foundation (NSF), National Oceanic and Atmospheric Administration (NOAA), and the National Aeronautic and Space Administration (NASA) whose goal is an improved understanding of the ecology and oceanography of HABs. In 1997, a multi-institutional research proposal led by Woods Hole Oceanographic Institution was funded under the ECOHAB program to study the ecology and oceanography of the harmful algal species, *Alexandrium*, in the GOM (ECOHAB-GOM). Within this proposal, some of the specific areas of study include the transport and distribution of *Alexandrium*, cyst dynamics, grazing rates, and the food-web transfer of toxins. Research is supported by numerical modeling to study the physical processes in the GOM as they relate to the distribution of *Alexandrium*. My thesis research investigates the use of satellite imagery as a tool for understanding the distribution of *Alexandrium* in the GOM. The overall goal is to quantify the extent to which satellite measured sea surface temperature and chlorophyll can model patterns of *Alexandrium* in time and space.

Riley (1946) showed that phytoplankton concentrations illustrate quantifiable relationships to specific physical and chemical parameters in their environment, but that the quantitative nature of their relationship varied in both time and space. An initial working hypothesis for this study is that quantifiable relationships will exist between satellite derived surface parameters and various *in situ* measurements but that the actual quantitative relationships will vary or even disappear, in time and/or space. For example

Kamykowski and Zentara (1991) documented a general inverse relationship between sea surface temperature and surface nutrient concentrations. In the GOM, however, this may hold true only for the spring and early summer and only in the more strongly physically forced areas such as the EMCC. However, if nutrient distributions are an important component of *Alexandrium* spatial distributions, relationships between satellite measured fields and nutrients could be a valuable tool in modeling *Alexandrium* distributions. Similarly, times and places where patterns of *Alexandrium* distribution have relationships with satellite-derived patterns can be expected to vary depending on the dominating processes. If physical processes dominate distributional ecology and *Alexandrium* is acting primarily as a Lagrangian tracer of flow structure, this hypothesis predicts a strong relationship to SST data. If phytoplankton ecological processes dominate and *Alexandrium* growth mimics that of the general phytoplankton biomass the hypothesis predicts a closer similarity to the surface chlorophyll patterns.

My hypothesis will be examined through qualitative and quantitative analyses of the relationships between surface *Alexandrium* concentrations from two years of ECOHAB cruise data (1998 and 2000) and coincident AVHRR SST and SeaWiFS chlorophyll data. Qualitative analyses will generally consist of examining the distribution of *Alexandrium* in the GOM in relation to the AVHRR SST and SeaWiFS data. More specifically, the analysis will look at the location of high *Alexandrium* cell densities in relation to the location of physical features in the GOM, such as the EMCC and include of a number of linear regression analyses using the *in situ* and the satellite data. Relationships revealed through these analyses will be quantified and applied to the satellite data to create a synoptic view of the *in situ* parameter. In addition to any linear

relationships, this regression analysis may reveal non-linear relationships groupings or clusters which imply ecological boundaries involved in *Alexandrium* distribution. Lastly, I will investigate the utility of satellite data in defining the connection between the EMCC and toxicity events in the western GOM. Assuming the high *Alexandrium* concentrations are in the EMCC, a connection of the EMCC to the western GOM is necessary to cause a toxicity event (Townsend et al., 2001). Quantification of this connection might allow satellite data to be used as a monitoring or management tool in predicting toxicity events in the western GOM in any given year.

# Chapter 2

# DATA AND METHODS

## 2.1. Data

### 2.1.1. *In Situ* Data

This study uses *in situ* data collected during the 1998 and 2000 ECOHAB field seasons. Three broad-scale survey cruises were conducted in 1998; June 6-16, July 6-16, and August 4-16. Two broad scale survey cruises were conducted in 2000; April 22-May 4 and June 5-15. The station locations for each of the five cruises are shown in Figure 2.1a-e with specific locations listed in Appendix A. In general, parameters measured at each station include vertical profiles of temperature, salinity, fluorescence, chlorophyll, pheopigments, dissolved nutrients ($NO_3$ and $NO_2$, $NH_4$, $PO_4$, $SiO_4$), and *Alexandrium* cells (see Appendix B). Redefinition of cruise objectives and methodologies resulted in differences between parameters measured in 1998 and 2000 (see Appendix B for details). Townsend et al. (2001) provide details on both lab and field protocols.

### 2.1.2. Satellite Data

**2.1.2.1. Ocean Color Data** Ocean color is measured by the reflectance of sunlight in the visible range (400 to 700 nanometers). Quantitative reflectance varies as a function of wavelength-dependant backscatter and absorption in the surface waters (Arnone and Gould, 1998) which in turn is a function of differences in concentrations of

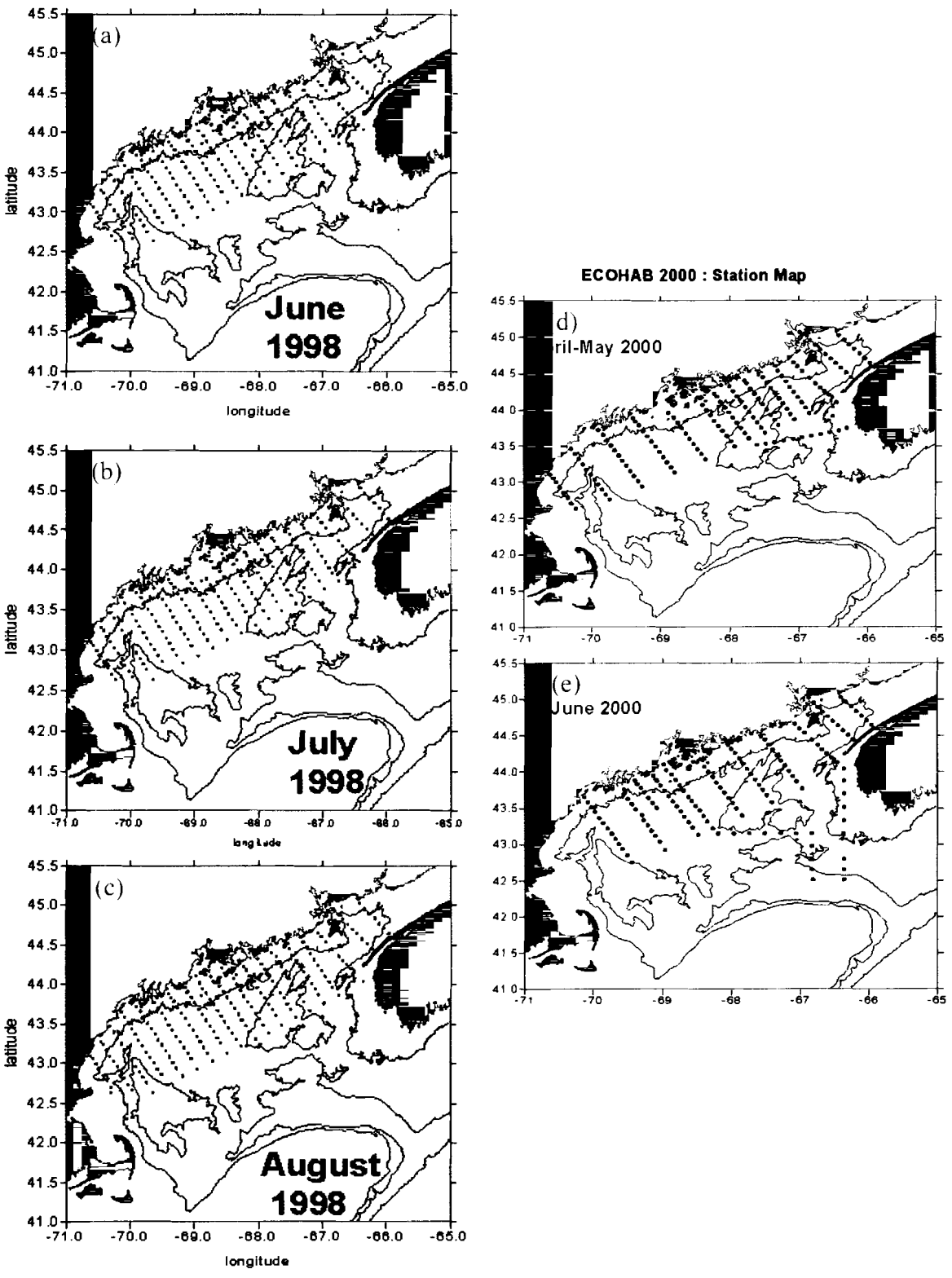


**Figure 2.1.** Maps of station locations for all five of the ECOHAB survey cruises; (a) June 1998, (b) July 1998, (c) August 1998, (d) May 2000, and (e) June 2000.

particles, primarily chlorophyll and sediment, in the water (Mobley, 1994). Reflected light is detected by the satellite and the concentration of substances in the water can be deduced if the nature of how they absorb and scatter light is understood (Mobley, 1994).

Remotely sensed ocean color measurements from Ocean Color and Temperature Sensor (OCTS), CZCS, SeaWiFS, and now the Moderate Resolution Imaging Spectroradiometer (MODIS) allow surface chlorophyll estimation from space. The earliest sensor, CZCS, provided an estimate of total pigment in the water (sum of both chlorophyll and pheopigments). Advances in spectral band selection and algorithms, allow SeaWiFS to make reliable estimates of chlorophyll from the detected water-leaving radiance in the open ocean. The color of the ocean, as seen from above, is the spectral and angular result of incident solar energy being backscattered and absorbed in the ocean surface and interior. Oligotrophic waters of the deep ocean central gyres appear dark blue because pure water absorbs red light and scatters mostly blue light. Closer to shore, productivity increases and chlorophyll, colored dissolved organic material (CDOM) and sediments become an increasing percentage of the particles in the water column. With increasing chlorophyll concentration, the water column absorbs more strongly in the blue wavelengths and shifts the spectral backscatter into green wavelengths. If the color-producing particles of the water are dominated by phytoplankton (case 1 water) the water will appear green due to the chlorophyll reflecting green light. Waters in which sediment and CDOM are dominant and pigment absorption is less important (case 2 waters) the waters will appear more brown or red (Morel and Prieur, 1977). The ocean color algorithms for SeaWiFS attempt to deal with the increased backscatter of sediments and

CDOM, but still tend to overestimate chlorophyll in coastal areas where case 2 waters dominate.

In addition to radiance backscattered out of the surface layer of the ocean, the radiance that is detected by the satellite includes that from the sky reflected off the ocean surface as well as that scattered back toward the satellite by atmospheric gases and particles (Mobley, 1994). This atmospheric component is modeled from radiance measurements made by the satellite and an atmospheric model, and then subtracted from the total signal. The largest source of error in satellite ocean color estimates results from this interference, which can account for up to 90% of the electromagnetic radiation received by the instrument. Sun glint can also be a large source of error in ocean color remote sensing but is avoided by tilting the sensor.

The ocean color data used in this study were received from the SeaWiFS instrument on the ORBIMAGE satellite, SeaStar, and sent to the Satellite Oceanography Data Lab at the University of Maine, monthly, from the National Aeronautic and Space Administration (NASA) Goddard Space Flight Center. L1A data (radiance values for each channel) are received and processed using NASA's SEADAS software resulting in L2 data (chlorophyll values). Both semianalytic and empirical models are used to make chlorophyll estimates, usually using the ratio of two sensor channels. Different algorithms, equations and band ratios are used to calculate chlorophyll in different optical water conditions. The SeaWiFS algorithm uses a modified cubic polynomial function with the ratio 490/555 to simulate the sigmoidal relationship between log radiance ratios and *in situ* chlorophyll concentrations found by O'Reilly et al. (1998):

$$[Chl] = -0.040 + 10^{[0.341 - 3.001 * X + 2.811 * X^2 - 2.041 * X^3]}$$

where X = LOG[Rrs(490)/ Rrs(555)].

Recent work has shown that a larger than expected area of the GOM is considered to be case 2 waters (work by M. Keller and Thomas, O' Reilly, personal communication, August 2001) and measurements derived from the SeaWiFS images may be overestimates of the actual concentrations. Algorithms are continually being improved to better derive chlorophyll concentrations in case 2 waters. Data used in this study were processed using the third SeaWiFS reprocessing (2000) algorithm coefficients.

**2.1.2.2. Sea-Surface Temperature Data** Sea surface temperature (SST) measurements are based on the quantification of infrared radiation leaving the ocean surface (Njoku, 1990) within the spectral range of 650 to 1200 nanometers. The largest source of uncertainty in SST measurements is interference from the atmosphere. The atmospheric constituent contributing most strongly to this uncertainty is water vapor. Clouds totally obscure the signal leaving the sea surface but even a "clear sky" contributes to the radiance measured (Minnett, 1995). Radiance contributed by the atmosphere, the largest component of which is water vapor, needs to be removed to calculate SST. The NOAA five-channel AVHRR data was the first to use multiple channels for both cloud masking and atmospheric attenuation corrections. In this method, three classes of cloud masking tests are used; visible and visible-near-infrared bi-directional reflectance thresholds, spatial coherence thresholds using visible and infrared data, and a multi-channel infrared intercomparison test. Pixels failing this test are masked as clouds and SST estimates are not possible from them. Accurate

measurements of SST depend on the isolation of cloud-free data and subsequent correction for interfering atmospheric absorption and radiation.

Once the cloud contaminated pixels are flagged, a multiple-window technique is used to calculate SST estimates from the remaining ocean pixels. This technique uses a linear relationship between brightness temperatures observed in two or more independent infrared channels and the SST. McMillin (1975) showed that a simple linear combination of radiances at two wavelengths gives a good estimate of the water leaving radiance, providing an SST estimate. A forward radiative transfer model is used to calculate the coefficients of the linear relationship, but due to uncertainties in the model and in the absolute calibration of the AVHRR, empirical adjustment of the coefficients is needed. The empirical adjustment is performed by regressing the brightness temperatures against a global array of collocated drifting buoy SST measurements. This method has a global accuracy of ~ 0.7°K (Bernstein, 1982).

The telemetry data stream from three NOAA satellites (NOAA-12, NOAA-14, NOAA-15) is downloaded at the University of Maine Satellite Oceanography Data Lab's (SODL) ground station. The three NOAA satellites each pass over the study area (the GOM) two to three times a day, allowing for six to nine images to be archived daily. The telemetry received is a full (2400 km wide) swath covering the east coast of the United States, including the GOM. In the lab, brightness temperatures in each channel are passed through a multi-channel SST (MCSST) algorithm, a linear algorithm with a weak dependence on view angle. The algorithm considers data in the three infrared channels; channel four and five are used in processing day images and channel three is used only when processing night images because the reflected solar radiation cannot be removed

during the day (Bates and Diaz, 1991). Channels one and two (visible wavelength reflectance) are used for cloud masking in daytime images.

The time period of satellite data examined for this study extended from five days prior to each cruise to five days after each cruise had ended. This allows cloud-free images from immediately outside the cruise period to contribute to any days at the beginning or end of the cruise period in which there were no cloud-free images. Appendix C is a list of the original data collected for this study. The AVHRR data were used not only to provide synoptic sea surface temperature fields, but also to calculate higher order descriptions of the ocean such as frontal location and strength, patterns indicative of advection, and current locations that may provide insight into *Alexandrium* distributions.

Archived, historical AVHRR data from the Pathfinder program, sponsored by NOAA and NASA, were used in an analysis of retrospective toxicity data. The goal of the Pathfinder program is to produce a long time-series of accurate SST data for global climate change studies. Intercalibration of sensors on the AVHRR instruments, as well as revised processing procedures and improved quality control algorithms make this data set a consistent and accurate estimate of SST over extended time periods (Kilpatrick et al., in press). For example, the Pathfinder SST data set makes use of a better cloud masking scheme than the MCSST data, using a two-tier technique. The first tier uses the same procedure as the MCSST algorithm. The second tier incorporates comparisons of the SST to a reference SST field defined from the actual time series and a match-up database. This two-tier approach makes the Pathfinder data set less noisy and more precise. In addition, because the Pathfinder algorithm regresses the satellite measured

SST estimates against buoy data, the measurements more closely represent the bulk temperature, not a surface skin temperature such as that returned by the original AVHRR SST algorithm (Schluessel et al., 1990).

High spatial resolution (1.25 km) Pathfinder data for the east coast of the United States are processed by the Graduate School of Oceanography at the University of Rhode Island. The individual images received from the University of Rhode Island were composited over eight-day periods, a time period that exceeds the mean decorrelation time scale of GOM SSTs, thus allowing each composite to be statistically independent. Composites covering the months in 1990 to 1999 coincident with the sampling period of toxicity data (March to August) provided by the Maine Department of Marine Resources (DMR) were used in this study.

### 2.1.3. Toxicity Data

Maine DMR samples shellfish for PSP toxicity at approximately 300 stations along the coast of Maine each year. Ten years of retrospective toxicity data (1990-1999) for all the stations were acquired for this analysis. A number of species of shellfish, including Atlantic and Arctic surf clams (*Spisula solidissima* and *Mactromeris polynyma*), horse mussels (*Modiolus modiolus*), razor clams (*Ensis directus*), soft shell clams (*Mya arenaria*), ocean quahogs (*Arctica islandica*), and most commonly, blue mussels (*Mytilus edulis*) are sampled at each station. The frequency of sampling for each site varies depending on the presence of toxin. Stations are sampled once a week, but when found to have increased or rising toxin levels they are more frequently monitored.

The level of toxicity in the shellfish is measured using a standard mouse bioassay method. A 100g sample of shellfish meat is collected and made into an extract. One ml of the extract is injected into each of three mice. The mouse is then weighed and the time of injection and apparent health and behavioral changes and/or time of death are recorded. Calculations are made to convert times to mouse units (MU) using Sommer's Table. The MU data is then corrected for weight by multiplying the time of death of each by a weight correction to give the corrected mouse unit (CMU) for each mouse. The median value of the three corrected mouse units is calculated and the concentration of toxin is determined using a standard formula which includes the CMU, a correction factor and a dilution factor (Bean, personal communication, September 2001). The level of toxin detection in mice is 40 μg/100g tissue, thus a toxin level of –40 μg/100g indicates no toxicity. If the toxin level at a station is at or approaching 80 μg/100g tissue, the area is closed to the taking of that species of shellfish (Bean, personal communication, January 2001).

The multiple shellfish species tested and the hundreds of stations sampled represent a wealth of information. To simplify the analysis, attention was focused on five specific DMR sampling sites that were relatively exposed and therefore determined to be more likely influenced by large-scale circulation patterns of the GOM rather than small-scale local processes occurring within individual bays and harbors. Similarly, I have used only the blue mussel (*Mytilus edulis*) as a key to general toxicity levels. *Mytilus edulis* is widely regarded in environmental and toxicity literature as an excellent indicator species. Timelines of toxicity level (μg/100g tissue) in *Mytilus edulis* over the sampling

season, usually from February to November, were created for the five sampling stations (four stations in western Maine and one in eastern Maine).

## 2.2. Methods

### 2.2.1. Noise Reduction

Day-to-day operations in the University of Maine SODL process the brightness temperatures of each AVHRR pass using the MCSST calculation and cloud masking algorithm set with seasonally-determined coefficients and thresholds. These generalized coefficients work for the majority of the images, but can be improved upon by customizing for specific study periods. All five channels of data are used in the determination of a cloud mask, but not all parameters have an equal impact on the amount of data masked. A sensitivity analysis was performed. The channel two maximum reflectance criteria and the channel four minimum temperature criteria were the threshold parameters that seemed to have the strongest influence on cloud masking success. The channel two maximum reflectance and channel four minimum temperature thresholds are adjusted seasonally at the University of Maine SODL to optimize the cloud masking. As the waters get colder in the GOM, the channel two maximum reflectance threshold needs to be increased and the channel four minimum temperature needs to be decreased.

In order to optimize the cloud masking for each individual AVHRR scene used in this study, the brightness temperature data were reprocessed using customized

coefficients for the atmospheric correction applied to either each cruise period or, in some cases, each individual image. Different thresholds were sometimes chosen for images coincident with the early part of the cruise and the late part of the cruise to obtain more rigorous cloud masking. Table 2.1 lists the thresholds used for each cruise period and each satellite.

| Cruise Period | Satellite | ch2_max | ch4_min_temp |
|---|---|---|---|
| June 1998 | 12 | 2 | 0 |
| | 14 | 3 | 6 |
| July 1998 | 12 | 2 | 0 |
| | 14 | 2 | 7 |
| August 1998 | 12 | 1.5 | 0 |
| | 14 | 2.2 | 6.91 |
| April - May 2000 | 12 | 1 | 2 |
| | 14 | 2 | 3 |
| | 15 | 2 | 3 |
| June 2000 | 12 | 2 | 5 (early) 7 (late) |
| | 14 | 2 (early) 3 (late) | 5 (early) 7 (late) |
| | 15 | 2 (early) 1 (late) | 7 |

**Table 2.1.** Thresholds used to reprocess AVHRR data for better cloud masking.

The largest problem with trying to improve the cloud masking, especially for those images in early spring, is that surface waters off the Scotian Shelf are sometimes just as cold, if not colder, than cloud surfaces. Attempts to mask all the clouds in these images based on thresholds often resulted in masking the coldest water as well. Optimal cloud masking in the five available channels of AVHRR data is an ongoing area of active research in Satellite Oceanography.

### 2.2.2. Composites

Temporal composites were created from the AVHRR and SeaWiFS image time series in order to map the mean pattern of physical and biological features representative of specific time periods (over a week or the entire cruise period). The compositing process also created images with better cloud-free coverage. Composites are not a true mathematical mean of the images used. A composite computes the mean at each pixel location using only valid (cloud-free) data from that location. Thus, the number of valid pixels entering into the calculation of the mean varies from location to location due to varying cloud cover.

All daily AVHRR and SeaWiFS images from the study period were visually inspected and any extremely cloudy images that would contribute little or no data to temporal composites were eliminated from the time series. The remaining images were used to form both weekly and cruise composites for each of the 1998 and 2000 ECOHAB cruise periods. The week one and week two split was determined by dividing the cruise period into two equal lengths. The dates used are specified in Table 2.2, along with the number if images used in each composite.

| Cruise | Week 1 Composite | Week 2 Composite |
|---|---|---|
| **June 1998** | | |
| Date Range: | June 6 - 11 | June 12t - 16 |
| Yeardays: | 152, 153, 155-158, 160-162 | 163 |
| # of images: | 9 | 1 |
| **July 1998** | | |
| Date Range: | July 6 - 11 | July 12 - 16 |
| Yeardays: | 183-185, 187, 189-192 | 193-196, 199, 200, 202-204 |
| # of images: | 8 | 9 |
| **August 1998** | | |
| Date Range: | August 4 - 10 | August 11 - 16 |
| Yeardays: | 213-218, 220-222 | 225, 226, 228, 231, 232, 234 |
| # of images: | 9 | 6 |
| **May 2000** | | |
| Date Range: | April 22 - 28 | April 29 - May 4 |
| Yeardays: | 108 | 120-125, 127 |
| # of images: | 1 | 7 |
| **June 2000** | | |
| Date Range: | June 5 - 10 | June 11 - 15 |
| Yeardays: | 155-157, 159, 160 | 166-168, 170-172 |
| # of images: | 5 | 6 |

**Table 2.2.** Date range, yeardays and number of images making up each weekly cruise composite.

Compositing can result in images with increased noise artifacts in areas where only a few temporally discontinuous pixels contribute to the mean. To reduce some of this noise, both 5 X 5 pixel mean and median spatial filters were applied sequentially to the AVHRR composites and a 5 X 5 pixel median filter was applied to the SeaWiFS composites.

### 2.2.3. Contours

Contours of the near surface (less than five meter depth) measurements of each of the *in situ* nutrient concentrations (nitrate/nitrite, ammonium, silicate, phosphate) and biological parameters (pheopigment, chlorophyll, *Alexandrium*, fluorescence) were

overlaid on the weekly, cruise and daily composites of both the AVHRR and SeaWiFS data to qualitatively investigate their relationship with the satellite data. Qualitative relationships evident from visual inspection were used in quantitative regression analyses, described below.

### 2.2.4. Two-Dimensional SST Gradients

If physical oceanographic processes in the GOM play a role in the distribution of *Alexandrium*, strong horizontal thermal gradients, or frontal zones, may be important. In addition to being hydrographic boundary regions, fronts are also regions of convergence. Using Van Woert's (1982) study of subtropical fronts as a model, two-dimensional SST gradient images were created by applying a two-dimensional gradient operator:

$$T(x,y) = 1/(2\Delta h)\ \{[T(x - \Delta h,y) - T(x + \Delta h,y)]^2 + [T(x,y - \Delta h) - T(x,y + \Delta h)]^2\}^{1/2}$$

to the AVHRR cruise composites for all five cruise periods. The operator is an unweighted central difference with final units of $°Ckm^{-1}$, where T is the temperature at any pixel location x,y in the image and $\Delta h$ is the pixel separation in the x and y direction over which the gradient is calculated. After sensitivity tests on the images, a $\Delta h$ of three (3.3 km) was used, resulting in gradients computed over seven pixels (~8 km) in the x and y directions. Surface *Alexandrium* concentrations for each cruise period were contoured on top of temporally respective gradient images to explore qualitative relationships between *Alexandrium* distribution and frontal zones.

### 2.2.5. Linear Regression Analyses

In order to quantify any relationships evident in the qualitative image/contour overlay comparisons, scatterplots were created using available spatially coincident satellite and *in situ* data. A line or a curve was fit to the data in a least-squares sense and a correlation coefficient was computed to examine the degree of relationship between the two. Two approaches were used. First all the data for the entire GOM were treated as a single data set and examined. Second, subsets of the GOM were analyzed individually. The second approach anticipates that statistically significant relationships between the satellite data and the *in situ* data might vary in time and space and thus not be evident in a treatment of the GOM as a whole. Subsets of the data (eastern Maine vs. western Maine and, more specifically, the EMCC, Jordan Basin, Scotian shelf, Wilkinson Basin or WMCC) were analyzed to determine if relationships improve if a particular area is isolated. Figure 2.2 shows the rough location of these subsets in the GOM and Appendix E lists the stations in each subset for each cruise.

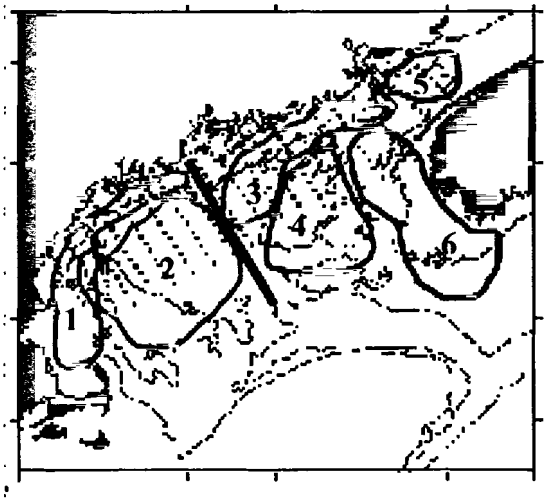


**Figure 2.2.** Location of subsets in GOM. (1) WMCC, (2) Wilkinson Basin, (3) EMCC, (4) Jordan Basin, (5) Bay of Fundy, and (6) Scotian Shelf

An additional set of scatterplots in which the distribution of a third parameter was represented in symbol was created for each cruise period. This allowed examination of any relationships between the third parameter and the other two data sets being regressed. Combinations of *in situ* and *in situ* data were plotted as well as combinations of *in situ* and satellite data to quantitatively assess relationships.

# Chapter 3

# RESULTS AND DISCUSSION

## 3.1. Contours

All nutrient and biological data contours were overlaid on daily, weekly and cruise composites of AVHRR SST and SeaWiFS chlorophyll. Dominant surface hydrographic features, such as the EMCC and mixing at the mouth of the Bay of Fundy, were more clearly evident in multiple day composites so daily composites are not presented.

*In situ* surface *Alexandrium* data contoured over AVHRR SST cruise composites are shown in Figures 3.1a-e. The contours for 1998 (Figures 3.1a,b,c) show a large population of *Alexandrium* at the mouth of the Bay of Fundy and extending southwest along the coast of eastern Maine associated with the colder SST of the EMCC consistent with advection. As the EMCC turns cyclonically offshore the *Alexandrium* cells are carried with it, resulting in an offshore population immediately south of Penobscot Bay. This *Alexandrium* population offshore decreases in concentration from June to August, the distribution pattern retracting back toward and into the mouth of the Bay of Fundy. These results are consistent with those of Townsend et al. (2001), who suggested the offshore populations of *Alexandrium* in the GOM were related to surface nutrient availability and the light field. They also found that the western GOM had uniformly low cell concentrations, most likely due to less than optimal growth conditions. Figure 3.1a-c

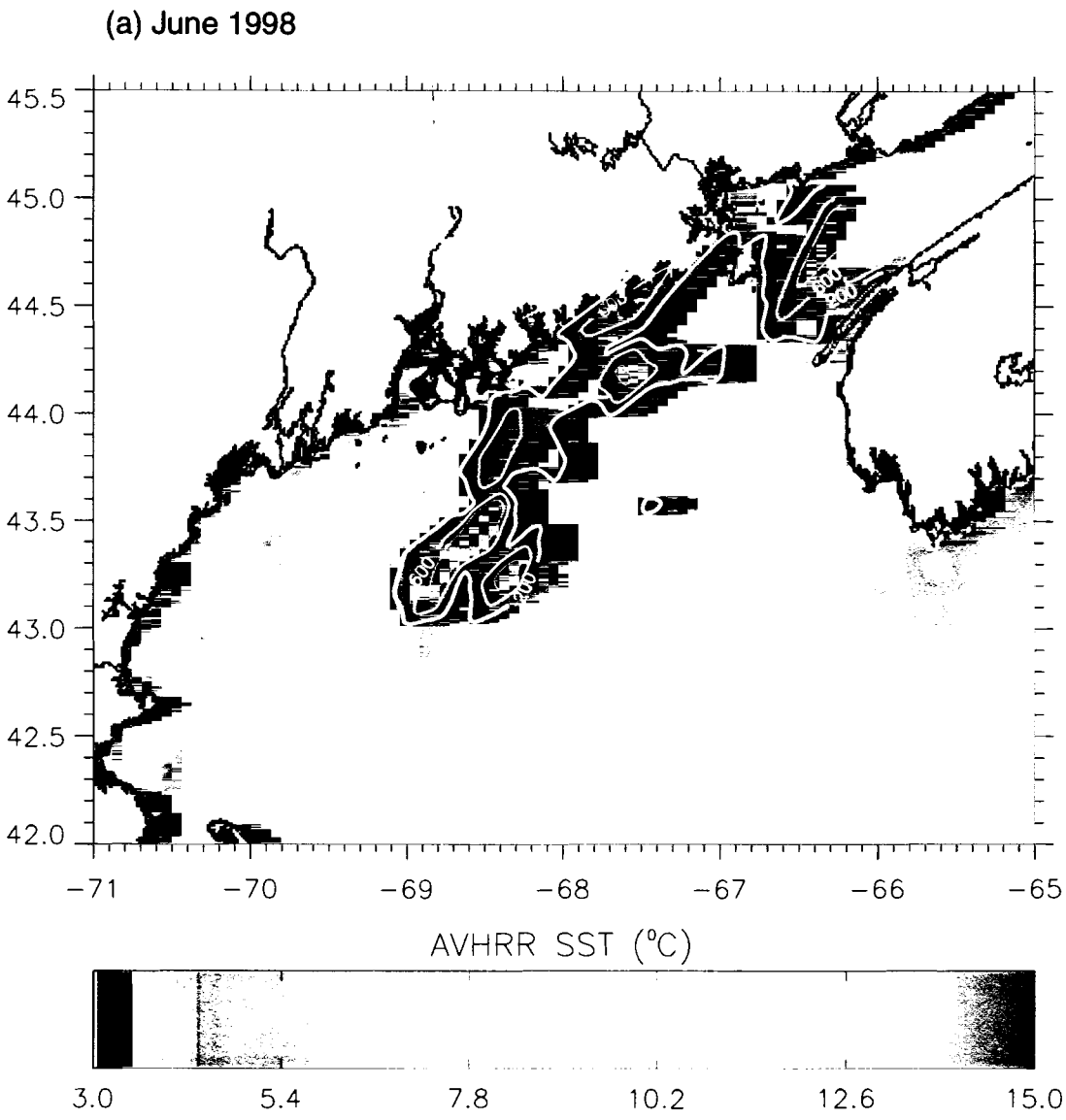


**Figure 3.1.** AVHRR SST cruise composites with surface *Alexandrium* concentration contours (cells/L) overlaid for (a) June 1998, (b) July 1998, (c) August 1998, (d) May 2000, and (e) June 2000.

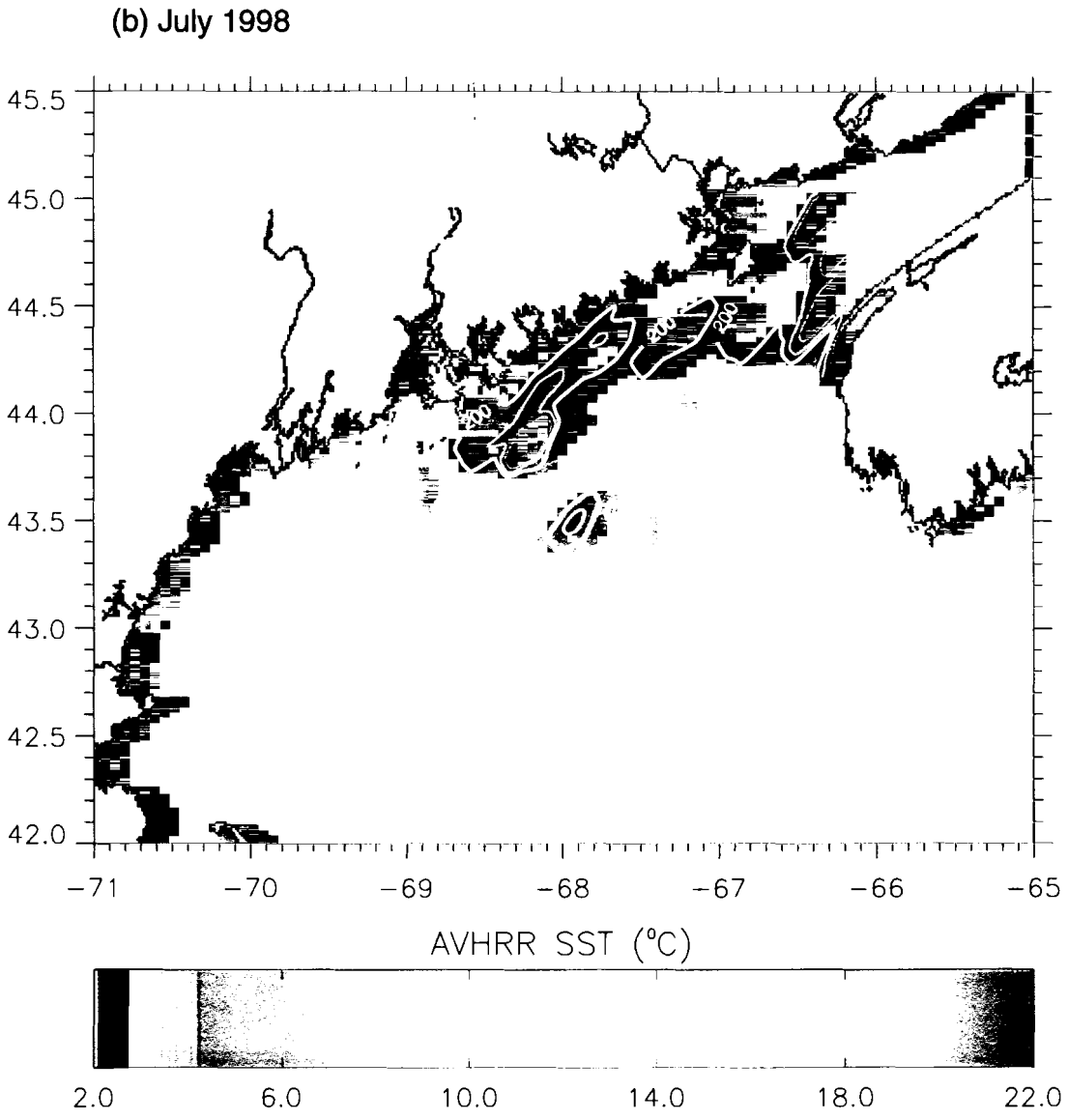


**Figure 3.1.** Continued

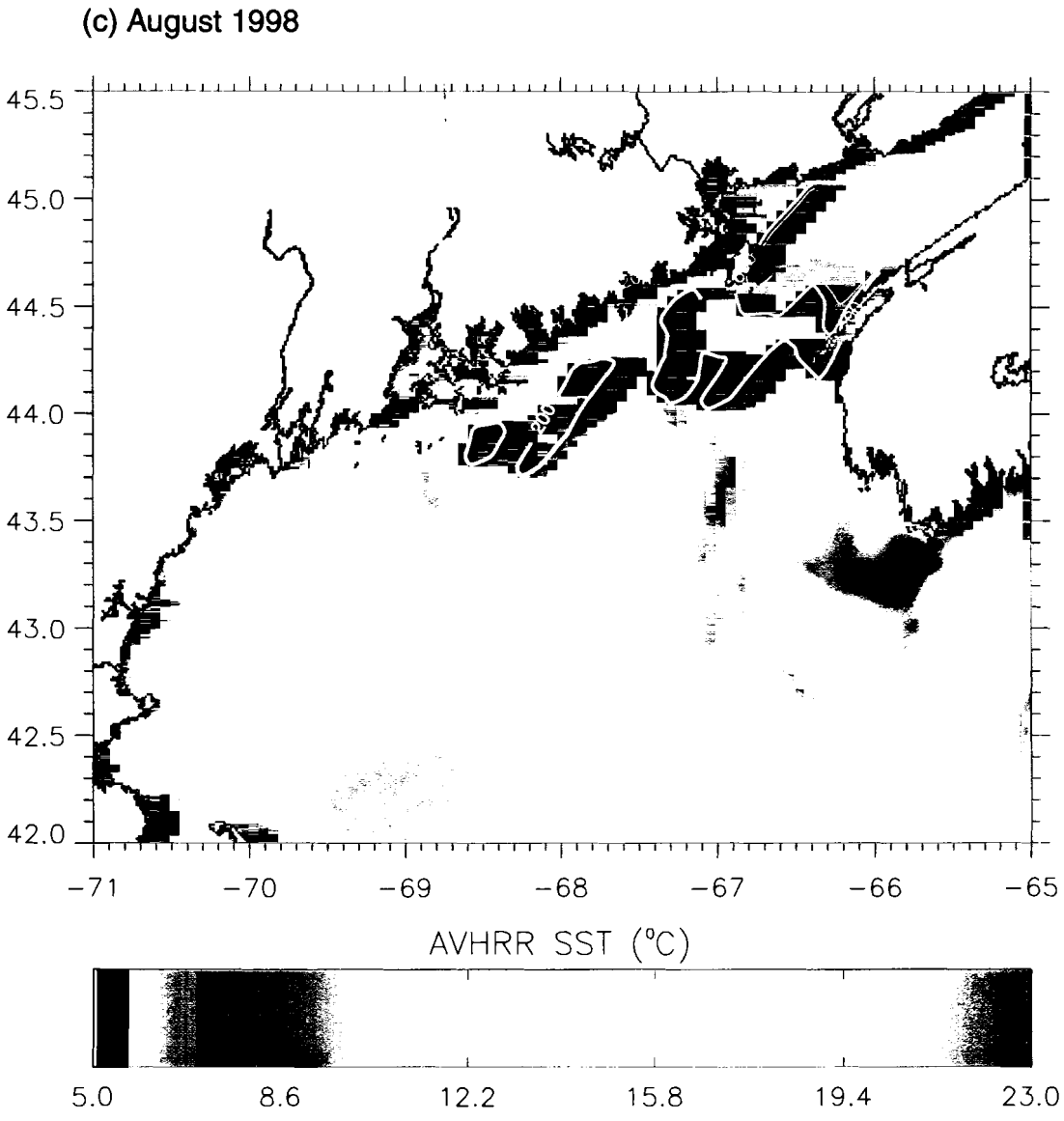


**Figure 3.1.** Continued

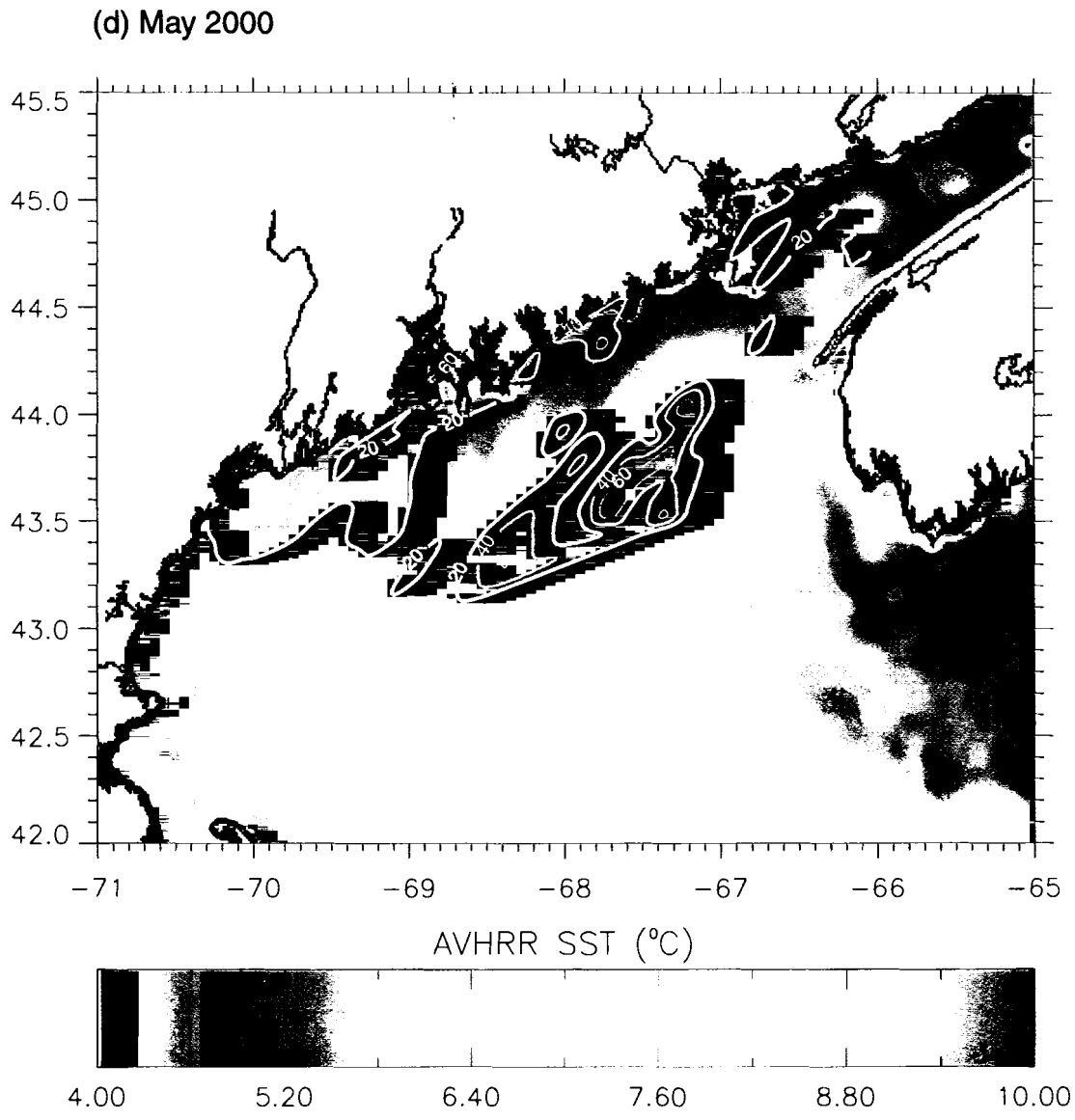


**Figure 3.1.** Continued

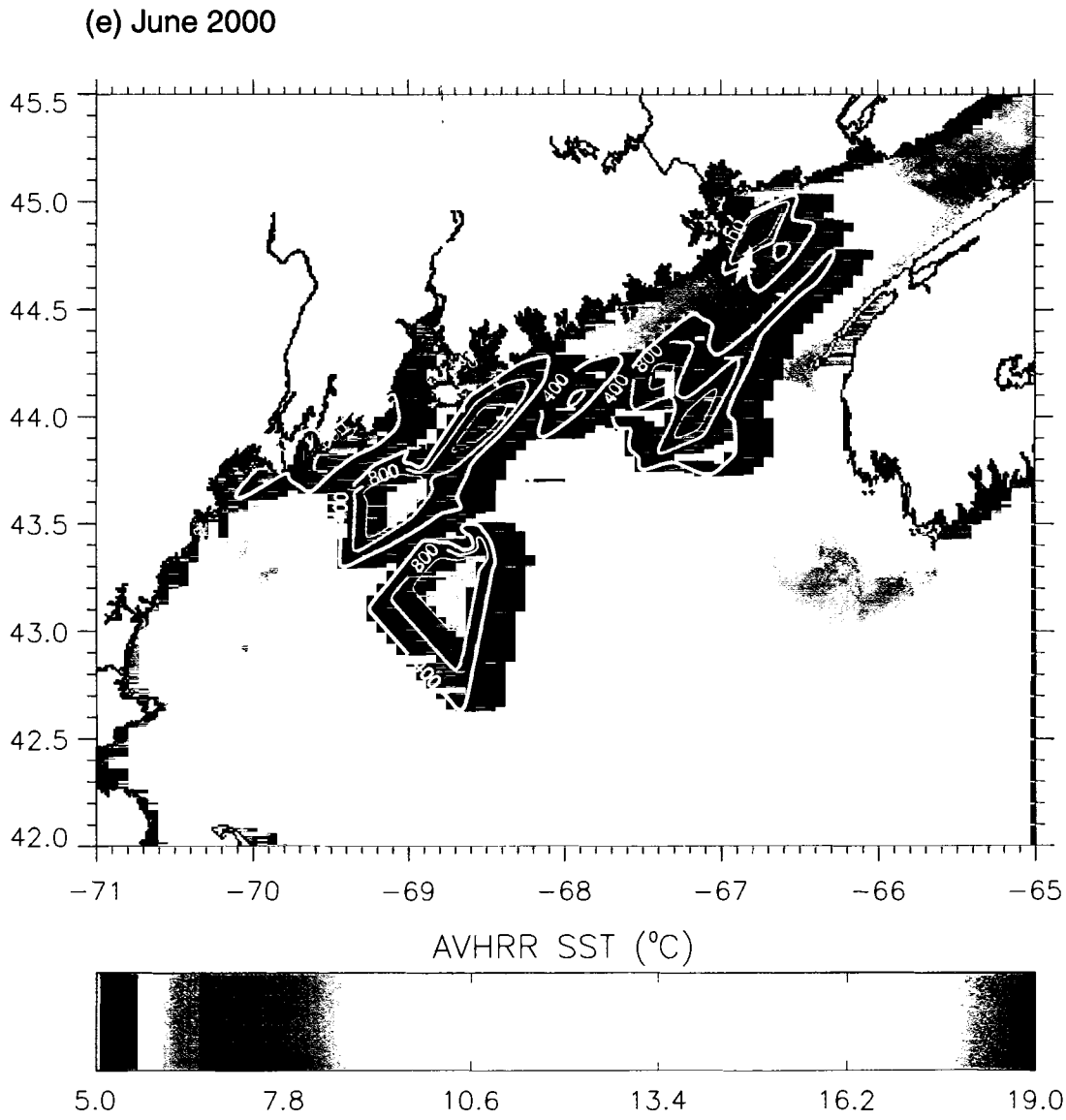


**Figure 3.1.** Continued

shows these results and illustrates the association of these low concentrations with warmer SSTs when compared with the station locations in Figure 2.1.

In May 2000 (Figure 3.1.d) *Alexandrium* was present in low concentrations throughout the entire GOM, showing both a different spatial pattern and relationship to AVHRR SST than was present in 1998. The populations are not spatially coincident with any specific surface physical feature. This is likely due to the fact that May is early in the season and detectable surface thermal features have not yet developed. By June 2000 (Figure 3.1e), the regular seasonal features of the GOM (Xue et al., 2000), such as the EMCC, have started to develop a surface SST expression, resulting in a more obvious relationship between SST and *Alexandrium* concentration. The distribution of *Alexandrium* in June 2000 is similar to that observed in each of the months in 1998, with highest *Alexandrium* concentrations associated with the cold waters of the EMCC, and thus consistent with the findings of Townsend et al. (2001). Two differences are noted, however. In June 2000 the EMCC turns offshore just south of the Penobscot Bay, whereas in 1998 it separates from the coast just north of the Penobscot Bay, consistent with variability in separation point observed by Brooks and Townsend (1989). In 2000 (Figure 3.1.d,e), there is also a population of *Alexandrium* in Jordan Basin that does not appear to be associated with the EMCC. In both 1998 and 2000, *Alexandrium* cells are not present in high concentrations near the frontal region separating the eastern and western GOM, as would be expected if dinoflagellates consistently congregate in frontal regions as Seliger et al. (1981) observed.

SeaWiFS cruise composites (Figure 3.2a-e) show high chlorophyll concentrations along the coast and near the frontal region which separates the eastern and western GOM

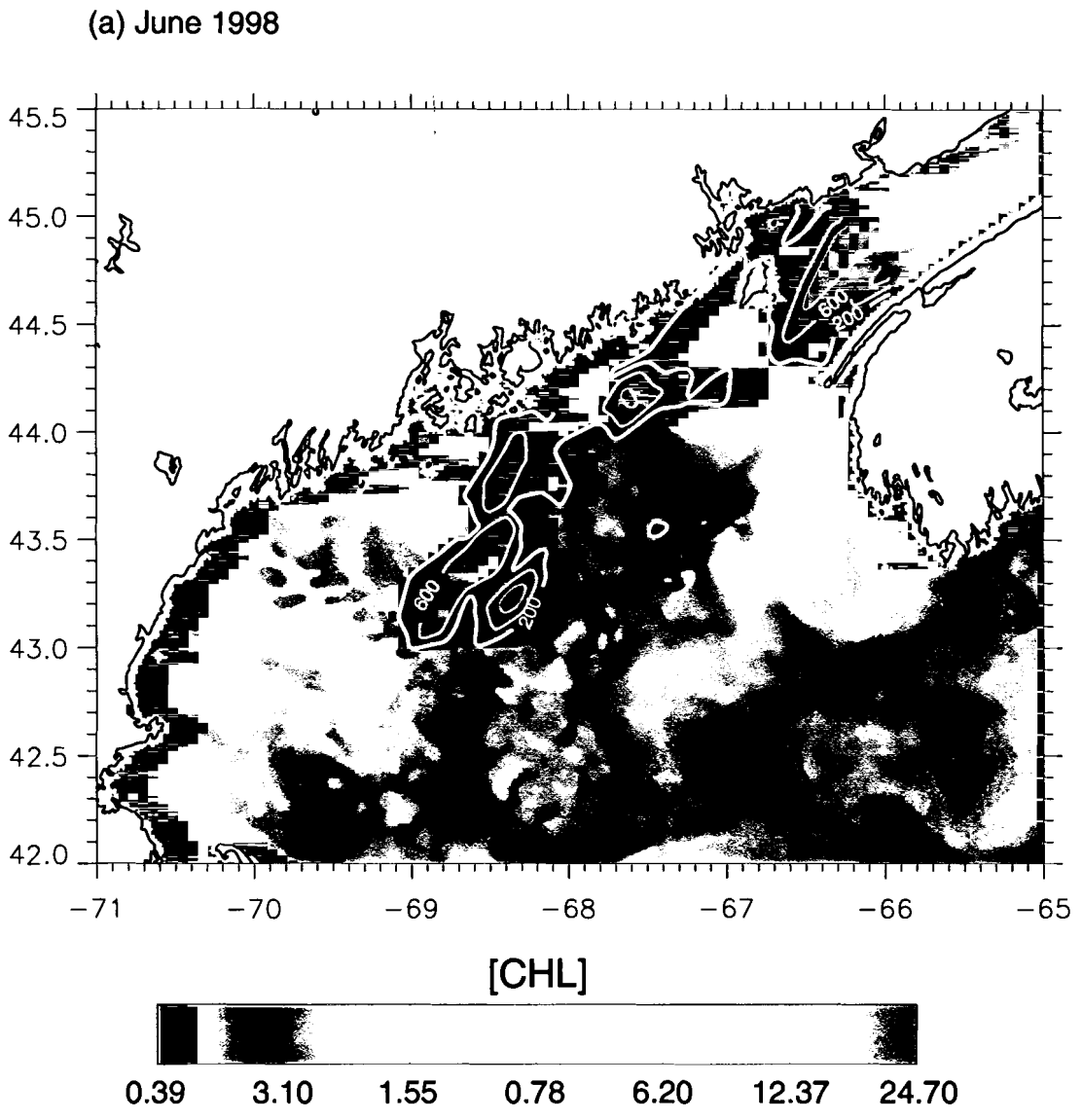


**Figure 3.2.** SeaWiFS chlorophyll cruise composites with surface *Alexandrium* concentration (cells/L) contours overlaid for (a) June 1998, (b) July 1998, (c) August 1998, (d) May 2000, and (e) June 2000.

(b) July 1998

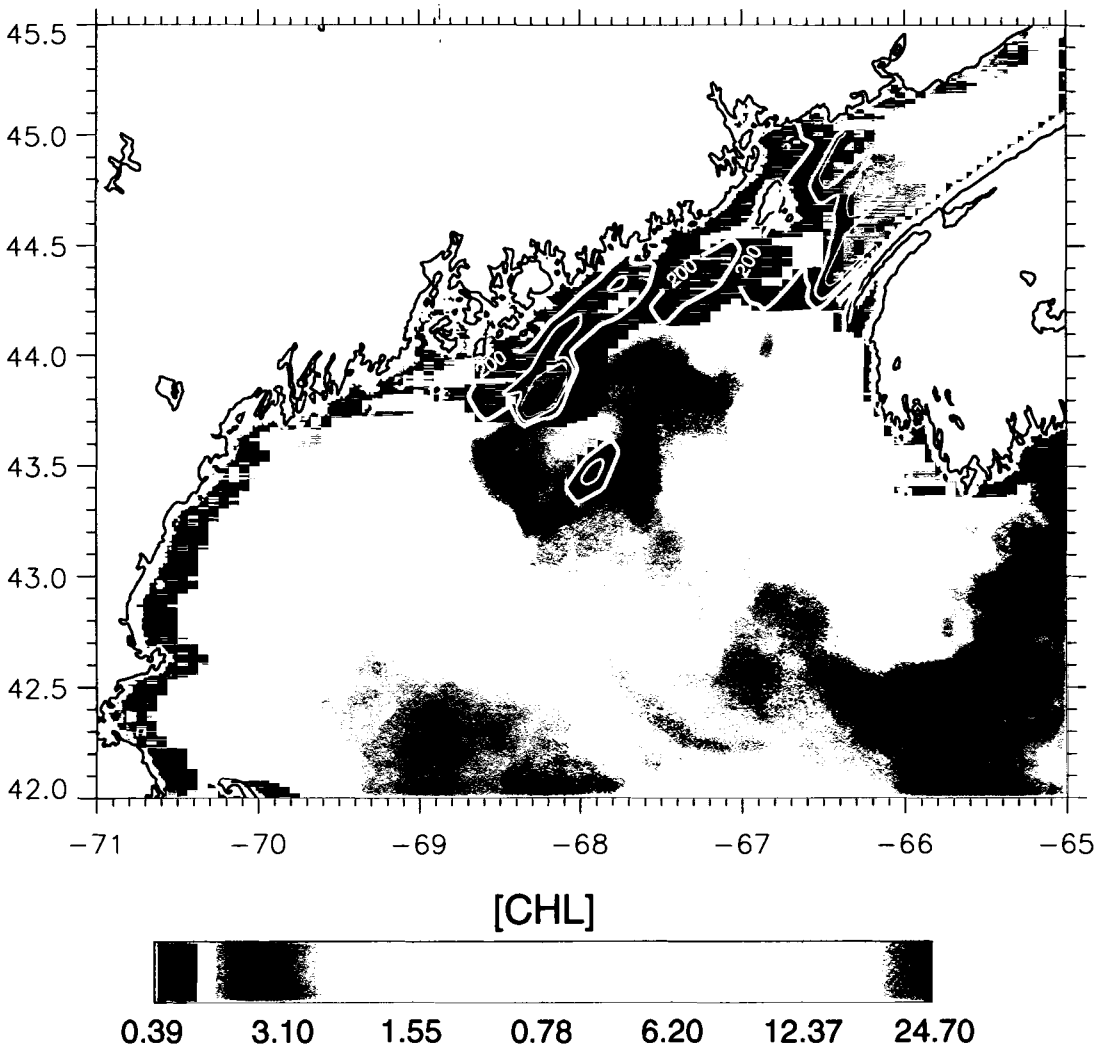


**Figure 3.2.** Continued

(c) August 1998

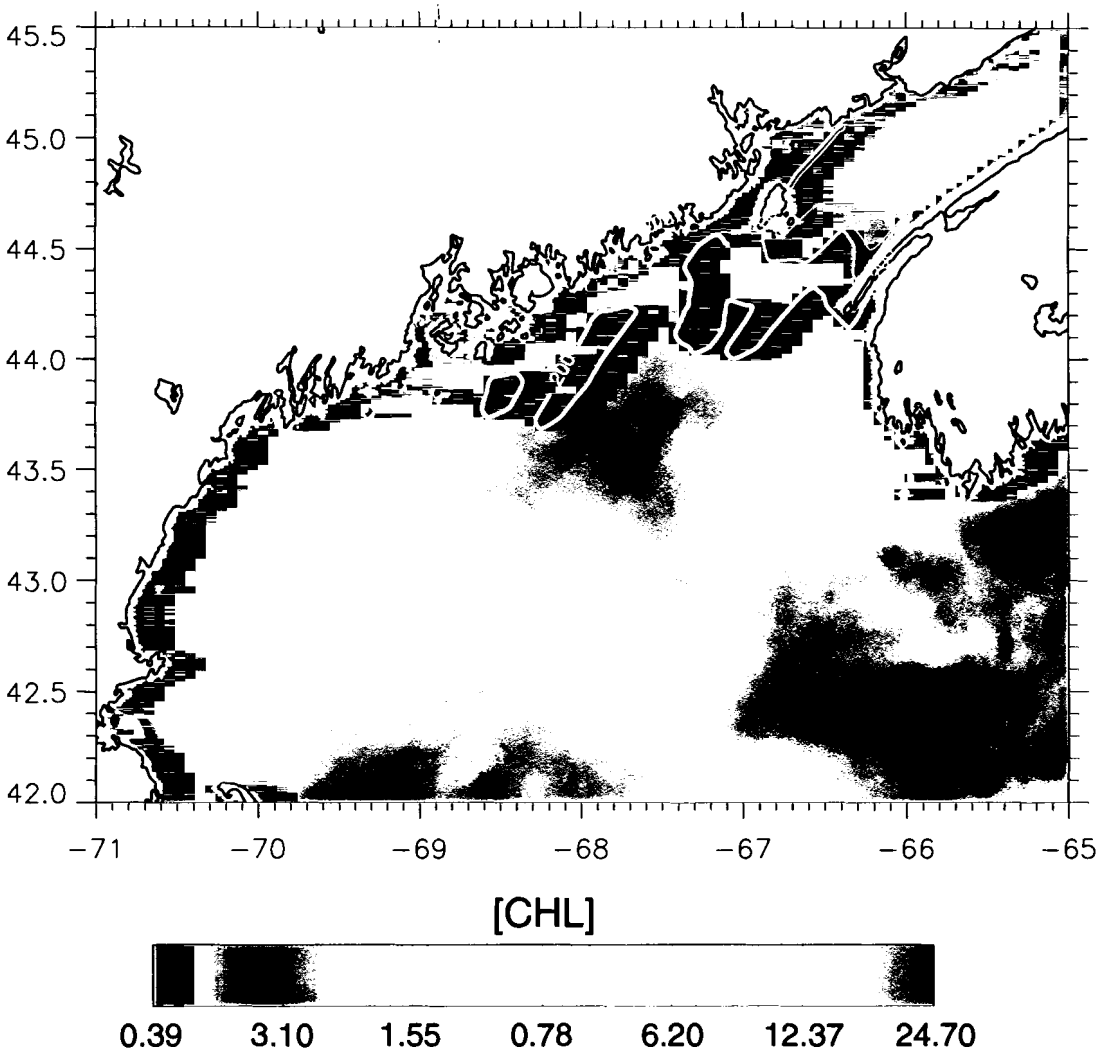


**Figure 3.2.** Continued

(d) May 2000

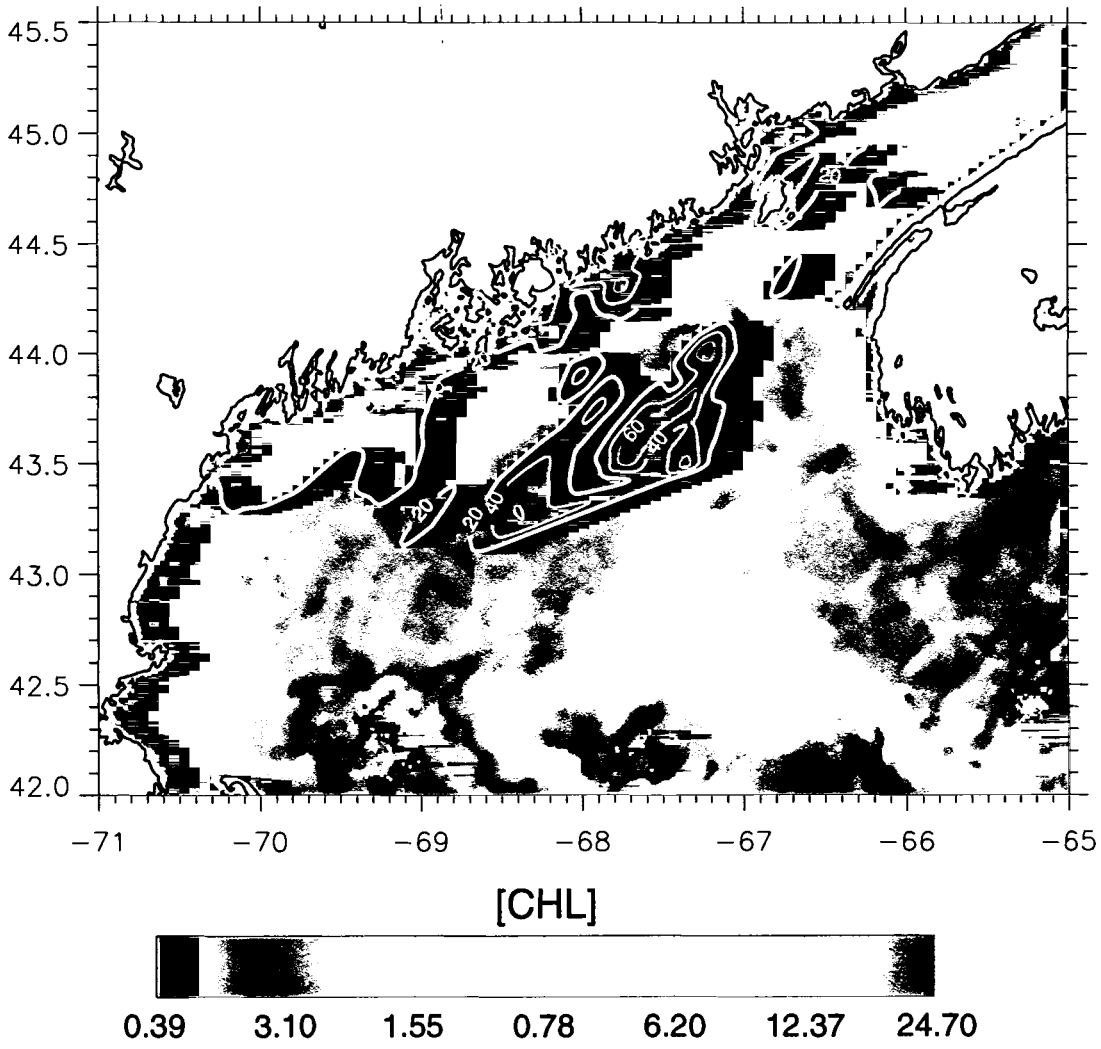


**Figure 3.2.** Continued

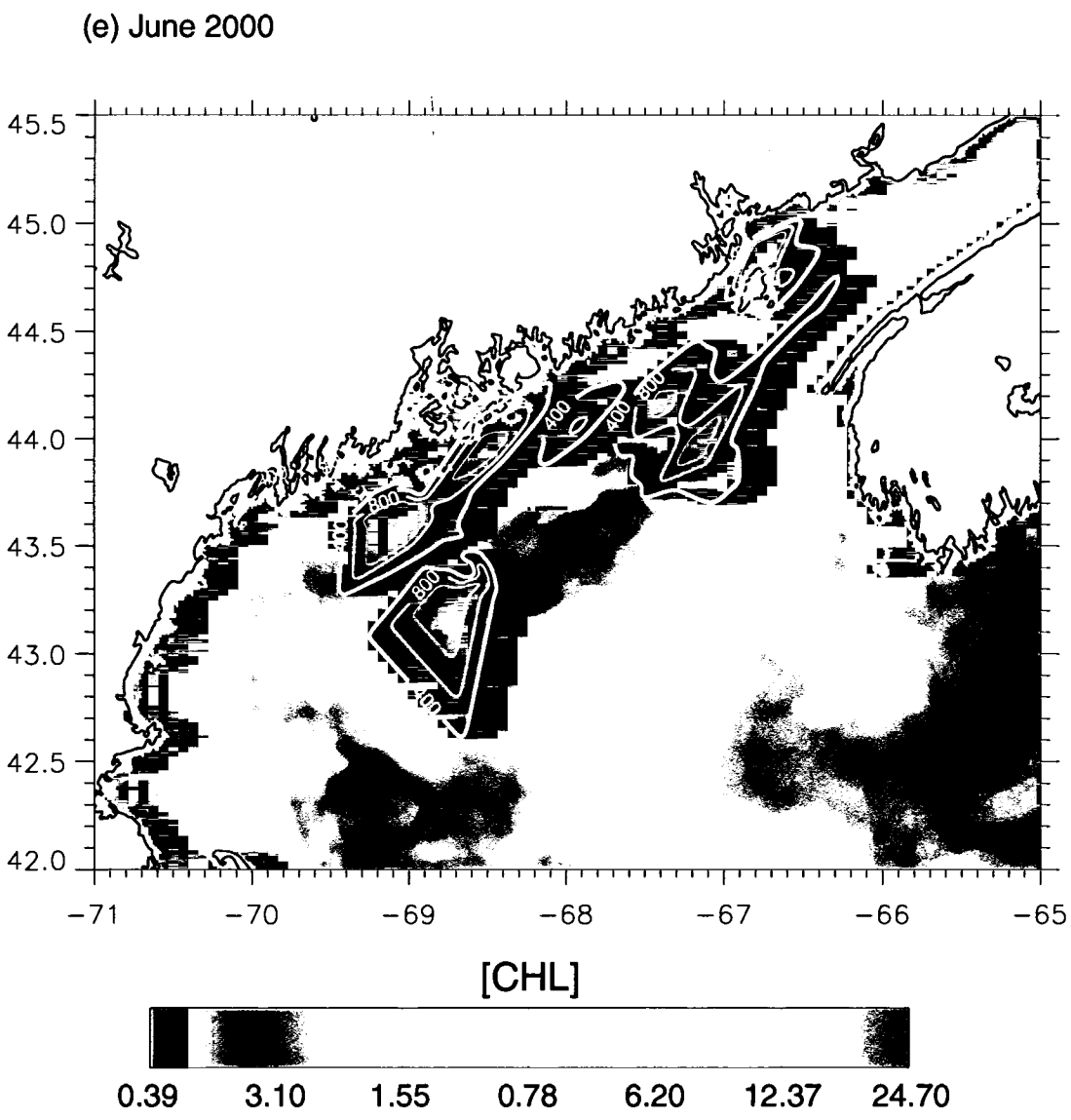


**Figure 3.2.** Continued

(see Figures 3.1a-e for exact location). Contours of *Alexandrium* concentration superimposed on these images show that cells are generally not found in high concentrations within areas of high chlorophyll. The decreased abundance of *Alexandrium* cells in the high chlorophyll regions indicates two things. First, *Alexandrium* is not the dominant chlorophyll pigment contributor to the signal detected by the SeaWiFS sensor and, second, that the dinoflagellate *Alexandrium* attains a competitive advantage in differing environmental conditions than diatoms (the major component of the SeaWiFS chlorophyll signal) and, therefore, tends to accumulate where overall chlorophyll concentrations are lower. Townsend et al. (2001) also observed that high chlorophyll regions were located shoreward of elevated *Alexandrium* concentrations in the GOM.

The distribution of other ship-measured parameters may also be important in the ecology and resulting spatial distribution of *Alexandrium* in the GOM. Nitrate, phosphate, and silicate were contoured over both the AVHRR SST and SeaWiFS chlorophyll composites for all five cruise periods. Qualitatively, contours of surface nutrient concentrations show a strong negative relationship to AVHRR SST, but no obvious relationship to SeaWiFS chlorophyll.

With the exception of May 2000, surface distributions of these nutrients were relatively consistent over each of the cruise periods. For this reason, Figure 3.3a-c shows only the June 1998 nutrient contours over the AVHRR SST composites. Elevated nitrate/nitrite distributions follow the surface temperature pattern of the EMCC with the highest concentrations in the cold core along the eastern Maine shore. This relationship arises because the EMCC is tidally well-mixed, forcing high nitrate and nitrite

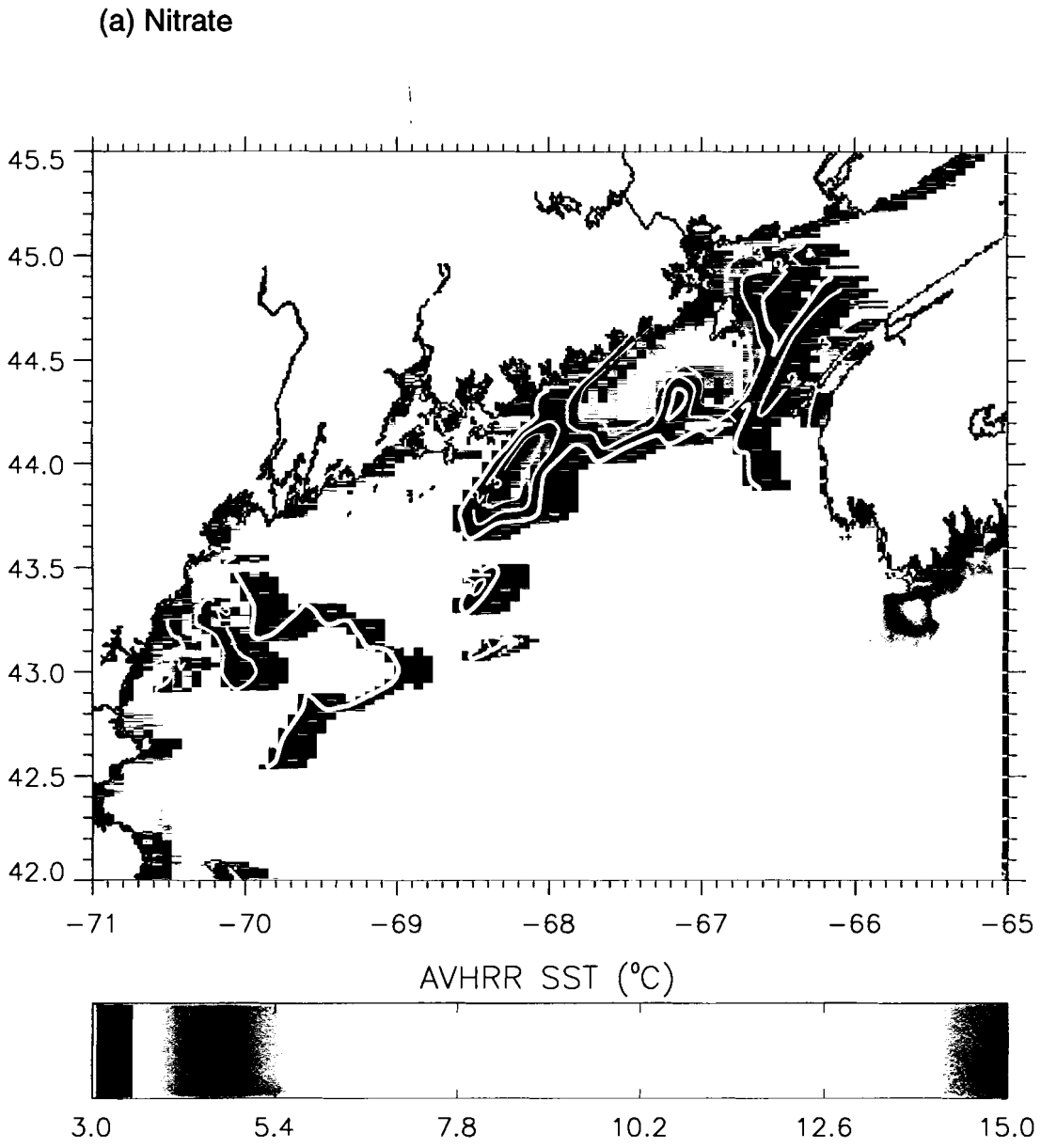


**Figure 3.3.** AVHRR SST cruise composites with surface *in situ* nutrient concentration (μg/L) contours overlaid; (a) nitrate , (b) silicate, and (c) phosphate.

(b) Silicate

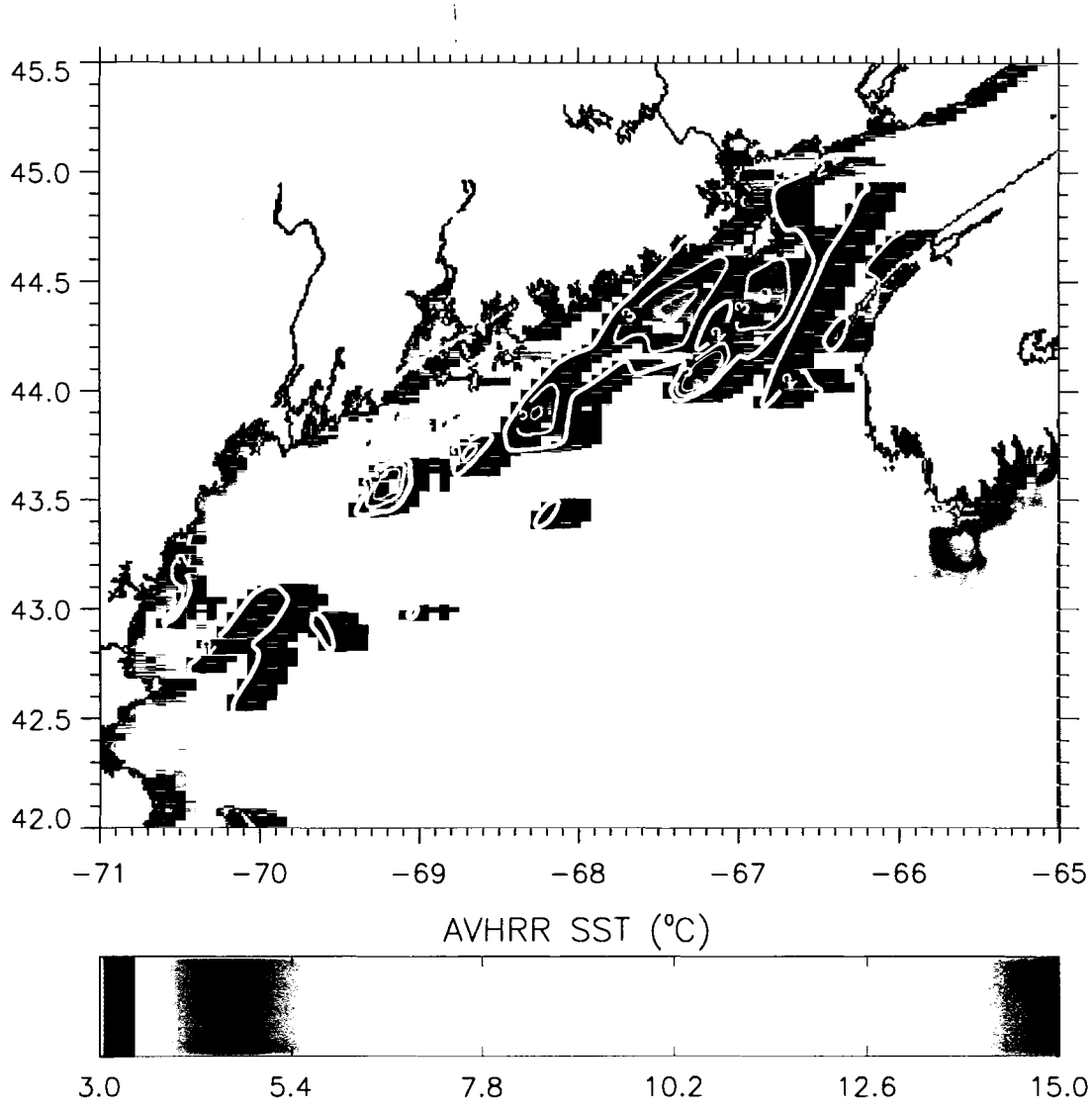


**Figure 3.3.** Continued

(c) Phosphate

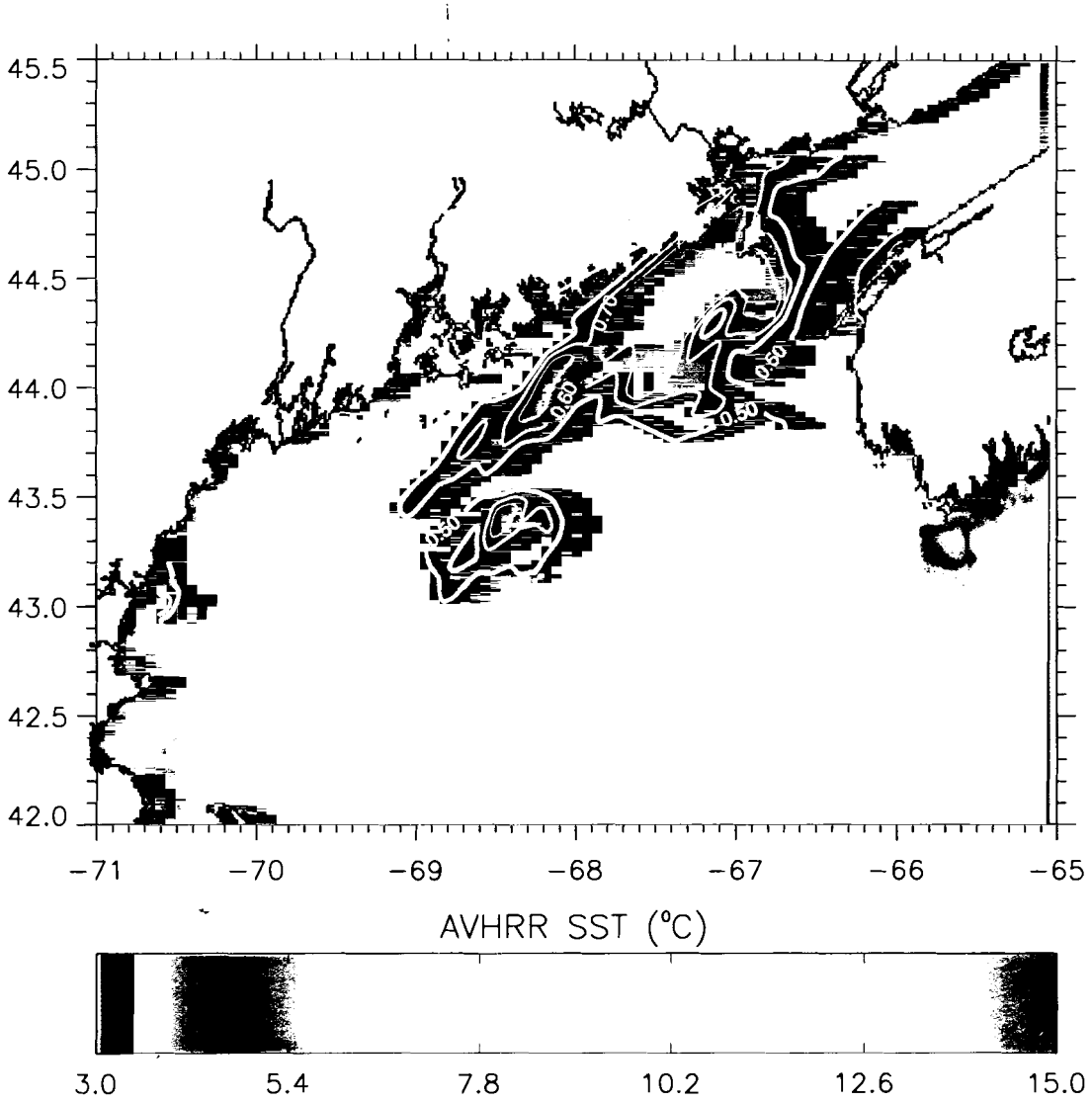


**Figure 3.3.** Continued

concentrations to the surface (Brooks and Townsend, 1989). While the distributions of *Alexandrium* show offshore populations, the nitrate distributions do not extend offshore. Concentrations of all nutrients decrease as the summer progresses, possibly due to uptake by phytoplankton. Silicate and phosphorus (Figure 3.3.b,c) have similar distributions except in May 2000.

In May 2000 the distribution of phosphate is similar to that of *Alexandrium*; uniformly low concentrations over the entire GOM. Nitrate, though, follows a pattern similar to the other cruise periods, with highest concentrations close to shore in eastern Maine. Silicate concentrations are highest along the entire coast of Maine, decreasing with increasing distance offshore, similar to the distribution of chlorophyll according to the SeaWiFS image for the cruise period. Concentrations of nutrients in May 2000 are higher than in any other cruise period, likely due to winter mixing and the data relative to seasonal hydrographic development. The distribution of nutrients in the GOM are those described by Townsend et al. (2001) presented in a manner which allows direct comparison to satellite-measured patterns.

Qualitatively, the nutrient data contoured over the SeaWiFS cruise composite images show little relationship between surface distributions of nutrients and the spatial patterns of chlorophyll in the GOM as measured by SeaWiFS. Surface nutrient distribution patterns are more similar to that of *Alexandrium* than that of chlorophyll concentrations. In the summer, increased (decreased) surface nutrients are associated with areas of decreased (increased) chlorophyll concentrations suggesting active uptake of nutrients by phytoplankton. These findings are consistent through each of the 1998 and the June 2000 cruise periods.

Measurements made early in the season (May 2000), however, show concentrations of all three nutrients are highest nearshore, associated with high chlorophyll concentrations. One explanation is that early in the season surface nutrients have not yet been depleted. It is also possible that the similar patterns at this time of year may be a result of nutrient loading due to increased runoff into coastal waters. This runoff could also cause an increase in colored organic material and suspended sediments which could lead to an overestimation of chlorophyll by SeaWiFS in coastal regions.

### 3.2. Two Dimensional SST Gradients

Qualitative examination of satellite patterns and *Alexandrium* distributions (Figure 3.1a-e) suggest that frontal zones may play a role as boundaries to the distribution of *Alexandrium* within the EMCC. Frontal areas can be identified in satellite SST images as cold, tidally mixed water adjacent to warm, stratified water (Yentsch and Garfield, 1981). SST spatial patterns transformed into two-dimensional SST gradient images (Figures 3.4 a-c) (see Chapter 2) revealed two major frontal systems in the ECOHAB study area in the 1998 cruise composites. First, strong fronts form inshore and offshore of the EMCC. Pettigrew et al. (1998) also observed the front on the offshore side of the EMCC that forms because of the intense tidal mixing over the eastern Maine shelf. The second system is a large front that developed just south of Penobscot Bay as the summer progressed in 1998. This front forms a boundary between the EMCC and the stratified western GOM surface water (Xue et al., 2000). In 2000, the May (Figure 3.3d) gradient image does not show any distinct fronts, due to the presence of relatively well-mixed waters throughout the GOM. Later in the season (June 2000), as stratification in the

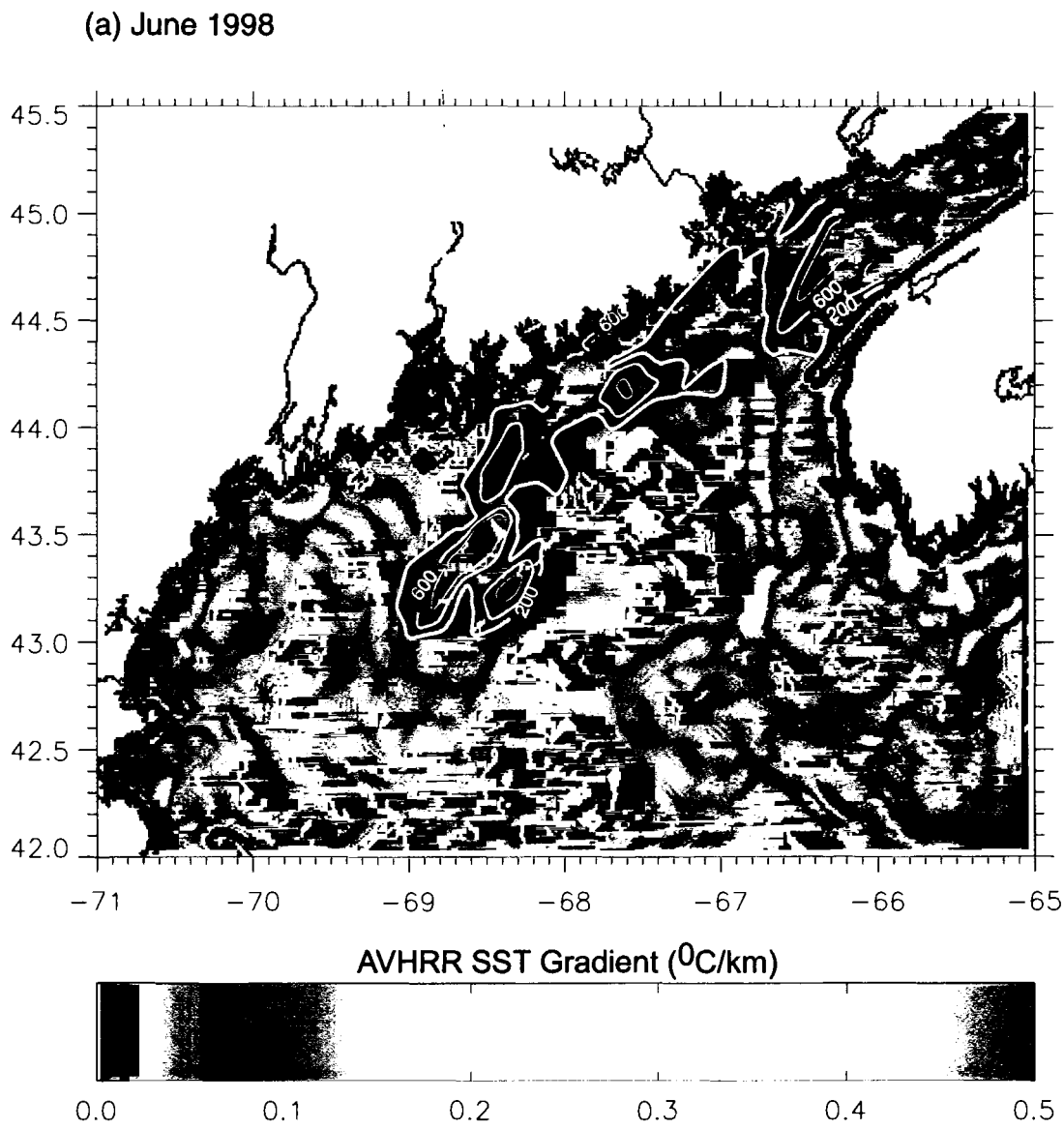


**Figure 3.4.** Two-dimensional SST gradient cruise composites with surface *Alexandrium* concentration (cells/L) contours overlaid for (a) June 1998, (b) July 1998, (c) August 1998, (d) May 2000, and (e) June 2000.

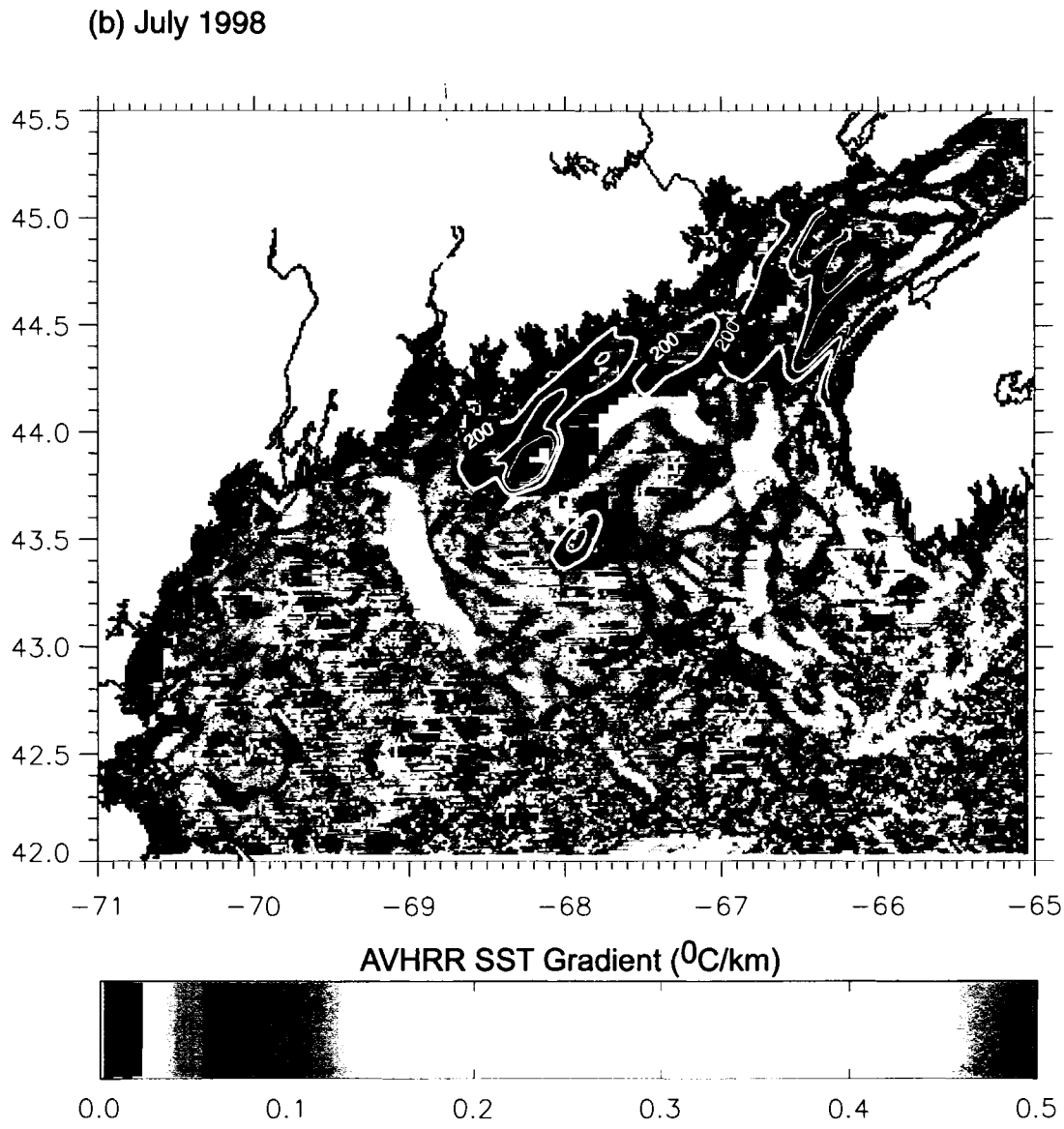


**Figure 3.4.** Continued

(c) August 1998

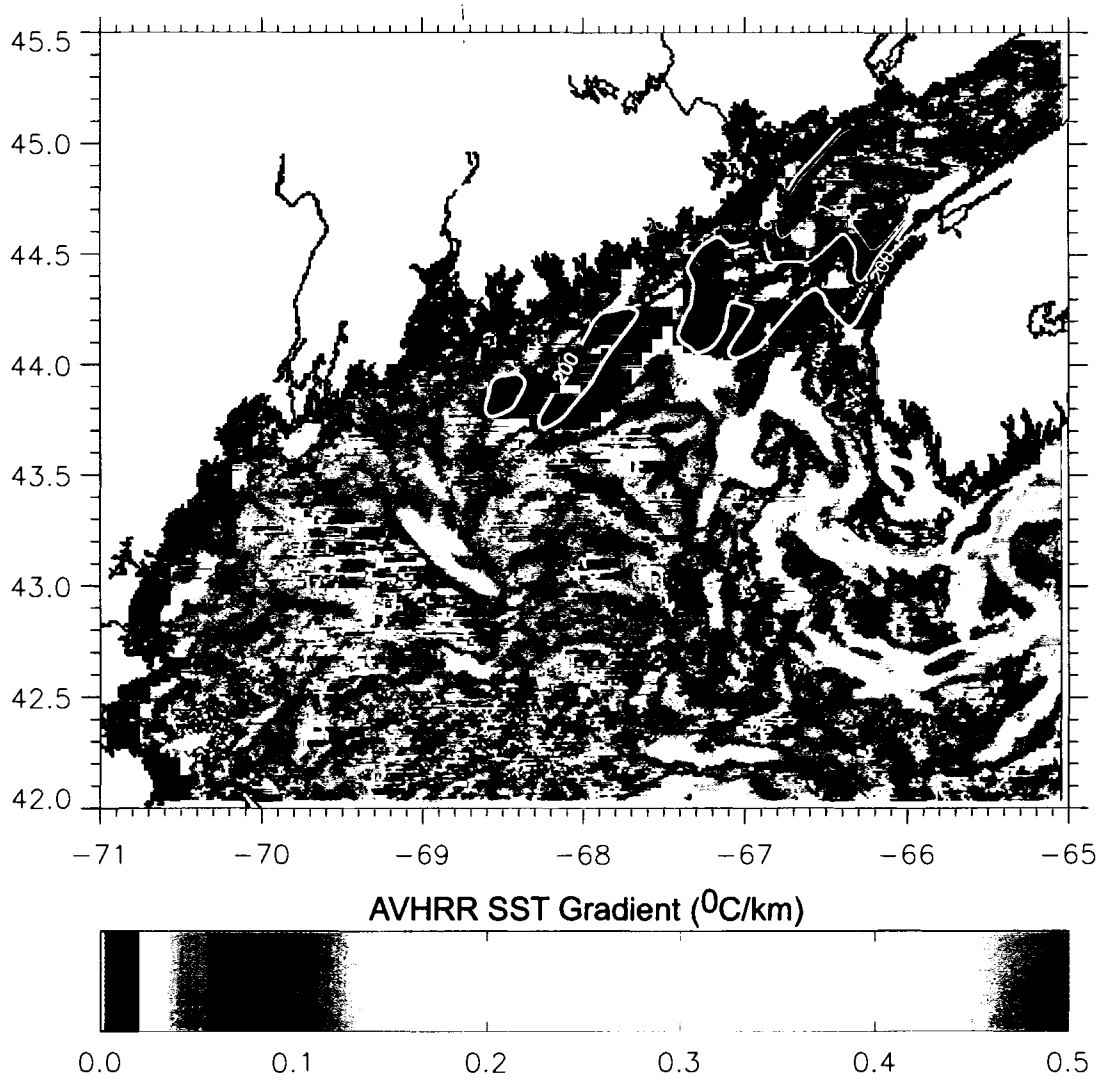


**Figure 3.4.** Continued

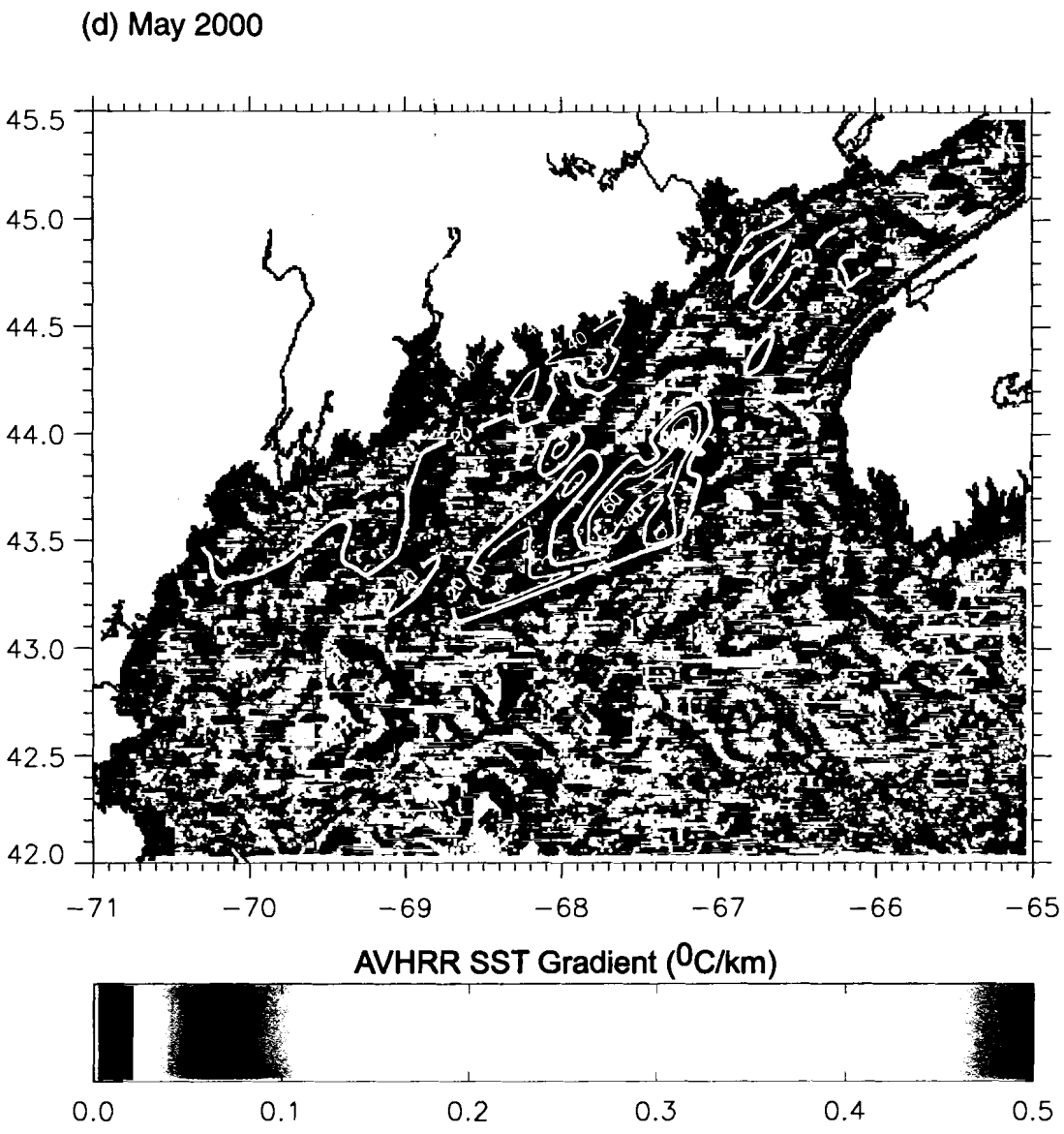


**Figure 3.4.** Continued

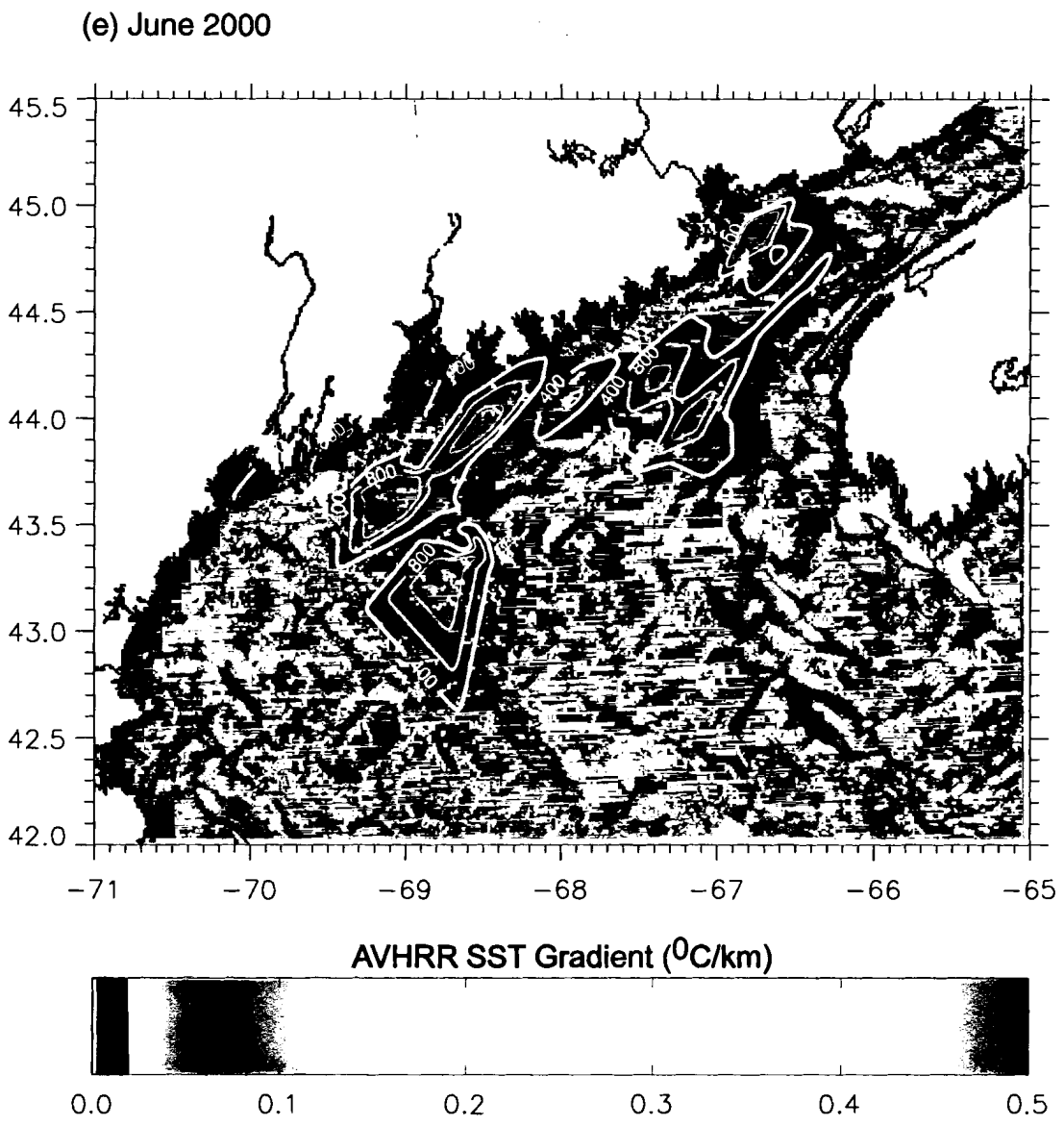


**Figure 3.4.** Continued

western GOM increases, the front separating the east and west surface water regimes develops and is seen in the cruise gradient image (Figure 3.3e). Contours of *Alexandrium* overlaid on these two-dimensional SST gradients suggest that high concentrations of *Alexandrium* are being constrained by the frontal regions defining the EMCC. In addition, the SST front just south of Penobscot Bay appears to consistently limit the east/west extent of *Alexandrium* distributions. Qualitatively, contours of *Alexandrium* on the June 2000 gradient image show a similar relationship to that of the 1998 images. These data suggest that frontal zones may play an important role in the spatial and temporal distribution of *Alexandrium* in the GOM. Significantly, satellite data are well suited to monitoring both the time, space and magnitude variability of these fronts.

### 3.3. Linear Regression Analyses

The analyses above indicate that there are qualitative relationships between satellite and *in situ* parameters that might be quantified. Linear regression analyses were conducted to determine if there are any direct correlations between the satellite data and *Alexandrium* distributions as well as other *in situ* measured parameters which may be important in their distributional ecology. Correlations that are consistently high could be used to model the spatial distribution of that parameter using readily available satellite data. This model would aid in the monitoring of blooms and bloom development in the GOM.

Prior to regression analysis, the distribution of each *in situ* parameter was tested for statistical normality. The nitrate, silicate, chlorophyll, fluorescence, and *Alexandrium*

concentrations proved not to be normally distributed and were log-transformed prior to regression with satellite data. Phosphate concentrations were normally distributed.

As a first step, satellite-measured SST and SeaWiFS chlorophyll from the cruise composites were regressed against *in situ* SST and surface chlorophyll to examine the ability of the ship data to reproduce satellite fields. The *in situ* temperature and AVHRR SST regression slope was 0.89 for June 1998, 1.19 for July 1998, 0.68 for August 1998, and 0.82 for June 2000. Each of these regressions explains over 50% of the variability in the data. In May 2000, the slope of the best-fit line was 0.34 and explained only 16% of the variability. The fact that the slope between the *in situ* and the satellite-measured SST is not one is due to the fact that the satellite measures surface skin temperature and the *in situ* measurements are of bulk temperature (<5 m below the surface) and to differences in the quantity actual sampled in space and time. These differences are also be the reason that the least-square fit regressions explain less than 100% of the variance. The *in situ* chlorophyll versus SeaWiFS chlorophyll (not LOG values) analysis for 1998 revealed slopes ranging from 0.15 in June 1998 to 0.53 in August 1998. In May 2000 the slope is -0.04 explaining 11% of the variability. In June 2000, the slope is 0.93 and explains 29% of the variance in the relationship. The deviation of the slopes in 1998 from a one-to-one relationship suggests that the NASA SeaWiFS algorithm was not doing an adequate job at predicting chlorophyll in the GOM. This could be due to an overestimate of chlorophyll in the coastal zone due to increased backscatter from other particles (not containing chlorophyll), increased absorption by CDOM, inadequate atmospheric correction or the mismatch of the *in situ* data with the satellite data in time and space.

Regressions of *in situ* surface *Alexandrium* with AVHRR SST showed a negative linear relationship over the five cruise periods that may be useful in creating a model of LOG*Alexandrium* distribution in the GOM from AVHRR SST data. Over all the cruises in 1998, a least squares fit to the data explained close to 50% of the variability in the log-transformed data; 48% in June (Figure 3.5.), 57% in July, and 59% in August. In 2000 the regression explains less of the variability; 15% in May 2000 and 14% in June 2000.

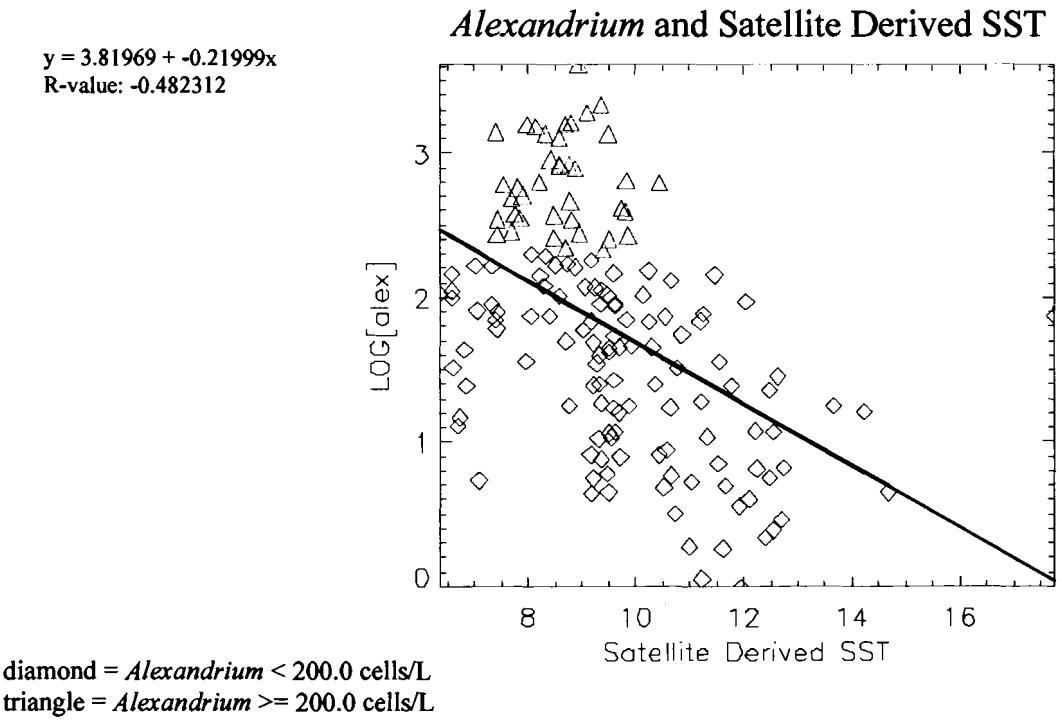


**Figure 3.5.** Plot of LOG*Alexandrium* (cells/L) versus AVHRR SST (°C) for the entire GOM for the June 1998 cruise. Sampling stations with *Alexandrium* concentrations above 200 cells/liter are represented in red triangles, showing the temperature range in which most *Alexandrium* are present.

The results of the linear regression analysis also showed consistent values for the slope and y-intercept of the least-squares fit line over the cruise periods in 1998. June regression coefficients were then applied to the July 1998 cruise SST composite in an attempt to model the distribution of LOG*Alexandrium* in the GOM. Figure 3.6.a shows

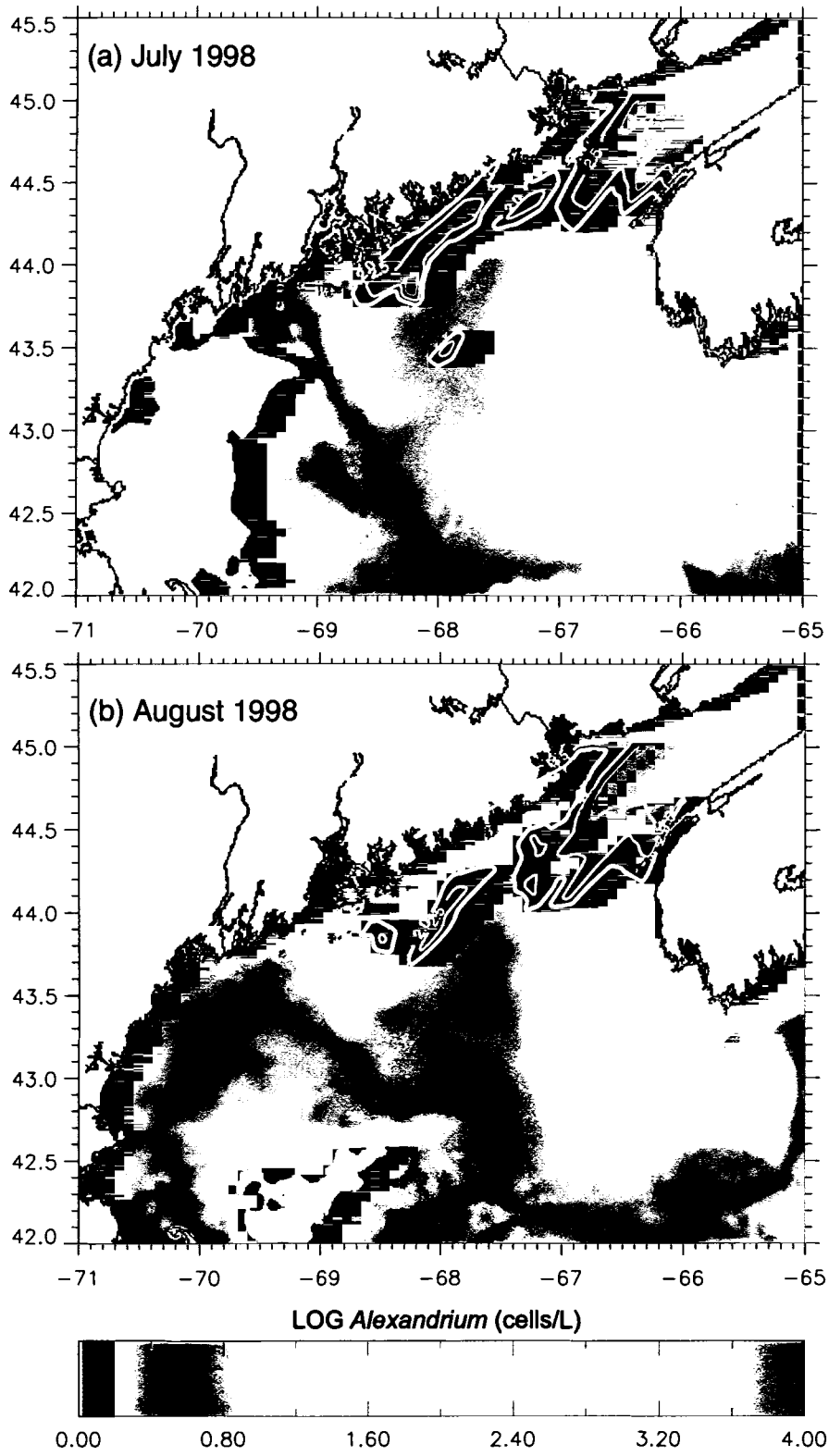


**Figure 3.6.** Modeled surface LOG*Alexandrium* cell distributions (cells/L) derived from linear regression results. June 1998 and July 1998 results are applied to (a) July 1998 and (b) August 1998 AVHRR SST cruise composites, respectively. Actual surface LOG*Alexandrium* concentrations (cells/L) from the same cruise period are overlaid.

the modeled distribution with contours of actual surface LOG*Alexandrium* concentrations for July 1998 superimposed and Figure 3.6.b shows the modeled distribution of LOG*Alexandrium* for August 1998, created from July 1998 regression coefficients, with the actual surface LOG*Alexandrium* cell densities superimposed. As expected, this simple model appears to do a good job of predicting elevated *Alexandrium* concentrations in the EMCC, but does not capture the offshore populations at all. Note also that the prediction of high *Alexandrium* concentrations on the Scotian Shelf cannot be verified as the survey cruises had no stations in that region in 1998. The model also does a good job of forecasting the low concentrations of *Alexandrium* in the western GOM. The prediction does well in terms of magnitude, predicting LOG*Alexandrium* concentrations on the order of 2 cells/L consistent with the contours. Predicted distributions do not, however, capture detail regarding the larger cell densities in the core of the EMCC. Regressions do not work well in the late spring (May 2000) when *Alexandrium* concentrations are uniformly low over the entire GOM and the SST dynamic range is low, explaining only 15% of the variability.

Regressions of *Alexandrium* concentration and AVHRR SST from both 1998 and 2000 also consistently show a group of stations (red triangles indicate *Alexandrium* concentrations >200 cells/liter in Figure 3.5.), suggesting that highest surface *Alexandrium* concentrations are found within an intermediate temperature range. The minimum and maximum values of this range increase as the summer progresses. In June 1998, this range is 8-10°C, in July 1998 the range extends to 8-12°C, and by August 1998 the range increases to 10-14°C. In May and June 2000 the ranges are 5-8°C and 11-

14°C, respectively. Although not pursued further here, these results are a potentially useful link between Alexandrium distributions and satellite data.

Correlation coefficients from the regression of SeaWiFS chlorophyll and *Alexandrium* concentrations are low (maximum of 0.20 in August 1998). The low correlations support the earlier suggestion that *Alexandrium* do not co-vary with the main population of diatoms, the dominant contribution to the signal measured by the SeaWiFS sensor.

Table 3.1 summarizes the correlations of *Alexandrium* and satellite data.

| Cruise | X,Y | Y intercept | Slope | R-value |
|---|---|---|---|---|
| June 1998 | AVHRR, *Alexandrium* | 3.87 | -0.23 | -0.48 |
| July 1998 | AVHRR, *Alexandrium* | 3.90 | -0.19 | -0.57 |
| August 1998 | AVHRR, *Alexandrium* | 4.78 | -0.23 | -0.59 |
| May 2000 | AVHRR, *Alexandrium* | 0.55 | 0.10 | 0.15 |
| June 2000 | AVHRR, *Alexandrium* | 1.40 | 0.08 | 0.14 |
| June 1998 | SeaWiFS, *Alexandrium* | 1.78 | 0.27 | 0.15 |
| July 1998 | SeaWiFS, *Alexandrium* | 1.56 | 0.38 | 0.04 |
| August 1998 | SeaWiFS, *Alexandrium* | 1.56 | 0.08 | 0.20 |
| May 2000 | SeaWiFS, *Alexandrium* | 1.16 | -0.007 | -0.002 |
| June 2000 | SeaWiFS, *Alexandrium* | 2.64 | -0.67 | -0.20 |

**Table 3.1.** Correlation results from regression analyses using satellite data and *in situ* surface *Alexandrium* concentrations for the entire GOM for all cruise periods. Note that *Alexandrium* and SeaWiFS chlorophyll concentrations are LOG concentrations.

The literature documents numerous instances of hydrographic and oceanographic parameters correlated with blooms of harmful phytoplankton (Holligan et al., 1983; Satsuki et al., 1989; Sullivan et al., 1993; Keafer and Anderson, 1993; Yentsch, 1989; Uno and Yokota, 1989; Tester and Stumpf, 1998; Goes et al., 1999). If similar linkages can be demonstrated in the GOM and these parameters can be modeled with satellite data, improved space and time predictions and/or extrapolations might be made. Townsend et al. (2001) suggest that surface nutrients might be important in determining *Alexandrium* distributions in the GOM. Morin et al. (1993) successfully estimated surface nitrate in a tidal front using a regression relationship to satellite-derived SST. They caution that the first order relationship they use will only work under specific conditions. For example, areas of strong advective diffusion might not show good relationships. In these areas, high surface nitrate concentrations (associated with cold, upwelled or mixed waters) are transported downstream and if biological uptake is slow the nitrate-rich surface waters will warm, destroying the linear relationship. Satellite-derived SST data were regressed with *in situ* surface nitrate measurements (Table 3.2.). In June 1998 the regression shows little relationship. In July and August 1998, however, SST explains over 50% of the variability in the nitrate data. These results suggest that satellite SST data could be used to model nitrate distributions in the GOM, another contribution that satellite data might provide to the understanding and/or monitoring of *Alexandrium* distributions.

| Cruise | X,Y | Y intercept | Slope | R-value |
|---|---|---|---|---|
| June 1998 | AVHRR SST, nitrate | 0.30 | -0.04 | -0.16 |
| July 1998 | AVHRR SST, nitrate | 2.24 | -0.22 | -0.59 |
| August 1998 | AVHRR SST, nitrate | 2.43 | -0.21 | -0.65 |
| May 2000 | AVHRR SST, nitrate | 1.47 | -0.13 | -0.51 |
| June 2000 | AVHRR SST, nitrate | 0.97 | -0.16 | -0.30 |

**Table 3.2.** Correlation results from regression analyses using LOG *in situ* surface nitrate and AVHRR SST for the entire GOM for all cruise periods.

Therriault et al. (1985) suggest that freshwater runoff, resulting in low salinity, high temperature, and high nutrients as well as an increased stability of the water column, is beneficial to the growth of dinoflagellates. Holligan (1985) found that the steepness of the pycnocline ultimately controls bloom development. Franks and Anderson (1992) show *Alexandrium* cells associated low salinity water from river outflow in the GOM. These results suggest that salinity may play a role in determining *Alexandrium* concentrations in the GOM. *In situ* salinity data and surface LOG*Alexandrium* concentrations were regressed. June and July 1998 show little relationship, explaining less than 40% of the variability. In August 1998 there is a better relationship, explaining 54% of the variance in the LOG*Alexandrium* data. These results indicate that at certain times of the year relationships might exist between low salinity waters and *Alexandrium* in the GOM as Franks and Anderson suggest. It is difficult, though, to separate a simple relationship of *Alexandrium* cells directly to salinity from a relationship to the structure of the water column. Temperature differences between river discharge and the waters of

the GOM often make plumes detectable in the AVHRR SST data. This possibility for AVHRR data to help monitor and predict HABs is only weakly tested here. Detailed sampling in the vicinity of river plumes would be needed to more fully explore this link.

Attempts to identify improved linear relationships by spatially isolating sub-regions (see Chapter 2) based on different hydrographic functions did not result in improved correlations with *in situ* parameters and satellite measured parameters.

All individual linear regression results are summarized in Appendix F.

### 3.4. *Alexandrium* and the EMCC

Qualitative comparisons between two-dimensional SST gradient patterns and *Alexandrium* distributions (Section 3.2) suggested high concentrations of *Alexandrium* in the EMCC were bound by frontal zones. Available *in situ* data allows an examination of the details of their relationships for comparison to the findings of Townsend et al. (2001), who observed high *Alexandrium* located within and at the frontal edges of the EMCC. This analysis compares the location of stations with high *Alexandrium* concentrations (typically >200 cells/liter) to the cross-shelf temperature structure of the EMCC to determine the consistency with which high *Alexandrium* cell densities lie within or at the frontal edges of the EMCC.

Surface temperature along the transects from just south of Penobscot Bay to Grand Manan Island were plotted and compared to stations at which surface *Alexandrium* cell concentrations were relatively high for that cruise period (>200 cells/liter in 1998, >40 cells/liter in May 2000, >300 cells/liter in June 2000). Figure 3.7 shows two example temperature transects illustrating the overall characteristics of the results.

Appendix G shows the transect plots for all the 1998 and 2000 cruises. In 1998 the transects indicate that stations with high *Alexandrium* concentrations are generally in the cold core and on the frontal edges of the EMCC, consistent with the findings of Townsend et al. (2001). In both cruises of 2000, however, stations with elevated *Alexandrium* concentrations are not exclusively in the EMCC and/or along its frontal edges. In May 2000, this could be due to the very weak frontal definition between the EMCC and the surrounding waters, since the GOM is still well mixed.

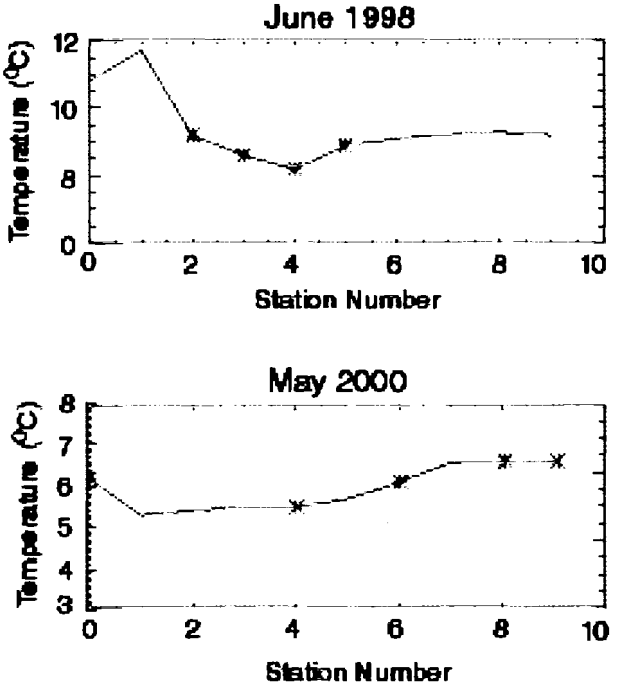


**Figure 3.7.** Examples of temperature transect plots for June 1998 and May 2000. Asterisks indicate stations along the transect where *Alexandrium* concentrations exceeded 200 cells/L for June 1998 and 30 cell/L for May 2000.

The results of this analysis are consistent with those from the previous qualitative analyses using contours of *Alexandrium* concentrations overlaid on AVHRR SST composite images and SST gradient images. Details revealed by these plots, however,

show inconsistencies in certain locations between *Alexandrium* concentration and both cross-shelf SST and its gradient. These inconsistencies are why the regressions are weak.

### 3.5. A Specific PSP Closure Case Study

In mid-May 2000, toxin concentrations greater than 80 μg/100g tissue in shellfish samples caused Maine DMR to issue a closure for all shellfish beds from the New Hampshire border to Marshall Point, Port Clyde (Hurst, personal communication, June 2000). This provided a localized, temporally specific, HAB event with concurrent AVHRR SST satellite data. The satellite images could be examined for patterns suggestive of mechanisms of advection or connection between a suspected source of *Alexandrium* cells in the EMCC and the closure area.

Townsend et al. (2001), and the data in Figure 3.1 identify elevated concentrations of *Alexandrium* in surface water of the EMCC and in offshore locations. A coastal closure in southern Maine therefore implies a mechanism for the transport of cells alongshore and onshore to the affected shellfish beds. Daily satellite SST data coincident with the May 2000 closure were examined for evidence of a surface pattern indicating onshore advection. A time series of these images bracketing the closure event is shown in Figure 3.8. In early May (May 2nd and 3rd), cold surface water continuous with that of the EMCC is observed pushing along the coast and past the mouth of Penobscot Bay. This pattern contrasts strongly with the later seasonal pattern (see Figure 3.1.) of the EMCC turning offshore. The continuous flow past Penobscot Bay is therefore capable of providing a mechanism for transporting *Alexandrium* populations from the eastern GOM to the western GOM. Evidence of surface onshore movement is

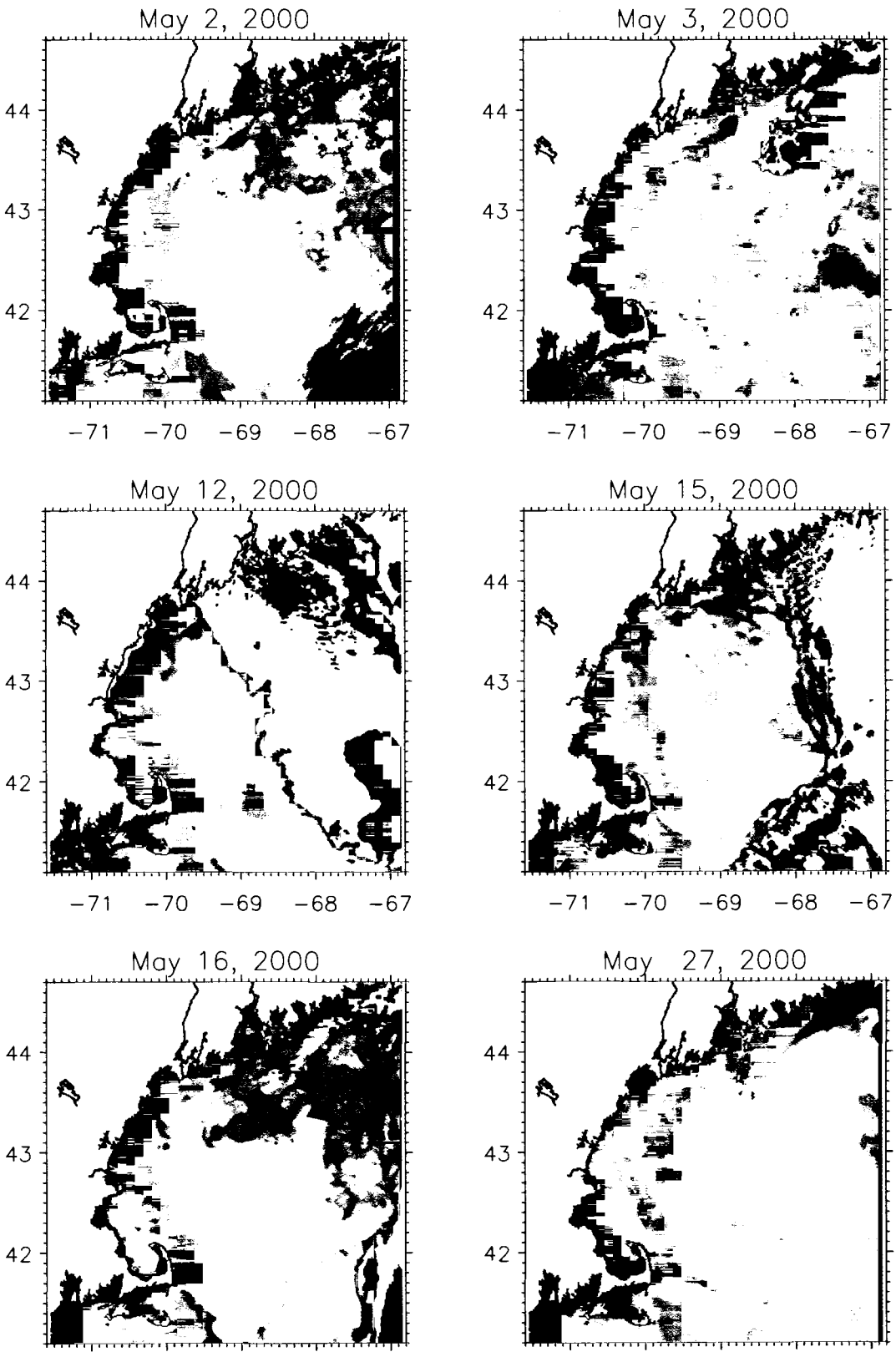


**Figure 3.8.** Time series of AVHRR SST images ($^0$C) around the time of the May 2000 closure showing the connection of the EMCC to the western GOM and Georges Bank.

also present in the satellite data. On May 12th a cold water plume from the EMCC is observed meandering inshore into close proximity of the coast near Wells Beach (Figure 3.8). This plume appears at the same time that the DMR PSP closure was imposed. These SST patterns, then, are consistent with an advective mechanism capable of transporting offshore populations of *Alexandrium* in the EMCC along the coast and, potentially causing toxicity events and shellfish bed closures in coastal areas of the western GOM. Townsend et al. (2001) also observed a filament of cold water at the end of the EMCC connecting to the coast in 1998.

Later in the month (May 15th and 16th), this shoreward meander of cold surface water disappears. At the same time, cold SST continuous with the EMCC is again observed pushing past the mouth of the Penobscot Bay. Here it continues all the way down the coast of western Maine, New Hampshire and Massachusetts and contributes to surface patterns indicative of circulation around Georges Bank (Figure 3.8). This feature is evidence of a direct transport mechanism for *Alexandrium* from the EMCC onto Georges Bank. The existence of *Alexandrium* cells on Georges Bank have been confirmed during GLOBEC field work (Townsend, personal communication, September 2001). By May 27th (at least the surface expression of) this feature is less obvious and the EMCC is observed turning offshore near Penobscot Bay.

Support for advective pathways inferred from the surface temperature patterns in the AVHRR SST data comes from two drifters deployed on April 30th, 2000 (#01915) and June 8th, 2000 (#21771) in the EMCC (J. Churchill, Woods Hole Oceanographic Institute, personal communication, July 2000). Paths of these drifters are plotted in Figure 3.9. Although not concurrent, the April drifter shows a connection of the EMCC

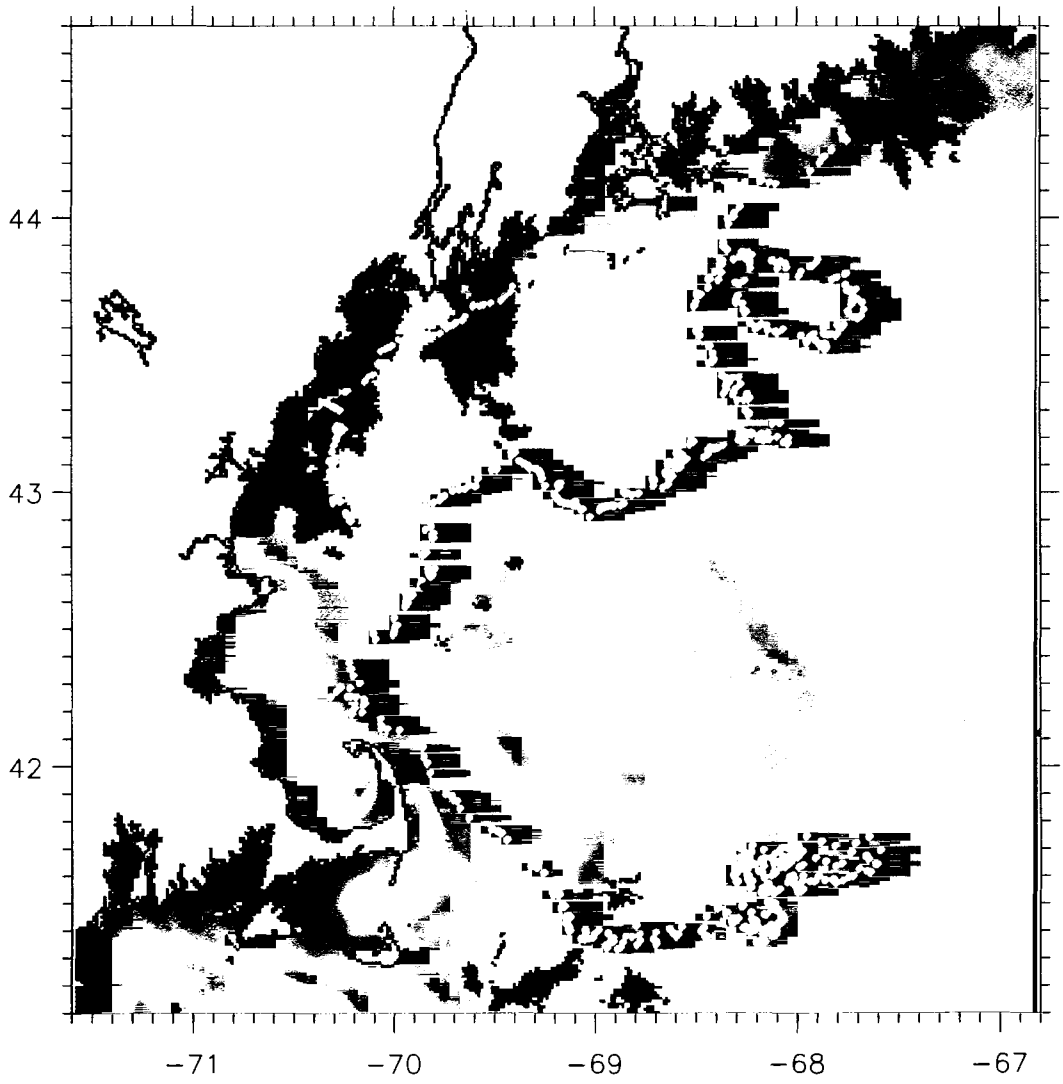


**Figure 3.9.** AVHRR SST image ($^0$C) from June 8, 2000 with drifter #01915 (white) and #21771 (pink) tracks overlaid.

to Georges Bank, confirming what was seen in the May 2000 AVHRR SST images. The June drifter followed a path past the mouth of Penobscot Bay and onshore near Wells Beach, confirming advection from the EMCC to the west and inshore to the coast.

Onshore wind-driven advection could also play a role in the transportation of an offshore population of *Alexandrium* into coastal shellfish beds through Ekman transport (Townsend et al., 2001). Franks and Anderson (1992) suggest that upwelling-favorable winds (from the southwest) push a plume of water running along the coast offshore, slowing any alongshore transport. They argue that downwelling-favorable winds (from the northeast) were found to constrict the plume close to shore and quicken the flow alongshore. Satellite-measured wind velocities from the SeaWinds instrument, a microwave scatterometer on the NASA QuikSCAT satellite are available twice daily for the May 2000 closure period. These data are delivered from the Jet Propulsion Lab to the Satellite Oceanography Data Lab at the University of Maine where they are processed and archived. These data were examined for the presence of southwesterly, downwelling-favorable winds associated with the May 2000 closure that would assist onshore transport.

Data from a six day window (four days before and two days after) around the date of the closure (yeardays 129-135 of 2000 with an ascending and descending pass each day) were examined for the presence of downwelling-favorable winds. The time series indicates downwelling favorable winds present only on May 10$^{th}$ (yearday 131), two days before the closure (See Figure 3.10.). Wind-driven onshore surface advection (and/or increased alongshore transport), consistent with the processes described by Franks and Anderson (1992) could therefore have resulted in *Alexandrium* cells being transported

from upstream and offshore locations to the coast, assuming the populations were relatively close to shore already. One day of downwelling-favorable winds would not transport the *Alexandrium* very far. The AVHRR data (Figure 3.8.) indicate that this water was continuous with cold SSTs of the EMCC.

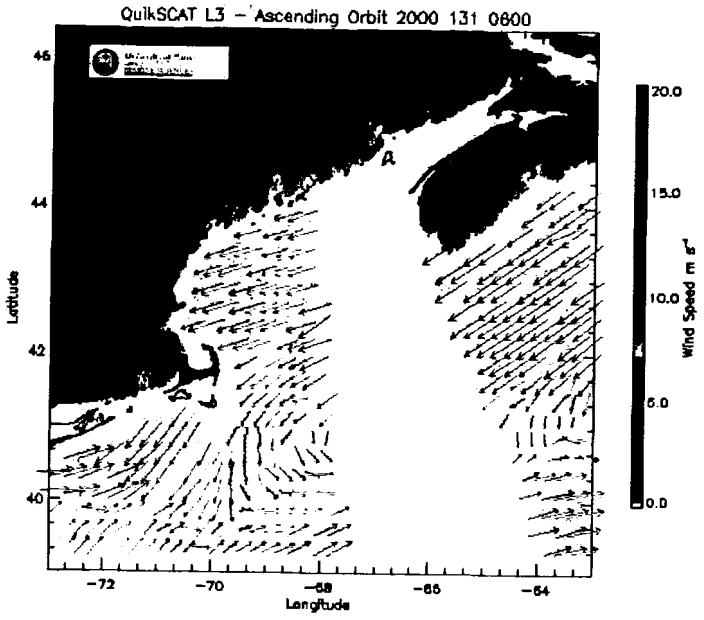


**Figure 3.10.** SeaWinds image from May 10th, 2000 (yearday 131, ascending pass) showing strong downwelling favorable winds (southwesterly) that could cause transport of toxic cells onshore and down the coast. Arrows indicate direction and magnitude of the wind. The color bar also indicates magnitude, high winds represented by red arrows and low winds represented by blue arrows.

### 3.6. GOM SST Patterns Associated with Toxicity Events

Specific oceanographic features evident in the satellite data during the May 2000 closure period suggested that SST patterns associated with surface water movement might be related to the location and/or timing of GOM PSP closures. Toxicity data (from Maine DMR) and coincident, archived Pathfinder AVHRR SST data for 1990-1999 were

used to investigate SST patterns at sampling sites where there was a high toxicity event to see if a consistent series of patterns could be observed.

The overwhelming majority of the DMR toxicity sampling stations are deep in bays and estuaries, likely quite removed and disconnected from the overall GOM circulation patterns. Small-scale, local processes are more likely to govern phytoplankton (and *Alexandrium*) ecology in these locations. The exact location of each sampling site was located on maps and charts. Five stations were subjectively chosen based on their location on points or outside bays. These stations were thought to be more exposed and therefore more strongly influenced by the large-scale circulation of the GOM.

The stations chosen reflect a focus on the western GOM, with three stations chosen in that area. One station was chosen in the eastern GOM so that the timing and amount of toxicity in both areas could be compared. One additional station was chosen in the transition area near Penobscot Bay where a front develops that is thought to restrict the flow of EMCC waters (and *Alexandrium* cells) to the western GOM. The stations are located at Ogunquit River, Cape Porpoise, Little River Kennebunkport, Pemaquid Point, and East Pond Cove (see Figure 3.11.).

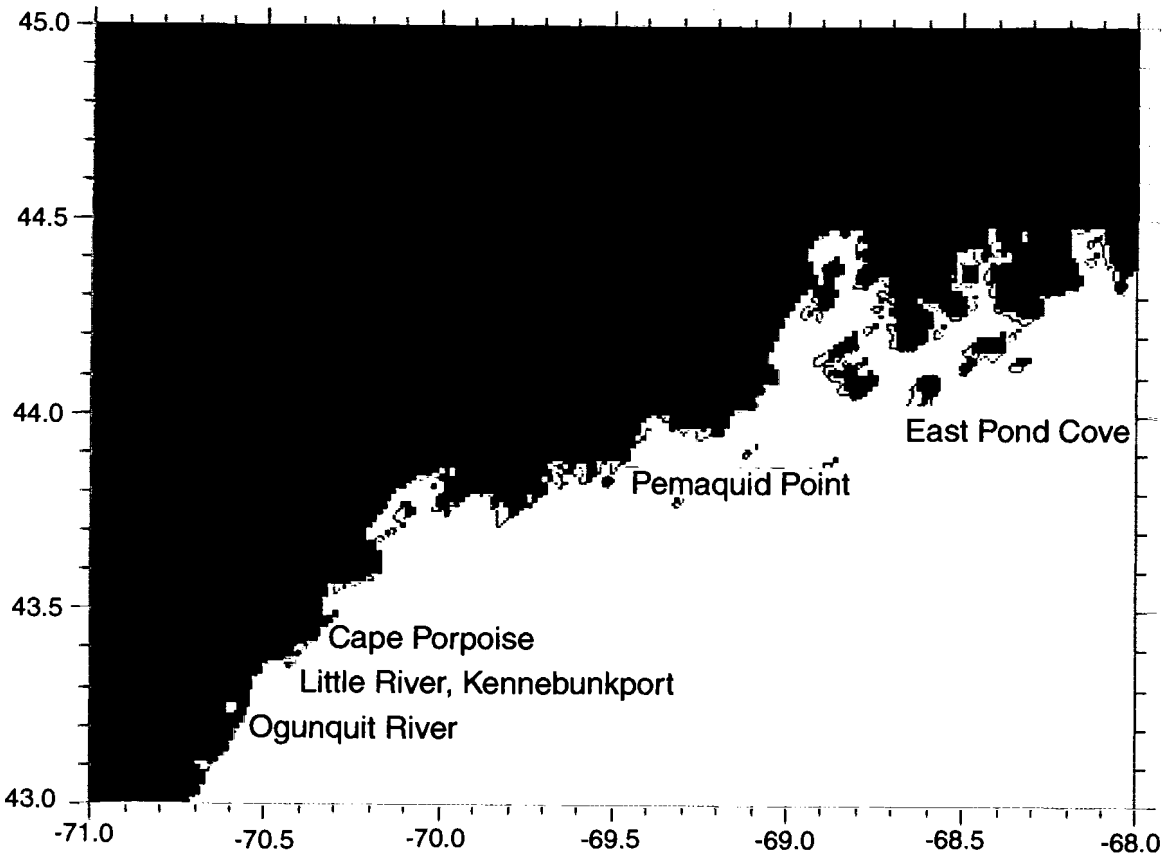


**Figure 3.11.** Map of the five stations chosen to study toxicity in the western GOM.

Toxicity was determined by the Maine DMR using mouse bioassay (see Chapter 2). The toxicity levels used in this analysis were only that of the blue mussel (*Mytilus edulis*), measured in μg toxin/100 g tissue. Time series of the toxicity level at each of the five sampling sites for all ten years were plotted (Figure 3.12a-e). These data show strong interannual variability in both the timing and magnitude of toxicity events in the GOM. In general, the data indicate that toxicity is consistently lowest at the eastern GOM station (East Pond Cove), second lowest at the central station (Pemaquid Point), and highest at the three western GOM stations (Ogunquit River, Little River Kennebunkport, and Cape Porpoise). The plots also showed that toxicity events in western GOM happen consistently earlier than toxicity events in the eastern GOM.

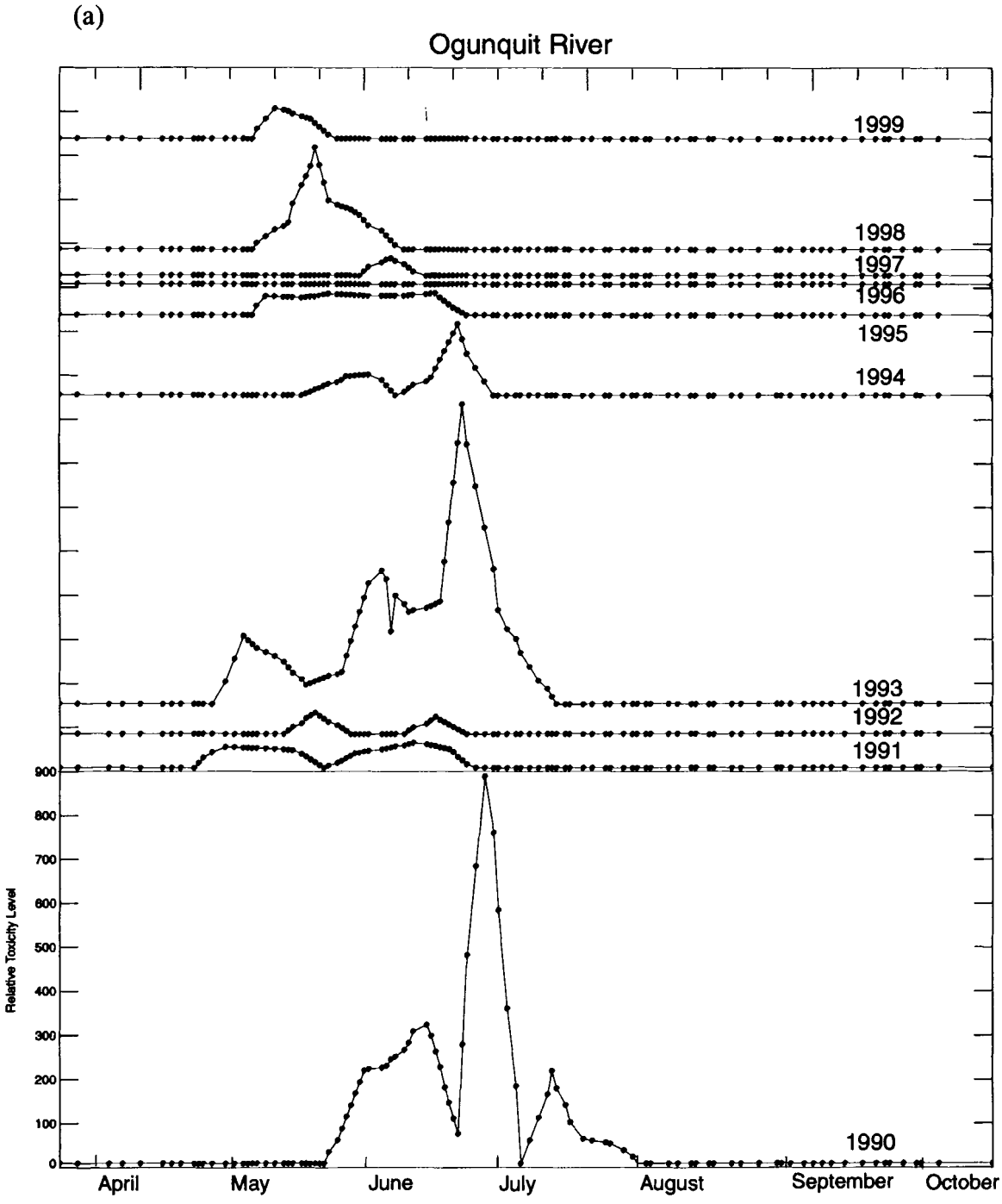


**Figure 3.12.** Timelines of relative toxicity level (μg toxin/100 g tissue) over the sampling season for all ten years of data available (1990-1999) at five DMR sampling stations; (a) Ogunquit River, (b) Cape Porpoise, (c) Little River, Kennebunkport, (d) Pemaquid Point, and (e) East Pond Cove .

(b)

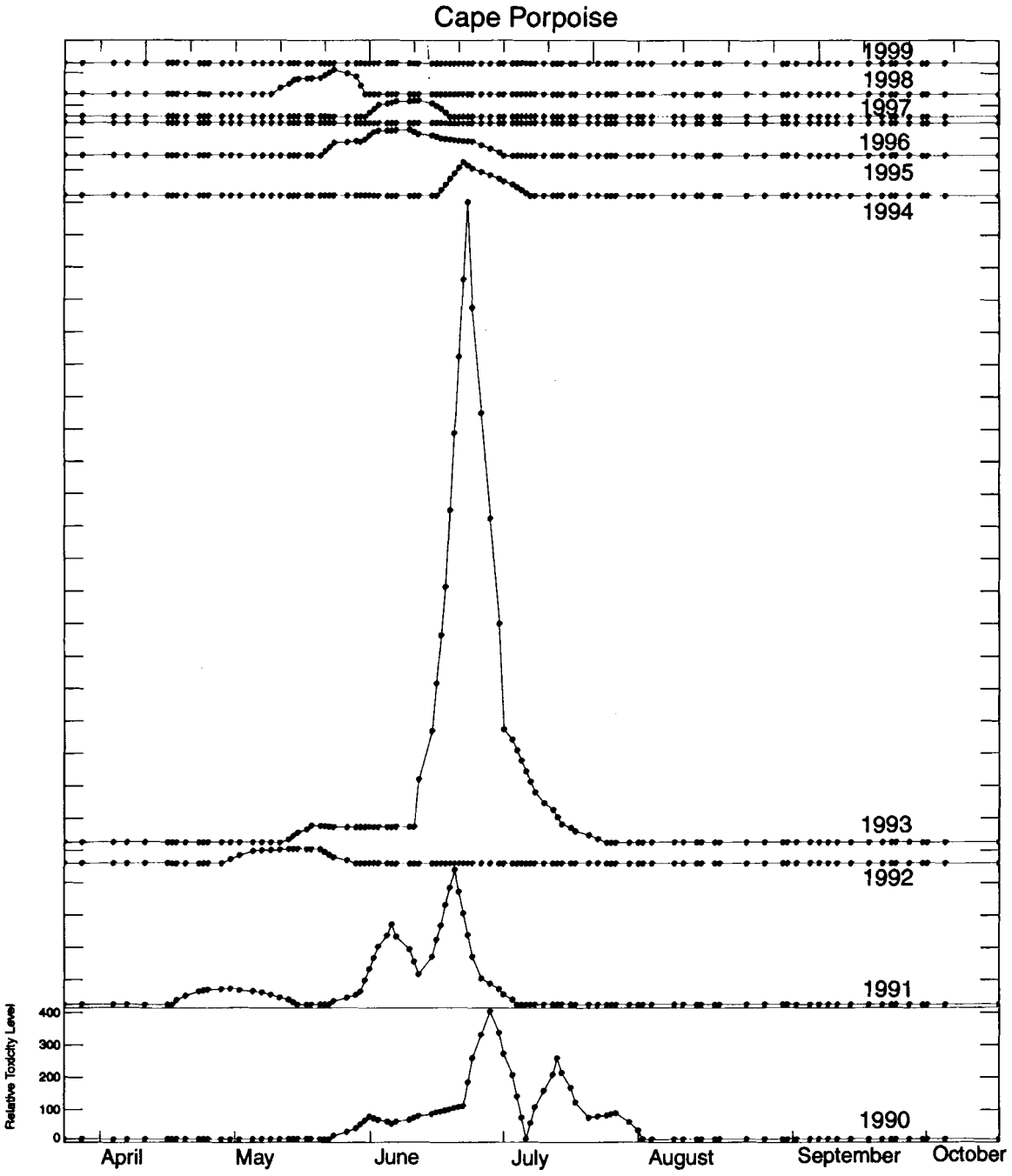


**Figure 3.12.** Continued

(c)

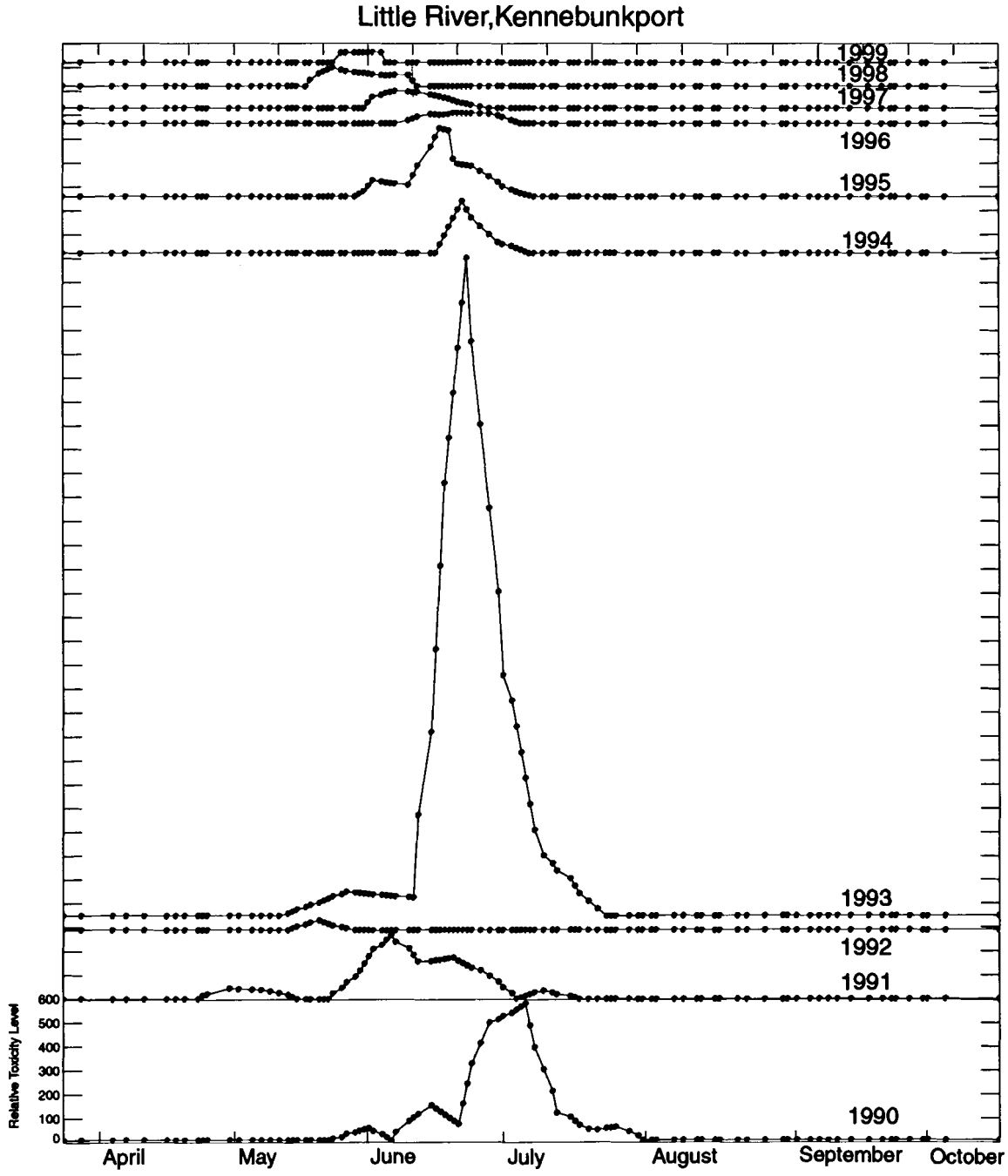


**Figure 3.12.** Continued

(d)

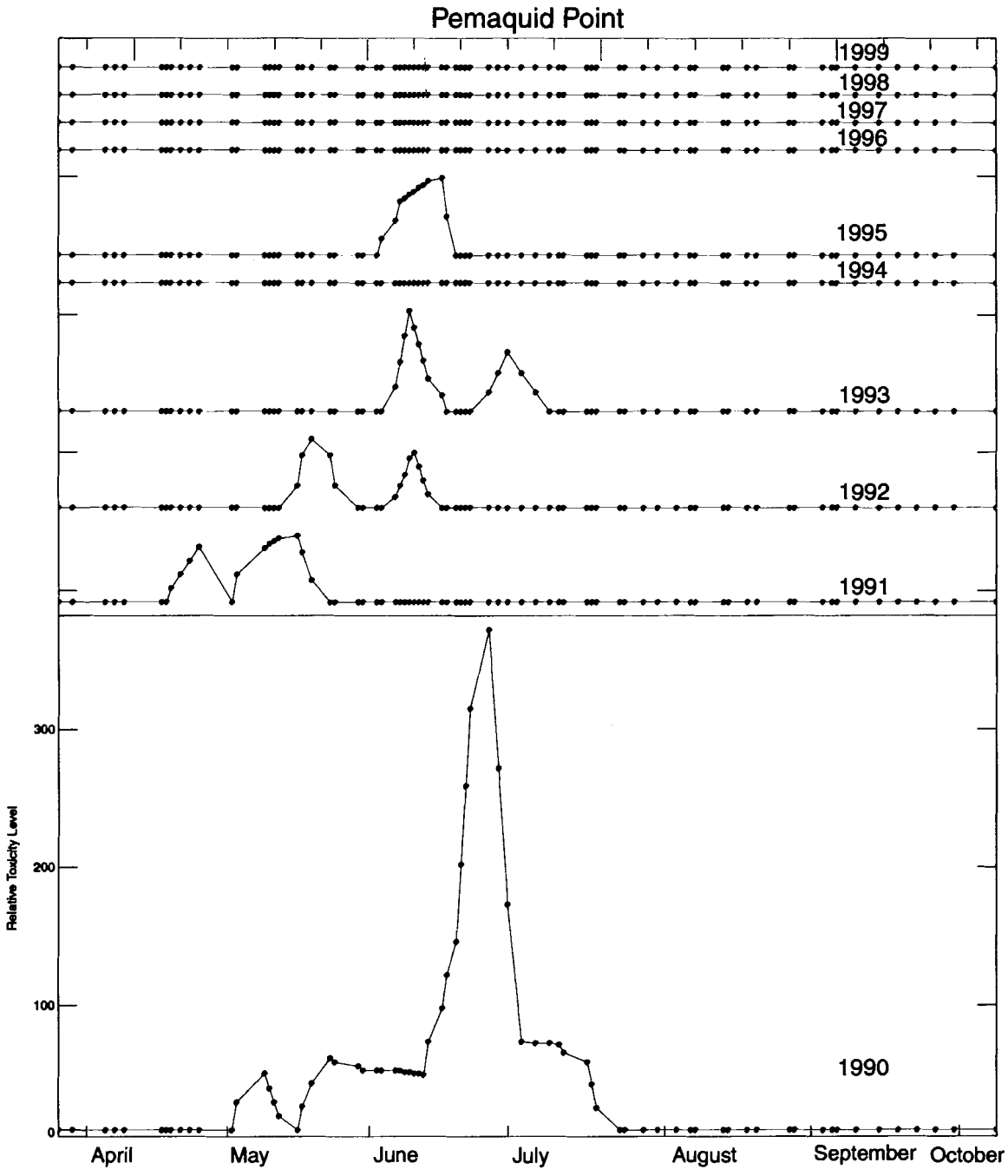


**Figure 3.12.** Continued

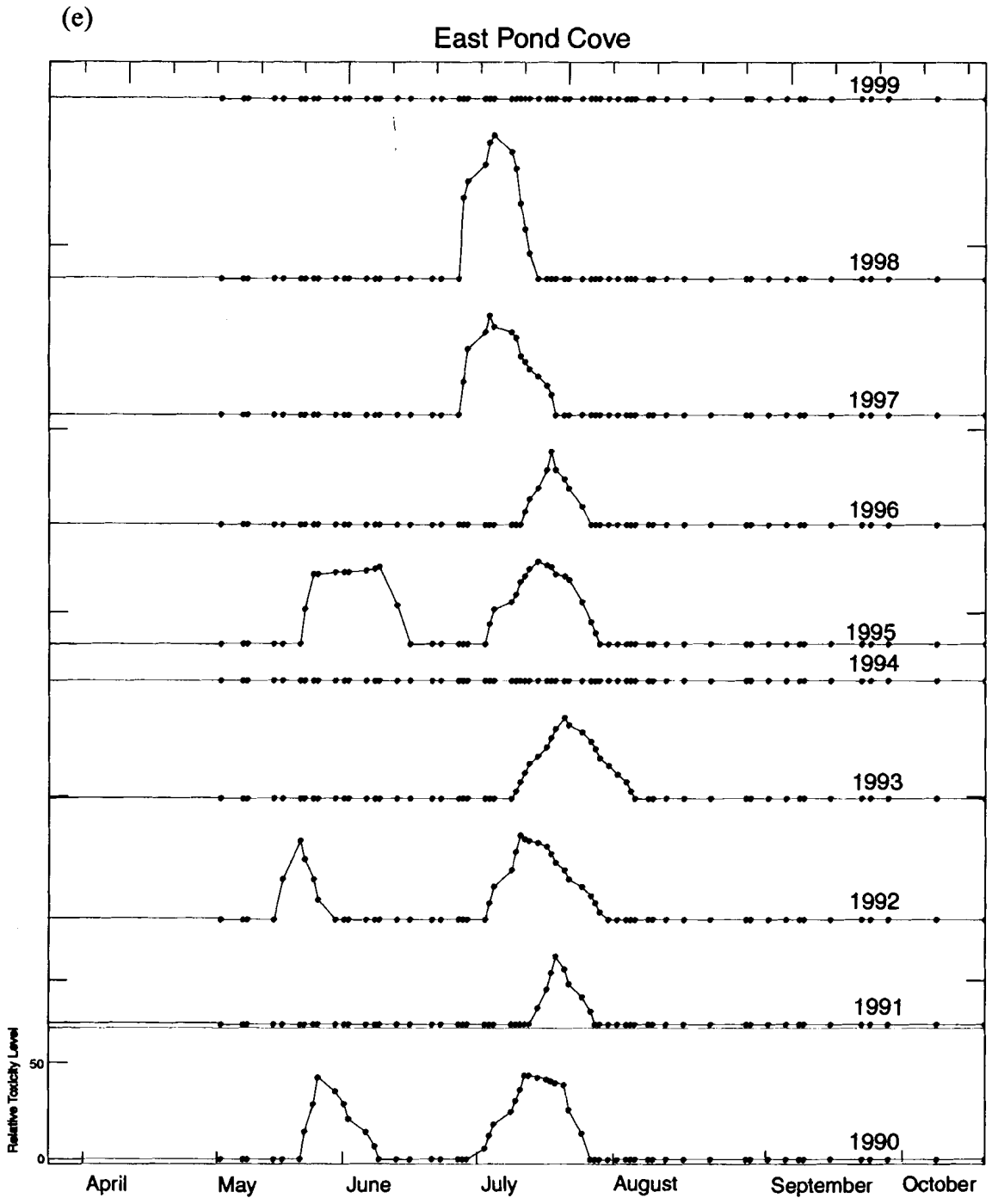


**Figure 3.12.** Continued

Toxicity events in the western GOM begin in May and early June. East of Penobscot Bay (Figure 3.12.e) toxicity events occur closer to the end of June and into July in all ten years.

One hypothesis explaining why toxicity events in the western and eastern GOM occur at different times of the year is based on the idea that the two regions have separate source populations. Anderson (1997) found the eastern and western GOM to be independent from one another with respect to *Alexandrium* populations. Franks and Anderson (1992) suggest that the onset of toxicity in the western GOM is due to a source population of *Alexandrium* located in the Androscoggin and Kennebec River estuary that is advected alongshore in a buoyant freshwater plume controlled by wind-forcing. In April the flow of freshwater runoff is greatest, thus there is an increase in the transport of toxic cells at that time. In eastern Maine the source population is thought to be in the Bay of Fundy and advection of those cells is controlled by the Scotian Shelf waters that drive the EMCC (Smith, 1983). The difference in source populations and advective mechanisms would account for the differing times of the toxicity events.

Another hypothesis explains why toxicity events in eastern GOM are later in the season. The EMCC is strongest in June (Xue et al., 2000), so any *Alexandrium* cells that are growing in the EMCC are promptly advected along the coast and into western GOM. By late July the front between the eastern and western GOM becomes well defined and the EMCC turns offshore, decreasing advection of EMCC waters to western GOM. When the strength of the EMCC begins to decline at the end of the summer, those cells growing in the EMCC are no longer advected so rapidly downstream (Xue et al., 2000), increasing the probability of a toxic event. In addition, there is a strong difference in the

seasonal temperature regime of the two regions early in summer (June) eastern Maine and the EMCC are still colder than the surrounding waters of the GOM so cells do not grow as fast, whereas in western GOM sea surface temperatures are warmer, thus phytoplankton grow more rapidly. Later in the season, the surface waters of eastern Maine increase in temperature, possibly creating conditions more favorable for *Alexandrium* growth.

Although toxicity events in the western GOM consistently occur early in the season, interannual variability is evident in the timing of the onset of toxicity (Figure 3.12.). Interannual variability in advection and east/west connection, which would affect the delivery of EMCC *Alexandrium* cells to the western GOM, could explain these variations in the timing of toxicity events from year to year. Increased connection and advection would occur before the development of the strong SST front separating eastern and western GOM. Differences in the timing of the development of this front would alter the timing or even the occurrence of an increase in toxicity.

This advective response could also be coupled with a nutrient response. The overall phytoplankton productivity in the GOM depends primarily on nutrient rich slope water and intense tidal mixing, especially in the EMCC (Brooks and Townsend, 1989). The transport of these nutrient rich waters to the stratified western and central gulf via the EMCC plays a significant role in the growth and transport of *Alexandrium* (Anderson, 1997), which may, in turn, lead to shellfish toxicity events in the western GOM.

Based on the above observations, the data presented by Townsend et al. (2001) and the results presented earlier in this thesis, I hypothesize that years with large toxicity

events in the western GOM should be years of increased or better connection between the EMCC and the western GOM.

The development of strong cross-shelf SST fronts, such as that evident in midsummer (Figure 3.13.), which suggest low connectivity, can be identified using satellite data. This front develops in the area where cold EMCC waters meet the warm stratified surface waters of western GOM. The front can be quantitatively located by plotting the average temperature along a path from western to eastern GOM. Two-dimensional SST gradient images (see Section 3.2.) make it easier to visualize location and magnitude of fronts in the GOM (Figure 3.13.) and quantify interannual variability of frontal development.

Eight-day composite Pathfinder AVHRR SST images from April 30-August 4 were used to create two-dimensional SST gradient images (see Chapter 2) quantifying the frontal (high gradient) regions in the GOM. Figure 3.13 shows an example eight-day composite and its respective gradient image showing the location of the fronts in relation to the SST patterns. Relative connection between the eastern and western GOM was characterized as the strength of the SST gradient within a 20 km wide box extending alongshore from 43.1°N, -70.5°W to 44.3°N, -68.1°W (see Figure 3.13.). Gradients within this box were quantified as the maximum SST gradient present at each alongshore location over the 20 km in the cross-shelf direction. Use of the maximum gradient rather than a simple cross-shelf mean prevented large frontal zones oriented away from a strictly cross-shelf direction from being averaged out. Figure 3.13 shows an example of the position and strength of the maximum SST gradient at each location between eastern and western GOM (from west to east) for the eight-day gradient image. An overview of

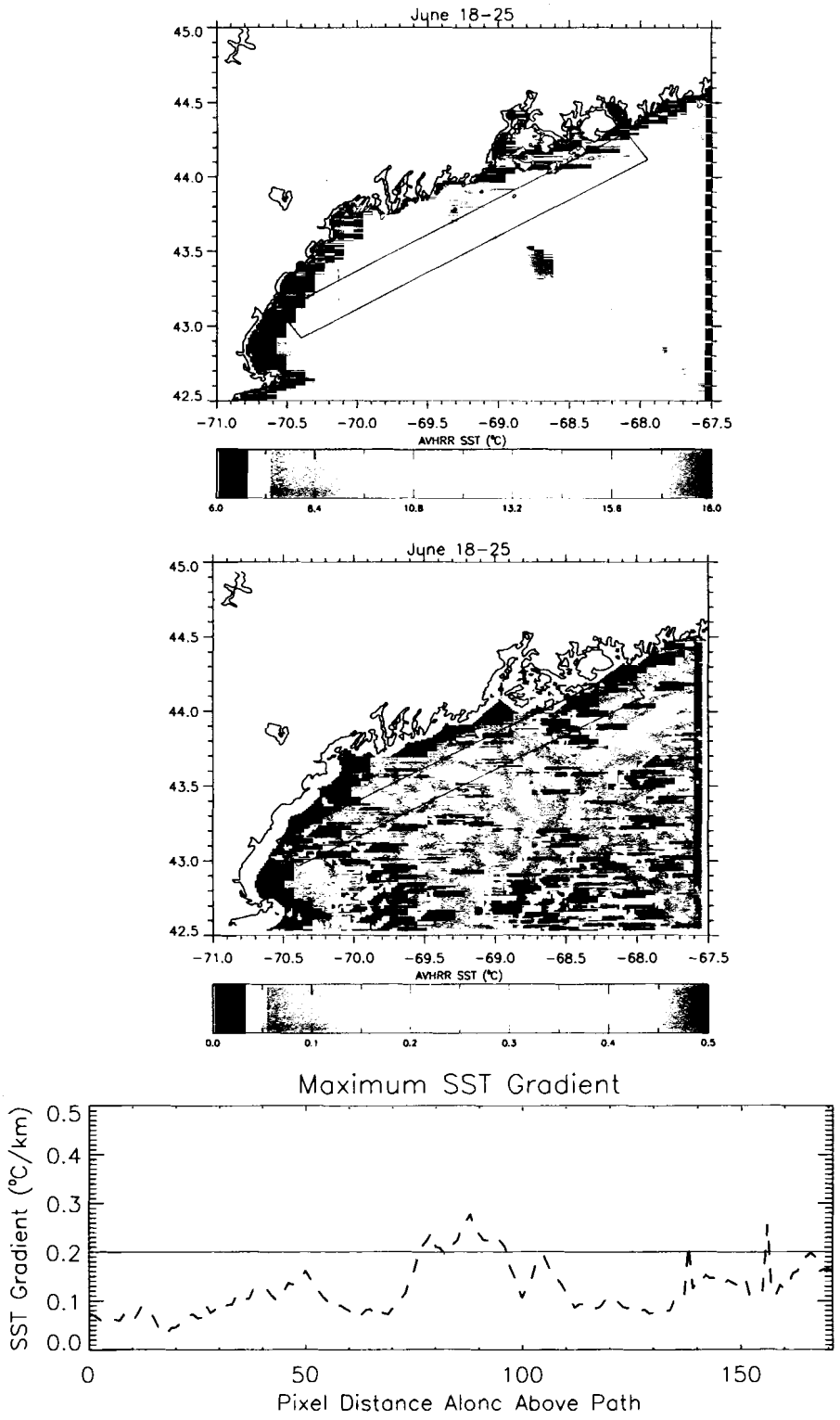


**Figure 3.13.** An example AVHRR SST 8-day composite ($^0$C) and its respective gradient image ($^0$C/km) - showing the box used to define an along shelf swath within which the maximum SST gradient is defined. The lower graph plots the maximum value of the gradient at each location along the transect, showing the 0.2$^0$C/km threshold used to define the "strong frontal zones."

the ten year time series suggested that stronger gradients were well characterized as those over 0.2°C/km. The strong front south of Penobscot Bay in Figure 3.13 is an example of such a front.

These SST gradients along the swath were contoured as a function of time and east/west location from the eight-day images from March 30 to August 4 (yearday 89-216) in each year to show the location and duration of fronts (Figure 3.14 a-j). The gradient operator is two-dimensional and therefore does not distinguish between alongshore and cross shelf fronts. Note that the 1998 and 1999 contours were created using the AVHRR SST data collected at the University of Maine ground station (cloud masking not as good) so the contours look slightly different from those created using the Pathfinder SST data.

The timelines of toxicity data were plotted beside each maximum thermal gradient contour for all ten years to illustrate similarities and differences between the timing and duration of frontal formation and that of the toxicity events for each year (see Figure 3.14a-j). Black bars between the plots indicate times of the year when the maximum gradient anywhere within the swath exceeds 0.2°C/km, indicating restricted connection (and perhaps flow of toxic cells) between the EMCC and the western GOM. The bars assist visualization of connections between frontal presence and toxicity events.

The toxicity time series reveal that 1999 and 1996 are years of little to no toxicity at most of the stations in western GOM and 1990 and 1993 are years of highest toxicity. The other years have moderate toxicity, with 1994, 1991 and 1998 having higher toxicity than 1992 and 1997. Comparison of these time series to the coincident maximum SST

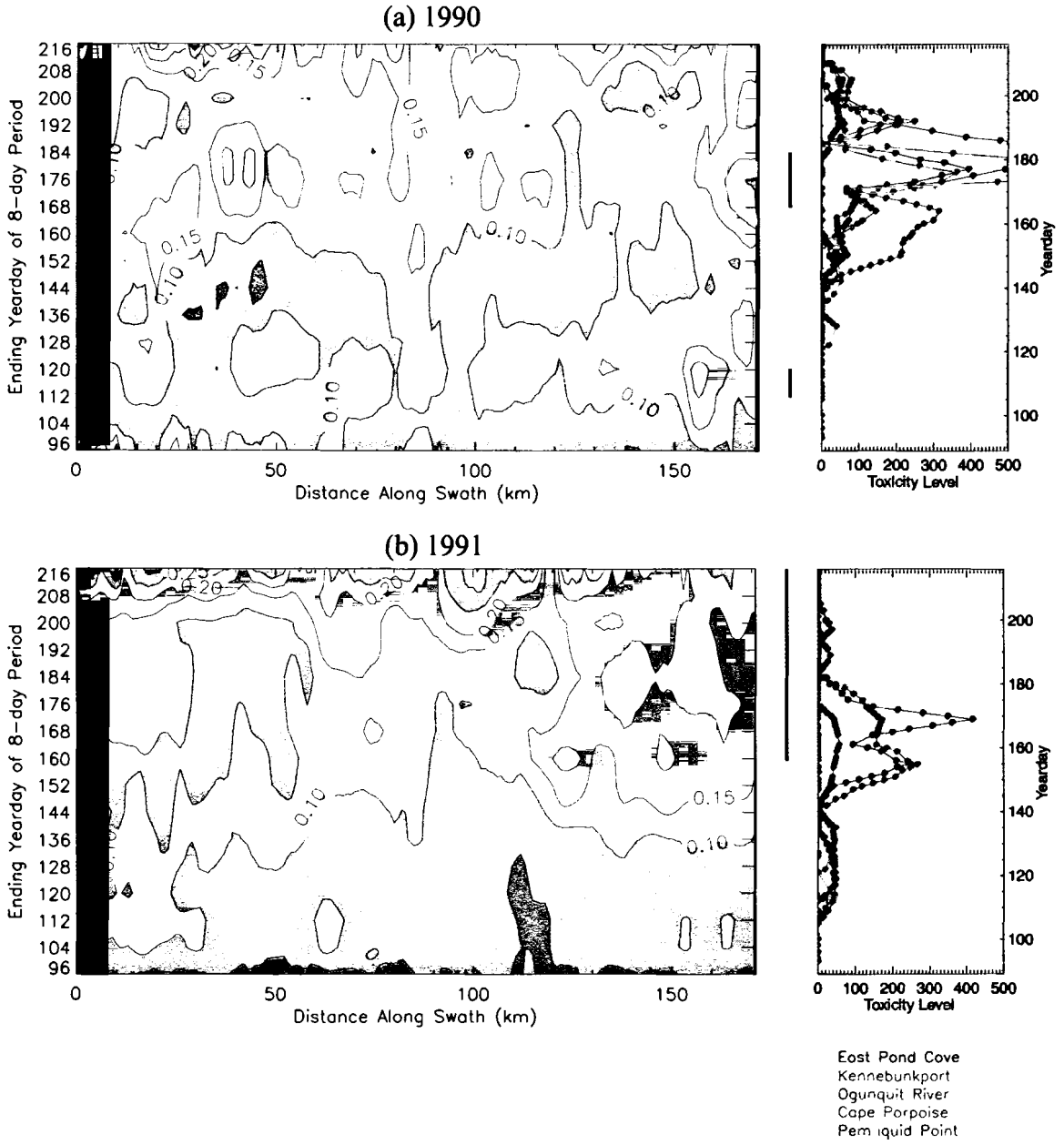


**Figure 3.14.** Contours of maximum two-dimensional SST gradient ($^0$C/km) along a swath from western to eastern GOM for the summer sampling season (April 30 - August 4) for ten years of available data; (a) 1990, (b) 1991, (c) 1992, (d) 1993, (e) 1994, (f) 1995, (g) 1996, (h) 1997, (i) 1998, and (j) 1999. Coincident toxicity timelines (μg toxin/100g tissue) for five sampling stations are shown on the right. The black bars between the plots indicate those images that had a maximum gradient of over 0.2 $^0$C/km somewhere along the swath, suggesting the presence of a front.

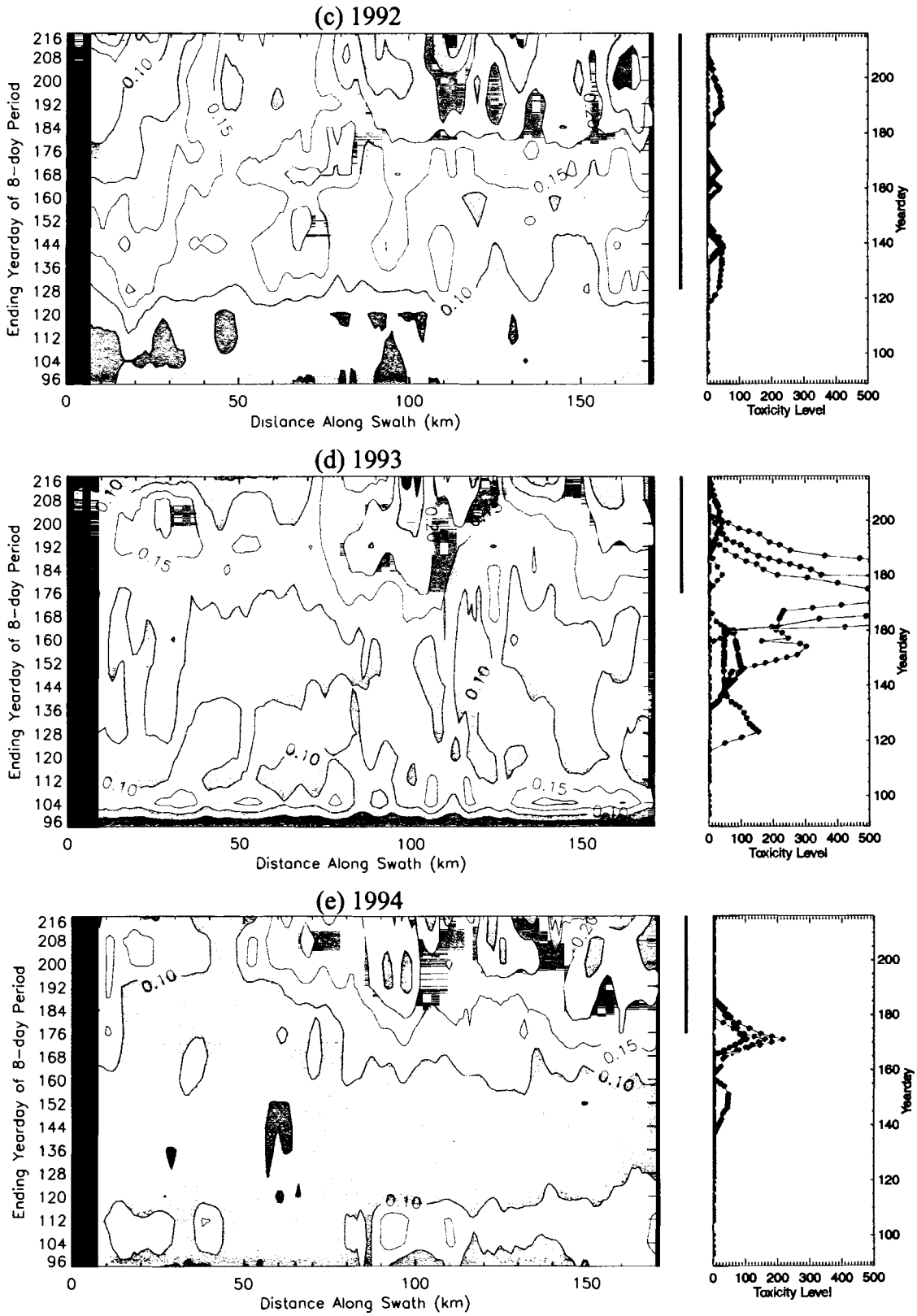


**Figure 3.14.** Continued

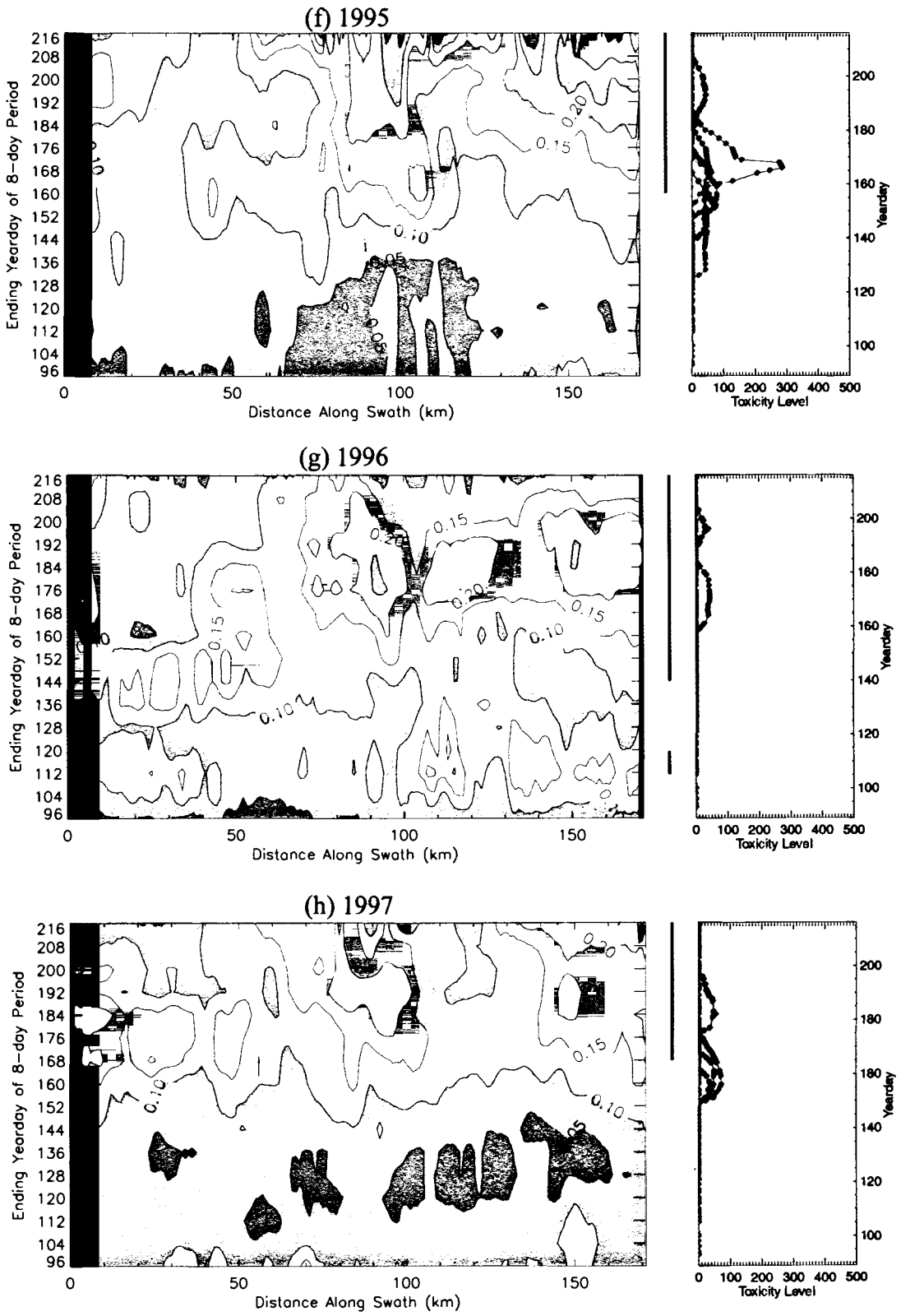


**Figure 3.14.** Continued

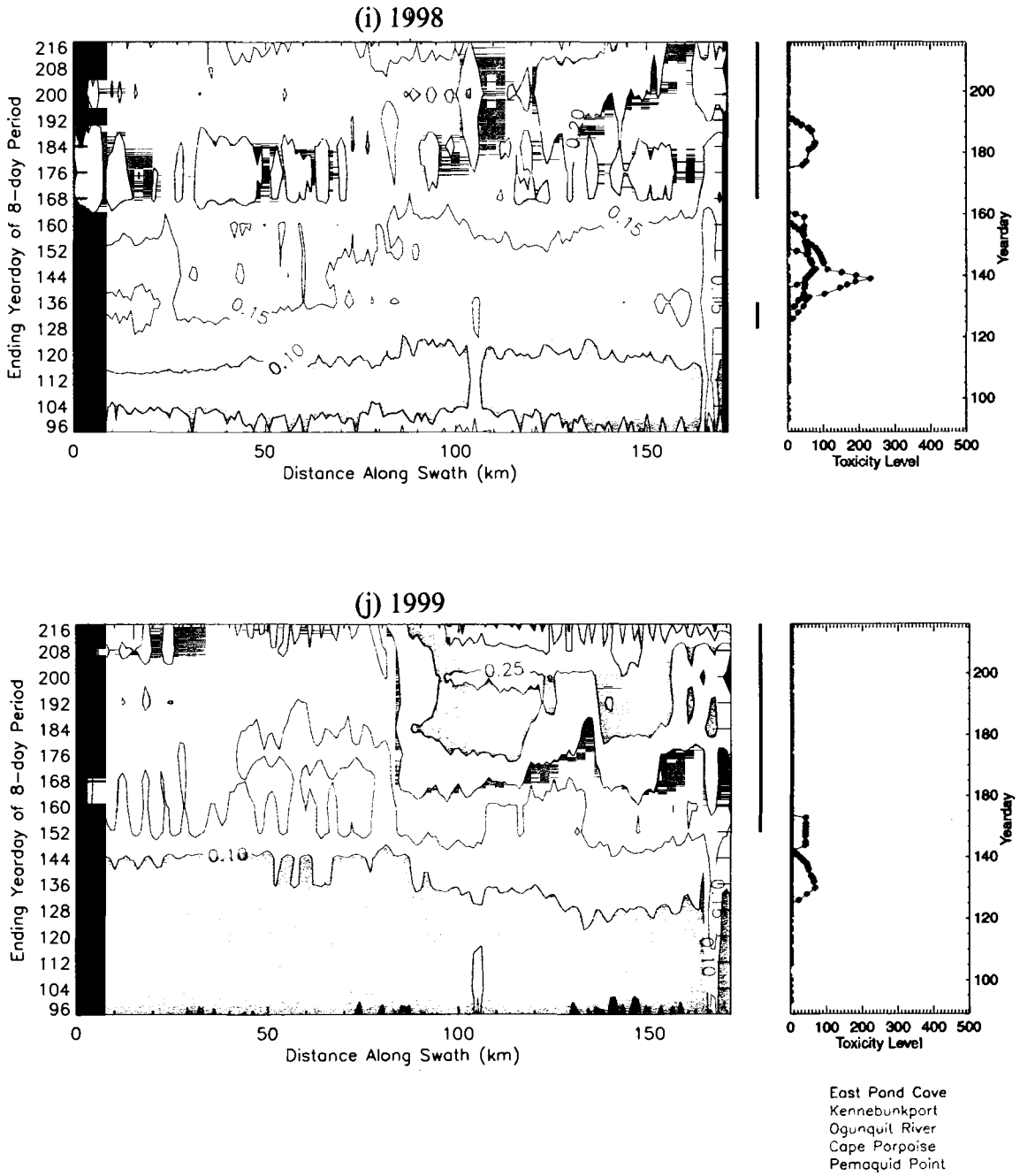


**Figure 3.14.** Continued

gradient contours indicates that the timing of frontal development plays a role in the year to year variability of the magnitude and timing of toxicity events.

The most important feature is the strong thermal gradient that develops between eastern and western GOM (50-100 km along the swath). Presence of this front indicates low connectivity of the EMCC to the western GOM, possibly restricting the transport of cells to the western GOM. Note that this front will not have any effect on the East Pond Cove station which is located upstream of the front, in eastern Maine.

Both 1990 and 1993, years of large toxicity events, show consistent patterns in frontal development and timing (Figure 3.14.a,d) that are different from other years. Strong (>0.2°C/km) SST gradients are present in relatively few (<6) eight day images along the path between eastern and western GOM. More importantly, when strong gradients are present in these years they develop late in the season (mid June) and/or far to the east, thus allowing a long period of connectivity of the EMCC to western GOM. Figure 3.15.a illustrates this idea that with the door open (little restriction of flow due to lack of frontal development) there would be an increased probability of high toxicity. In 1991, toxicity levels were relatively high and, as expected, the cross shelf front between eastern and western GOM developed later in the season (early July), allowing ample time for *Alexandrium* cells to be transported to western GOM in the EMCC. The strong gradients seen earlier in the time series in 1991 likely have little influence on the connectivity between the EMCC and western GOM because they occur in the eastern GOM (>100 km along the swath). The fronts represented in the 1991 contours are similar to those seen in Figure 3.4 b and c occurring on the outer edge of the EMCC.

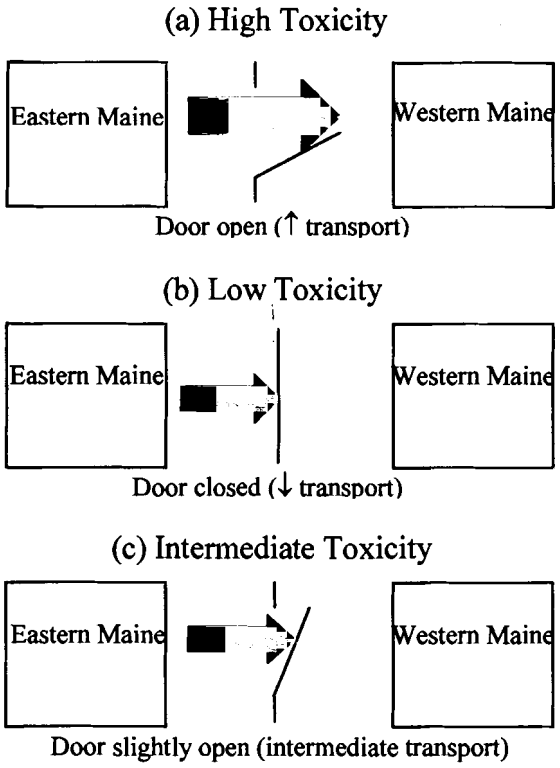


**Figure 3.15.** Illustration of the three toxicity scenarios; (a) high toxicity due to increased connectivity of the EMCC to western GOM (door open), (b) low toxicity due to low connectivity (door closed); and (c) intermediate toxicity due to moderate connectivity (door slightly open).

The connectivity implied by the gradient contours between the EMCC and the western GOM in years of high toxicity is markedly different from that of years that experienced little to no toxicity in the western GOM (1992, 1996 and 1999). Contours in these years (Figure 3.14c,g,j) indicate strong thermal gradients present throughout most of the sampling season, starting relatively early in the season (by beginning of June) (illustrated in Figure 3.15.b). The connection between the EMCC and western GOM is not present long, if at all, and may limit the amount of *Alexandrium* cells transported to western GOM. As strong SST gradients persist throughout the summer, the early season

represents the only delivery of cells to the western GOM, possibly leading to small toxicity events in these three years.

Years with moderate toxicity (1994, 1995, 1997, 1998) represent the intermediate situation (Figure 3.15.c). They develop a strong front between 50 and 100 km later in June than years with little toxicity. This later development of the front allows for an early period of enhanced connectivity. Assuming environmental conditions are favorable to dinoflagellate growth, a toxic event could occur. Nutrient concentrations decrease with time due to uptake by phytoplankton, however, SST and light increase with time. At some point optimal growth conditions will occur when there is ample supply of all three parameters. The timing of the development and/or breakdown of the front in relation to the when optimal growth conditions are present could explain the variability of the magnitude of toxicity events in these years. If the front breaks down, allowing connectivity to re-establish, when optimal growth conditions are present in western GOM a large toxicity event could occur. If the connectivity is re-established before or after favorable growth conditions are present, cells will not grow as well and a smaller toxicity event is expected.

The issue of global climate change is important in this situation as well. With the changing climate the frequency and intensity of storms is thought to increase (M. Wells, personal communication, November 2001). Increased wind events and runoff in the GOM could affect the occurrence of toxicity blooms, due to their effects on frontal structure.

These comparisons of frontal development and toxicity explain much of the interannual variation in the magnitude of the toxicity events in the western GOM. The

results indicate that years when the front between eastern and western GOM forms later in the sampling season there is high toxicity. These results are consistent with the situation, allowing a large population of *Alexandrium* cells to be transported into the western GOM. The sustained transport of toxic cells throughout the season allows for development of a bloom when growth conditions are optimal. Contours of nitrate concentrations superimposed on May 2000 AVHRR SST cruise composite indicate that the western GOM is still vertically mixed and nitrate concentrations are high. As the western GOM begins to stratify, surface *Alexandrium* populations will have favorable conditions for growth – high nutrients and warm surface temperatures.

It is important to consider the fact that the timing of the development of the front between eastern and western GOM affects only the TRANSPORT of *Alexandrium* cells to the western GOM. Large toxicity events in the western GOM still require optimal environmental conditions in order for *Alexandrium* cells to bloom. Biological conditions required for optimal growth are not necessarily linked to the connection described here.

Toxicity events at the East Pond Cove (eastern Maine) occurred consistently later in the season than the western GOM toxicity events. This could be due to the fact that early in the season when western Maine is experiencing toxicity events, the waters in eastern Maine are still too cold for cells to grow fast enough to elevate toxicity. Toxicity levels were also consistently lower than those in western GOM with little variation in magnitude, consistent with the idea that simple seasonal forcing, such as surface temperature, might be a controlling factor. No relationship was found between the magnitude of events in western GOM and those in eastern GOM. The sampling station at Pemaquid Point showed consistently lower toxicity levels than those in western GOM,

with the exception of 1992 and 1996 when all stations had little to no toxicity. The fact that this station is located very close to what Shumway et al. (1980) call the "PSP Sandwich," could explain why there are very few toxicity events there.

The results of this toxicity analysis present a relatively consistent story linking large-scale hydrographic features of the GOM to interannual variability of toxicity events in the western GOM at stations that are most likely influenced by the large-scale circulation of the GOM. If we assume that *Alexandrium* is present in low numbers quite ubiquitously, then DMR sampling stations deep within bays and estuaries are probably not going to have toxicity records affected by the transport of cells from the EMCC. These sampling stations will have toxicity records more strongly influenced by the local processes within bays and harbors.

# Chapter 4

# CONCLUSIONS

Consistent *qualitative* relationships between patterns of sea surface temperature and spatial distributions of *Alexandrium* in the GOM were observed using contours of *Alexandrium* concentration superimposed on time averages (composites) of satellite SST data representing the cruise periods. Elevated *Alexandrium* concentrations were present primarily in offshore regions associated with cold EMCC water. Low cell densities were present in regions of warm SST. This qualitative relationship was present during each of the cruises in 1998 (June, July and August) and in June 2000. It was not present in May 2000, most likely due to the fact that stratification in unmixed waters had not yet developed so the EMCC was not visible in the AVHRR SST cruise composite. Composites of SeaWiFS chlorophyll with *Alexandrium* contours overlaid do not show a consistent relationship. *Alexandrium* makes up a small proportion of the phytoplankton community in the GOM. Other phytoplankton with differing distributions make up the pigment signal measured by SeaWiFS. The *Alexandrium* concentration is so small comparably that it is undetectable. Contours did show that high chlorophyll regions are located shoreward of *Alexandrium*. Townsend et al. (2001) suggest this pattern indicates that chlorophyll has a high nanophytoplankton contribution.

Statistically significant *quantitative* relationships between either *Alexandrium* or other ship-measured parameters important to the distributional ecology of *Alexandrium*, and the satellite data would allow the distribution of the *in situ* parameters to be modeled

from the satellite data. Attempts to quantify the above relationships using linear regressions did produce some significant results. A relationship between AVHRR SST and *Alexandrium* concentrations in the GOM was found to be consistent throughout the cruise periods in 1998. Using the regression results of this analysis, models of the distribution of *Alexandrium* for July and August 1998 were created allowing extrapolation and interpolation between measurement sites. The regression analyses show that there is a temperature range in which *Alexandrium* seem to congregate. Regressions based on subsets of the overall data set were examined for simple relationships between satellite and *in situ* data parameters to test the hypothesis that isolated regions of the GOM may be oceanographically similar and thus result in better correlations. Some correlations of subsets improved but the relationships were not consistent.

Tester et al. (1991) suggest that dinoflagellate blooms are generally a result of cell transportation into an area of environmental conditions favorable for bloom development. It is hard to separate alongshore advection of cells from local growth responding to locally favorable conditions. Franks and Anderson (1992) suggest that *Alexandrium* in western GOM is a result of vegetative cells being advected down the coast by a buoyant wind-driven plume of freshwater. In this study it is shown that *Alexandrium* cell densities are highest in the Bay of Fundy and the EMCC and patterns are consistent with advection down the coast of eastern Maine in the EMCC, possibly delivering cells to western GOM.

Transformation of SST patterns into two dimensional gradient images reveals the presence and location of large thermal gradients, or fronts. These occur preferentially

along the inshore and offshore edges of the EMCC and separate stratified western GOM surface waters from the eastern GOM. Contours of surface *Alexandrium* concentrations overlaid on the frontal patterns show elevated cell densities to be constrained by the fronts, supporting the strong hydrographic linkage evident in the SST patterns.

Further evidence of strong hydrographic control of *Alexandrium* populations in the GOM was obtained during a shellfish harvesting closure issued by the Maine DMR in May 2000. The timing and location of this closure in the western GOM was compared to AVHRR SST patterns just before the time of the closure. Results suggested one mechanism whereby offshore dynamics could explain the closure. In 2000, EMCC was observed in the AVHRR SST data to flow past Penobscot Bay and into coastal regions of the western GOM. In addition, AVHRR SST patterns showed a plume of cold water, continuous with the EMCC, connecting to the coast of western Maine on the day of the closure. These two features could have provided a mechanism for *Alexandrium* cells to move from the EMCC into the western GOM and then onshore. Drifter tracks and wind data support this hypothesized mechanism.

The qualitative relationships between *Alexandrium* and SST patterns and dynamics associated with the May 2000 closure suggest that toxicity events in coastal regions of the western GOM require a mechanism for delivery of offshore eastern GOM *Alexandrium* populations. Enhanced connections between the EMCC and the western GOM would provide such a mechanism. Analysis of ten years of coastal toxicity data and coincident SST patterns suggest that the occurrence of strong surface thermal gradients, or frontal zones, in the EMCC/WMCC region influence the occurrence of toxicity events in the western GOM. Years with little toxicity are years when relatively

strong gradients (> 0.2 °C/km) are present during most of the growing season. Years with delayed increases in toxicity have a front early in the season, and cell advection into the western GOM is restricted until later in the season. Years of higher toxicity have reduced fronts until later in the season, allowing delivery of cells into western GOM.

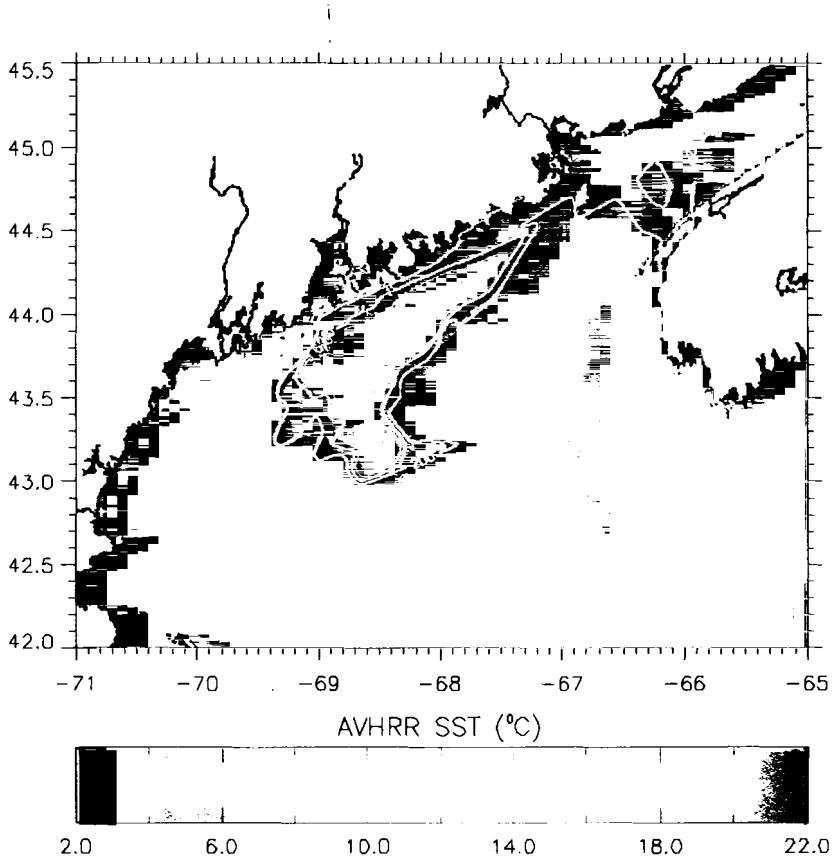


**Figure 4.1.** July 2001 AVHRR SST cruise composite (July 6-16) with surface *Alexandrium* concentration contours overlaid

The results of this study point to a story linking surface hydrologic processes, advection and water mass distribution with spatial patterns of *Alexandrium* concentration and the occurrence of toxic events in the coastal regions of the GOM. Despite their inability to directly measure *Alexandrium* concentrations, satellite data are clearly able to measure and monitor many surface oceanographic parameters indicative of these

hydrologic processes. In some specific cases, the satellite data can even be used to model *in situ* parameters potentially useful in predicting and monitoring HABs in the GOM.

Future work will test the temporal integrity of the relationships presented in this study. As an initial extrapolation, surface *Alexandrium* concentrations for July 2001 are superimposed on the cruise composite AVHRR SST image (Figure 4.1.). These data are clearly consistent with my observations that, during summer, higher *Alexandrium* concentrations are associated with colder waters of the EMCC and furthermore, advective transport of cells into offshore regions of the GOM is affected by the cyclonic turn of the EMCC in the vicinity of Penobscot Bay.

A better spatial clarification of ecological regimes based on other oceanographic parameters available from the satellite data may prove useful in future work. For example, SeaWiFS data provides estimates of the depth of the 10% light level and the diffuse attenuation coefficient, both of which are indicative of the vertical light regime which Townsend et al. (2001) deem important in the distribution of *Alexandrium*. Lastly, this study shed some light on interannual differences in the timing and magnitude of toxicity events in the western GOM. Future research might investigate the timing and magnitude of toxicity events in the very different hydrographic regime of the eastern GOM and their relationship with patterns evident in satellite data.

## BIBLIOGRAPHY


Anderson, D. M. "Bloom dynamics of toxic *Alexandrium* species in the northeastern U.S." *Limnology and Oceanography*. Vol 42. 1997. pp 1009-1022.

Anderson, D. M. "Effects of temperature conditioning on development and germination of *Gonyaulax tamarensis* (Dinophyceae) hypnozygotes." *Journal of Phycology*. Vol 16. 1980. pp 166-172.

Anderson, D. M. "Toxic Algal Blooms and Red Tides: A Global Perspective." IN: *Red Tides: Biology, Environmental Science, and Toxicology*. New York: Elsevier Science Publishing Co., Inc., 1989. pp 11-16.

Arnone, R. A. and R. W. Gould. "Coastal Monitoring Using Ocean Color." *Sea Technology*. September 1998. pp 18-27.

Bates, J. J. and H. F. Diaz. "Evaluation of Multichannel Sea Surface Temperature Product Quality for Climate Monitoring: 1982-1988." *Journal of Geophysical Research*. Vol 96. No C11. November 15, 1991. pp 20613-20622.

Bernstein, R. L. "Sea-Surface Temperature Estimates Using NOAA 6 Satellite Advanced Very High Resolution Radiometery." *Journal of Geophysical Research*. Vol 87. 1982. pp 9455-9965.

Blasco, D. "Red Tides in the Upwelling Regions." IN: *Proceedings of the First International Conference on Toxic Dinoflagellate Blooms*. Wakefield: Massachusetts Science and Technology Foundation, 1975. pp 113-119.

Blaxter, J. H. S. and A.J. Southward. *Advances in Marine Biology: The Biogeography of the Oceans*. San Diego: Academic Press, 1997. pp 596.

Broeknuizen, N. "Simulating motile algae using a mixed Eulerian-Lagrangian approach: does motility promote dinoflagellate persistence or co-existence with diatom?" *Journal of Plankton Research*. Vol 21. No 7. 1999. pp 1191-1216.

Brooks, D. A. "Vernal Circulation in the Gulf of Maine." *Journal of Geophysical Research*. Vol 90. No C5. 1985. pp 4687-4705.

Brooks, D. A. "A model study of the buoyancy-driven circulation in the Gulf of Maine." *Journal of Physical Oceanography*. Vol 24. 1994. pp 2387-2412.

Brooks, D. A. and D. W. Townsend. "Variability of the coastal current and nutrient pathways in the eastern Gulf of Maine." *Journal of Marine Research*. Vol 47. 1989. pp 303-321.

Charton, B. and J. Tietjen. "Dinoflagellates." *The Facts on File Dictionary of Marine Science*. New York: Facts on File, 1988. pp 77-78.

Eppley, R. W., J. N. Rogers, J. J. McCarthy. "Half-saturation constants for uptake of nitrate and ammonium by marine phytoplankton." *Limnology and Oceanography*. Vol 14. 1969. pp 912-920.

Franks, P. J. S. and D. M. Anderson. "Alongshore transport of a toxic phytoplankton bloom in a buoyancy current: *Alexandrium tamarense* in the Gulf of Maine." *Marine Biology*. Vol 112. 1992. pp 153-164.

Goes, J. I., T. Saino, H. Oaku, D. L. Jiang. "A Method for Estimating Sea Surface Nitrate Concentrations from Remotely Sensed SST and Chlorophyll *a* – A Case Study for the North Pacific Ocean Using OCTS/ADEOS Data." *IEEE Transactions on Geoscience and Remote Sensing*. Vol 37. No 3. May 1999. pp 1633-1644.

Hallegraeff, G. M. "Harmful algal blooms: A global overview." IN: *Manual on Harmful Marine Microalgae*. France: UNESCO, 1995. pp 1-21.

Hastings, J. W. and B. M. Sweeney. "Phased cell division in the marine dinoflagellates." IN: *Synchrony in cell division and growth*. New York: John Wiley and Sons, 1964. pp 307.

Holligan, P. M., M. Viollier, C. Dupouy, J. Aiken. "Satellite Studies on the Distribution of Chlorophyll and Dinoflagellate Blooms in the Western English Channel." *Continental Shelf Research*. Vol 2. 1983. pp 81-96.

Holligan, P. M. "Marine Dinoflagellate Blooms - Growth Strategies and Environmental Exploration." IN: *Toxic Dinoflagellates*. New York: Elsevier Science Publishing Co., Inc., 1985. pp 133-139.

Kamykowski, D. and S. J. Zentara. "Spatio-Temporal and Process-Oriented Views of Nitrite in the World Ocean as Recorded in the Historical Data Set." *Deep Sea Research*. Vol 38. 1991. pp 445-464.

Keafer, B. A. and D. M. Anderson. "Dinoflagellate cyst dynamics in coastal and estuarine waters." IN: *Toxic Dinoflagellates: Proceedings of 3rd International Conference*. New York: Elsevier Science Publishing Co., Inc., 1985.

Keafer, B. A. and D. M. Anderson. "Use of Remotely-Sensed Sea Surface Temperatures in Studies of *Alexandrium tamarense* Bloom Dynamics." IN: *Toxic Phytoplankton in the Sea: Proceedings of 5th International Conference on Toxic Marine Phytoplankton.* 1993. pp 763-768.

Kilpatrick, K. A., G. P. Podesta, R. Evans. "Overview of the NOAA/NASA AVHRR Pathfinder algorithm for Sea Surface Temperature and associated Matchup Database." *Journal of Geophysical Research.* (in press).

Lalli, C. M. and T. R. Parson. *Biological Oceanography: An Introduction.* New York: Pergamon Press, 1993. pp 301.

Landsberg, J. H. and K. A. Steidinger. "A Historical Review of *Gymnodinium breve* Red Tides Implicated in Mass Mortalities of the Manatee (*Trichechus manatus latirostris*) in Florida, USA." *Journal of Phycology.* Vol 34. 1998. pp 431.

Lewis, C. M., C. M. Yentsch, B. Dale. "Distribution of *Gonyaulax excavata* resting cysts in the sediments of Gulf of Maine." IN: *Toxic dinoflagellate blooms: Proceedings of 2nd International Conference.* New York: Elsevier Science Publishing Co., Inc., 1979.

Lynch, D. R., M. J. Holboke, C. E. Naimie. "The Maine coastal current: spring climatological circulation." *Continental Shelf Research.* Vol 17. No 6. 1997. pp 605-634.

Maine Environmental Properties Project. "Report from the Steering Committee, Consensus Ranking of Environmental Risks Facing Maine." State House Station, Augusta, Maine 04333, January 1996.

Martin, J. L. and A. W. White. "Distribution and Abundance of the Toxic Dinoflagellate *Gonyaulax excavata* in the Bay of Fundy." *Canadian Journal of Fisheries and Aquatic Science.* Vol 45. 1988. pp 1968-1975.

McMillin, L. M. "Estimation of sea surface temperatures from two infrared window measurements with different absorption." *Journal of Geophysical Research.* Vol 80. 1975. pp 5113-5117.

Minnett, P. J. "SST from Along Track Scanning Radiometer." IN: *Oceanographic Applications of Remote Sensing.* Boston: CRC Press, Inc., 1995. pp 131-143.

Mobley, C. D. "Remote Sensing." *Light and Water: Radiative Transfer in Natural Waters.* Boston: Academic Press, 1994. pp 487-496.

Morel, A. Y. and L. Prieur. "Analysis of Variations in Ocean Color." *Limnology and Oceanography.* Vol 22. 1977. pp 709-722.

Morin, P., M. V. M. Wafar, P. LeCorre. "Estimation of Nitrate Flux in a Tidal Front From Satellite-Derived Temperature Data." *Journal of Geophysical Research.* Vol 98. No C3. March 15, 1993. pp 4689-4695.

Njoku, E. G. "Satellite remote sensing of sea surface temperature." IN: *Surface Waves and Fluxes, Vol II.* Dordrecht: Kluwer Academic Publishers, 1990. pp 311-338.

Njoku, E. G. and O. B. Brown. "Sea Surface Temperature." IN: *Atlas of Satellite Observations Related to Global Change.* New York: Cambridge University Press, 1993. pp 237-249.

O'Reilly J. E., S. Maritorena, B. G. Mitchell, D. A. Siegel, K. L. Carder, S. A. Garver, M. Kahru, C. McClain. "Ocean Color Chlorophyll Algorithms for SeaWiFS." *Journal of Geophysical Research.* Vol 103. No C11. October 15, 1998. pp 24937-24953.

Pettigrew, N. R., D. W. Townsend, H. Xue, J. P. Wallings, P. J. Brickley, R. D. Hetland. "Observations of the Eastern Maine Coastal Current and its offshore extensions in 1994." *Journal of Geophysical Research.* Vol 103. No C13. December 15, 1998. pp 30,623-30,639.

Pingree, R. D., P. K. Pugh, P. M. Holligan, and G. R. Forester. "Summer phytoplankton blooms and red tides along tidal fronts in the approaches to the English Channel." *Nature* (London). Vol 258. 1975. pp 672-677.

Raymont, J. E. G. "The Phytoplankton." *Plankton and Productivity in the Oceans.* New York: The MacMillan Company, 1963. pp 93-113.

Riley, G. A. "Factors Controlling Phytoplankton Populations on Georges Bank." *Journal of Marine Research.* Vol 6. 1946. pp 54-73.

Ryther, J. H. "The measurement of primary productivity." *Limnology and Oceanography.* Vol 1. 1965. pp 72-84.

Satsuki, M., H. Fukushima, and Y. Sugimori. "Remotely Sensed Phytoplankton Pigment Concentrations Around Japan Using the Coastal Zone Color Scanner." IN: *Red Tides: Biology, Environmental Science and Toxicology.* New York: Elsevier Science Publishing Co., Inc., 1989. pp 185-188.

Schluessel, P., W. J. Emery, H. Grassel, T. Mammen. "On the Bulk-Skin Temperature Difference and its Impact on Satellite-Remote Sensing of Sea Surface Temperature." *Journal of Geophysical Research.* Vol 95. 1990. pp 13341.

Seliger, H. H., K. R. McKenley, W. H. Biggla, R. B. Rivkin, and K. R. H. Aspden. "Phytoplankton patchiness and frontal regions." *Marine Biology.* Vol 61. pp 119-131.

Shumway, S. E., S. Sherman-Caswell, J. W. Hurst. "Paralytic shellfish poisoning in Maine: Monitoring a monster." *Journal of Shellfish Research*. Vol 7. 1988. pp 643-652.

Sieracki, M. E., P. G. Verity, D. K. Stoecker. "Plankton community response to sequential silicate and nitrate depletion during the 1989 North Atlantic spring bloom." *Deep Sea Research II*. Vol 40. No1/2. 1993. pp 213-225.

Smith, P. C. "Mean and seasonal circulation off southwest Nova Scotia." *Journal of Physical Oceanography*. Vol 13. 1983. pp 1034-1054.

Stewart, R. H. "Observations Using Infrared Radiation." *Methods of Satellite Oceanography*. London: Scripps Institute of Oceanography, 1985. pp 128-152.

Sullivan, C. W., K. R. Arrigo, C. R. McClain, J. C. Comiso, J. Firestone. "Distributions of Phytoplankton Blooms in the Southern Ocean." *Science*. Vol 262. December 1993. pp 1832-1837.

Tester, P. A. and R. P. Stumpf. "Phytoplankton Blooms and Remote Sensing: What is the Potential for Early Warning." *Journal of Shellfish Research*. Vol 17. No 5. 1998. pp 1469-1471.

Tester, P. A., R. P. Stumpf, F. M. Vukovich, P. K. Fowler, J. T. Turner. "An expatriate red tide bloom: Transport, distribution, and persistence." *Limnology and Oceanography*. Vol 36. 1991. pp 1053-1061.

Therriault, J. C., J. Painchaud, M. Levasseur. "Factors Controlling the Occurrence of *Protogonyaulax tamarensis* and Shellfish Toxicity in the St. Lawrence Estuary: Freshwater Runoff and the Stability of the Water Column." IN: *Toxic Dinoflagellates*. New York: Elsevier Science Publishing Co., Inc., 1985. pp 141-146.

Townsend, D. W., N. R. Pettigrew, A.C. Thomas. "Offshore blooms of the red tide Dinoflagellate, *Alexandrium* sp., in the Gulf of Maine." *Continental Shelf Research*. Vol 21. 2001. pp 347-369.

Uno, S. and M. Yokota. "Applications of Remote Sensing Techniques for the Mapping of Red Tide Distribution in Coastal Areas." IN: *Red Tides: Biology, Environmental Science, and Toxicology*. New York: Elsevier Science Publishing Co., Inc., 1989. pp 189-192.

Van Woert, M. "The Subtropical Front: Satellite Observations During FRONTS 80." *Journal of Geophysical Research*. Vol 87. 1982. pp 9523-9536.

Walker, L. M. "Life Histories, Dispersal, and Survival in Marine, Planktonic Dinoflagellates." IN: *Marine Plankton Life Cycle Strategies*. Boca Raton, FL: CRC Press, Inc., 1984. pp 19-32.

White, A. W., and C. M. Lewis. "Resting cysts of the toxic red tide dinoflagellate *Gonyaulax excavata." Canadian Journal of Fisheries and Aquatic Science*. Vol 39. 1982. pp 1185-1194.

Xue, H., F. Chai, N. R. Pettigrew. "A Model Study of the Seasonal Circulation in the Gulf of Maine." *Journal of Physical Research*. Vol 30. May 2000. pp 1111-1135.

Yentsch, C. S. "Monitoring Algal Bloom, the Use of Satellites and Other Remote Sensing Devices." IN: *Red Tides: Biology, Environmental Science, and Toxicology*. New York: Elsevier Science Publishing Co., Inc., 1989. pp 181-184.

Yentsch, C. S. and N. Garfield. "Principal areas of vertical mixing in the waters of the Gulf of Maine, with reference to the total productivity of the area." IN: *Oceanography from Space*. 1981. pp 303-312.

# APPENDICES

# Appendix A

## LATITUDE AND LONGITUDE LOCATIONS FOR EACH CRUISE STATION

| June 1998 | | | July 1998 | | | August 1998 | | |
|---|---|---|---|---|---|---|---|---|
| Station # | Latitude | Longitude | Station # | Latitude | Longitude | Station # | Latitude | Longitude |
| 1 | 43.1032 | -70.6107 | 1 | 43.0985 | -70.6138 | 1 | 43.102 | -70.6112 |
| 2 | 43.0662 | -70.5825 | 2 | 43.0635 | -70.5815 | 2 | 43.0635 | -70.582 |
| 3 | 42.9938 | -70.5253 | 3 | 42.9945 | -70.5252 | 3 | 42.9967 | -70.5232 |
| 4 | 42.9238 | -70.4658 | 4 | 42.9247 | -70.4658 | 4 | 42.9258 | -70.4672 |
| 5 | 42.854 | -70.4095 | 5 | 42.8533 | -70.4088 | 5 | 42.854 | -70.4093 |
| 6 | 42.7807 | -70.351 | 6 | 42.7792 | -70.3502 | 6 | 42.7805 | -70.3512 |
| 7 | 42.7055 | -70.297 | 7 | 42.706 | -70.2975 | 7 | 42.7072 | -70.2987 |
| 8 | 42.6337 | -70.2365 | 8 | 42.634 | -70.2373 | 8 | 42.6327 | -70.2977 |
| 9 | 42.6663 | -69.9703 | 9 | 42.6652 | -69.9698 | 9 | 42.665 | -69.9698 |
| 10 | 42.7403 | -70.0168 | 10 | 42.741 | -70.0188 | 10 | 42.7405 | -70.0233 |
| 11 | 42.8163 | -70.0843 | 11 | 42.8155 | -70.084 | 11 | 42.8182 | -70.0903 |
| 12 | 42.8913 | -70.1335 | 12 | 42.8918 | -70.1333 | 12 | 42.8937 | -70.1332 |
| 13 | 42.9577 | -70.1917 | 13 | 42.9592 | -70.1898 | 13 | 42.961 | -70.191 |
| 14 | 43.0243 | -70.2495 | 14 | 43.0263 | -70.2483 | 14 | 43.0262 | -70.2493 |
| 15 | 43.1003 | -70.3092 | 15 | 43.1007 | -70.307 | 15 | 43.0983 | -70.3075 |
| 16 | 43.1715 | -70.3627 | 16 | 43.1715 | -70.362 | 16 | 43.1705 | -70.3612 |
| 17 | 43.2445 | -70.4182 | 17 | 43.2442 | -70.4175 | 17 | 43.2447 | -70.4167 |
| 18 | 43.2798 | -70.4483 | 18 | 43.2797 | -70.4478 | 18 | 43.2787 | -70.4485 |
| 19 | 43.4695 | -70.3048 | 19 | 43.4692 | -70.3052 | 19 | 43.4682 | -70.3055 |
| 20 | 43.3992 | -70.2465 | 20 | 43.3973 | -70.2468 | 20 | 43.399 | -70.2453 |
| 21 | 43.3267 | -70.1877 | 21 | 43.326 | -70.1887 | 21 | 43.326 | -70.1875 |
| 22 | 43.2535 | -70.1333 | 22 | 43.2532 | -70.1325 | 22 | 43.2522 | -70.1322 |
| 23 | 43.1815 | -70.0757 | 23 | 43.18 | -70.079 | 23 | 43.1803 | -70.078 |
| 24 | 43.1082 | -70.023 | 24 | 43.1088 | -70.0218 | 24 | 43.1095 | -70.021 |
| 25 | 43.0405 | -69.9607 | 25 | 43.0392 | -69.9623 | 25 | 43.04 | -69.9622 |
| 26 | 42.9697 | -69.9065 | 26 | 42.97 | -69.9093 | 26 | 42.9702 | -69.9092 |
| 27 | 42.9018 | -69.8512 | 27 | 42.9005 | -69.8535 | 27 | 42.9013 | -69.8533 |
| 28 | 42.8297 | -69.7953 | 28 | 42.829 | -69.7982 | 28 | 42.8292 | -69.7982 |
| 29 | 42.7592 | -69.7398 | 29 | 42.7595 | -69.7403 | 29 | 42.7602 | -69.7395 |
| 30 | 42.8623 | -69.5095 | 30 | 42.8625 | -69.5083 | 30 | 42.8612 | -69.5107 |
| 31 | 42.9355 | -69.5708 | 31 | 42.9367 | -69.5698 | 31 | 42.9357 | -69.5708 |
| 32 | 43.0077 | -69.6262 | 32 | 43.0083 | -69.626 | 32 | 43.008 | -69.6263 |
| 33 | 43.0783 | -69.684 | 33 | 43.0775 | -69.6818 | 33 | 43.0777 | -69.6837 |
| 34 | 43.1485 | -69.743 | 34 | 43.1485 | -69.7413 | 34 | 43.1487 | -69.7423 |
| 35 | 43.2217 | -69.8017 | 35 | 43.2203 | -69.7987 | 35 | 43.2208 | -69.8018 |
| 36 | 43.297 | -69.8595 | 36 | 43.295 | -69.8572 | 36 | 43.295 | -69.8605 |
| 37 | 43.3698 | -69.9157 | 37 | 43.368 | -69.9135 | 37 | 43.3695 | -69.9152 |
| 38 | 43.4415 | -69.9717 | 38 | 43.4428 | -69.9732 | 38 | 43.4412 | -69.973 |
| 39 | 43.5145 | -70.033 | 39 | 43.5132 | -70.0317 | 39 | 43.5138 | -70.0335 |
| 40 | 43.5842 | -70.087 | 40 | 43.5847 | -70.084 | 40 | 43.5838 | -70.0838 |
| 41 | 43.6543 | -70.142 | 41 | 43.6532 | -70.141 | 41 | 43.6542 | -70.1413 |
| 42 | 43.7258 | -69.907 | 42 | 43.7252 | -69.9098 | 42 | 43.7248 | -69.9078 |
| 43 | 43.6595 | -69.8342 | 43 | 43.6603 | -69.835 | 43 | 43.6603 | -69.8355 |
| 44 | 43.583 | -69.7788 | 44 | 43.5832 | -69.7782 | 44 | 43.5832 | -69.7773 |
| 45 | 43.5112 | -69.7235 | 45 | 43.5117 | -69.7237 | 45 | 43.5112 | -69.7223 |
| 46 | 43.444 | -69.666 | 46 | 43.4427 | -69.6665 | 46 | 43.4432 | -69.6657 |
| 47 | 43.3702 | -69.6103 | 47 | 43.3692 | -69.6098 | 47 | 43.3702 | -69.6088 |
| 48 | 43.3003 | -69.557 | 48 | 43.2988 | -69.5563 | 48 | 43.299 | -69.556 |
| 49 | 43.2292 | -69.4998 | 49 | 43.2305 | -69.4987 | 49 | 43.2338 | -69.4978 |
| 50 | 43.1572 | -69.4428 | 50 | 43.1587 | -69.4432 | 50 | 43.159 | -69.4425 |

| June 1998 | | | July 1998 | | | August 1998 | | |
|---|---|---|---|---|---|---|---|---|
| 51 | 43.0848 | -69.3897 | 51 | 43.0865 | -69.3903 | 51 | 43.0872 | -69.387 |
| 52 | 43.015 | -69.3305 | 52 | 43.0142 | -69.3317 | 52 | 43.0147 | -69.3303 |
| 53 | 42.942 | -69.275 | 53 | 42.9408 | -69.273 | 53 | 42.9407 | -69.2733 |
| 54 | 43.0593 | -69.0477 | 54 | 43.06 | -69.048 | 54 | 43.0583 | -69.0472 |
| 55 | 43.131 | -69.103 | 55 | 43.1338 | -69.1032 | 55 | 43.1315 | -69.1023 |
| 56 | 43.2043 | -69.1615 | 56 | 43.2027 | -69.1613 | 56 | 43.2023 | -69.1592 |
| 57 | 43.274 | -69.2182 | 57 | 43.275 | -69.2155 | 57 | 43.275 | -69.212 |
| 58 | 43.3478 | -69.2745 | 58 | 43.3475 | -69.274 | 58 | 43.3462 | -69.2773 |
| 59 | 43.419 | -69.3332 | 59 | 43.4195 | -69.3312 | 59 | 43.4188 | -69.3335 |
| 60 | 43.4893 | -69.3848 | 60 | 43.4925 | -69.386 | 60 | 43.4905 | -69.3888 |
| 61 | 43.5615 | -69.4455 | 61 | 43.5613 | -69.4457 | 61 | 43.5627 | -69.4478 |
| 62 | 43.6328 | -69.5057 | 62 | 43.6347 | -69.5035 | 62 | 43.6333 | -69.5053 |
| 63 | 43.7062 | -69.5613 | 63 | 43.7068 | -69.5597 | 63 | 43.7048 | -69.5627 |
| 64 | 43.766 | -69.6388 | 64 | 43.778 | -69.6353 | 64 | 43.7697 | -69.6318 |
| 65 | 43.8887 | -69.4027 | 65 | 43.8878 | -69.403 | 65 | 43.888 | -69.402 |
| 66 | 43.8398 | -69.3677 | 66 | 43.8393 | -69.3683 | 66 | 43.8342 | -69.3627 |
| 67 | 43.7895 | -69.3155 | 67 | 43.7892 | -69.3153 | 67 | 43.7917 | -69.3158 |
| 68 | 43.708 | -69.2515 | 68 | 43.7052 | -69.2543 | 68 | 43.7058 | -69.2517 |
| 69 | 43.6355 | -69.1928 | 69 | 43.6357 | -69.1965 | 69 | 43.6352 | -69.191 |
| 70 | 43.5637 | -69.1363 | 70 | 43.5635 | -69.1363 | 70 | 43.5647 | -69.1347 |
| 71 | 43.494 | -69.0762 | 71 | 43.4945 | -69.0777 | 71 | 43.4952 | -69.0753 |
| 72 | 43.4187 | -69.0198 | 72 | 43.4172 | -69.02 | 72 | 43.4172 | -69.018 |
| 73 | 43.3488 | -68.964 | 73 | 43.349 | -68.9617 | 73 | 43.3472 | -68.9603 |
| 74 | 43.2755 | -68.9087 | 74 | 43.2753 | -68.9083 | 74 | 43.2762 | -68.907 |
| 75 | 43.2037 | -68.8492 | 75 | 43.2033 | -68.8493 | 75 | 43.2018 | -68.8475 |
| 76 | 43.132 | -68.793 | 76 | 43.1313 | -68.7938 | 76 | 43.1298 | -68.7913 |
| 77 | 43.2597 | -68.5823 | 77 | 43.2603 | -68.582 | 77 | 43.2615 | -68.5845 |
| 78 | 43.3317 | -68.6408 | 78 | 43.3305 | -68.6407 | 78 | 43.328 | -68.64 |
| 79 | 43.4038 | -68.6967 | 79 | 43.4027 | -68.695 | 79 | 43.4027 | -68.6982 |
| 80 | 43.4767 | -68.7558 | 80 | 43.4763 | -68.7538 | 80 | 43.4743 | -68.7563 |
| 81 | 43.5465 | -68.8137 | 81 | 43.5472 | -68.8125 | 81 | 43.5462 | -68.8132 |
| 82 | 43.6207 | -68.87 | 82 | 43.62 | -68.8688 | 82 | 43.6168 | -68.8708 |
| 83 | 43.6923 | -68.9267 | 83 | 43.6925 | -68.9263 | 83 | 43.6915 | -68.9263 |
| 84 | 43.7658 | -68.986 | 84 | 43.7648 | -68.9862 | 84 | 43.7657 | -68.9873 |
| 85 | 43.8383 | -69.0442 | 85 | 43.838 | -69.0442 | 85 | 43.8393 | -69.0438 |
| 86 | 43.9093 | -69.0993 | 86 | 43.9108 | -69.1003 | 86 | 43.9112 | -69.0987 |
| 87 | 43.9662 | -69.1438 | 87 | 43.9655 | -69.1428 | 87 | 43.9653 | -69.1492 |
| 88 | 44.1088 | -68.9825 | 91 | 43.8917 | -68.8098 | 88 | 44.1085 | -68.9807 |
| 89 | 44.0288 | -68.9472 | 92 | 43.8188 | -68.7528 | 89 | 44.0223 | -68.9098 |
| 90 | 43.962 | -68.8647 | 93 | 43.7467 | -68.6943 | 90 | 43.9518 | -68.8688 |
| 91 | 43.8915 | -68.8103 | 94 | 43.6732 | -68.633 | 91 | 43.8927 | -68.8065 |
| 92 | 43.818 | -68.7523 | 95 | 43.5995 | -68.578 | 92 | 43.8198 | -68.7498 |
| 93 | 43.747 | -68.6928 | 96 | 43.5285 | -68.5202 | 93 | 43.7477 | -68.6933 |
| 94 | 43.6747 | -68.6372 | 97 | 43.454 | -68.464 | 94 | 43.6758 | -68.6372 |
| 95 | 43.6005 | -68.579 | 98 | 43.3847 | -68.4065 | 95 | 43.6015 | -68.578 |
| 96 | 43.5298 | -68.522 | 99 | 43.314 | -68.3483 | 96 | 43.531 | -68.5232 |
| 97 | 43.4573 | -68.4643 | 100 | 43.41 | -68.137 | 97 | 43.455 | -68.4645 |
| 98 | 43.3853 | -68.4087 | 101 | 43.483 | -68.1963 | 98 | 43.3865 | -68.4048 |
| 99 | 43.3148 | -68.349 | 102 | 43.555 | -68.2537 | 99 | 43.3145 | -68.3495 |
| 100 | 43.4115 | -68.1383 | 103 | 43.6263 | -68.3102 | 100 | 43.4107 | -68.138 |
| 101 | 43.4833 | -68.1968 | 104 | 43.6995 | -68.3678 | 101 | 43.4832 | -68.1962 |

| June 1998 | | | July 1998 | | | August 1998 | | |
|---|---|---|---|---|---|---|---|---|
| 102 | 43.5553 | -68.2527 | 105 | 43.7707 | -68.427 | 102 | 43.5545 | -68.254 |
| 103 | 43.6262 | -68.3103 | 106 | 43.8415 | -68.485 | 103 | 43.6268 | -68.3077 |
| 104 | 43.6997 | -68.3683 | 107 | 43.914 | -68.5417 | 104 | 43.7012 | -68.3648 |
| 105 | 43.774 | -68.4303 | 108 | 43.9863 | -68.6017 | 105 | 43.7685 | -68.4273 |
| 106 | 43.8418 | -68.484 | 109 | 44.0332 | -68.7015 | 106 | 43.8422 | -68.4855 |
| 107 | 43.9127 | -68.5422 | 110 | 44.106 | -68.7422 | 107 | 43.9128 | -68.542 |
| 108 | 43.9873 | -68.6007 | 111 | 44.1712 | -68.7672 | 108 | 43.9873 | -68.6025 |
| 109 | 44.0347 | -68.7053 | 112 | 44.137 | -68.5497 | 109 | 44.0363 | -68.7008 |
| 110 | 44.1053 | -68.742 | 113 | 44.2073 | -68.3993 | 110 | 44.103 | -68.7402 |
| 111 | 44.1715 | -68.7665 | 114 | 44.0732 | -68.396 | 111 | 44.1693 | -68.7653 |
| 112 | 44.1392 | -68.55 | 115 | 44.002 | -68.3343 | 112 | 44.139 | -68.5342 |
| 113 | 44.2082 | -68.3995 | 116 | 43.9278 | -68.278 | 113 | 44.2068 | -68.3968 |
| 114 | 44.0737 | -68.3985 | 117 | 43.8558 | -68.2178 | 114 | 44.074 | -68.3938 |
| 115 | 44.0013 | -68.3327 | 118 | 43.7845 | -68.1612 | 115 | 44.0035 | -68.3355 |
| 116 | 43.927 | -68.2758 | 119 | 43.7143 | -68.1028 | 116 | 43.9287 | -68.2782 |
| 117 | 43.8565 | -68.2173 | 120 | 43.6427 | -68.0457 | 117 | 43.8572 | -68.2192 |
| 118 | 43.7858 | -68.0766 | 121 | 43.5707 | -67.9867 | 118 | 43.7855 | -68.16 |
| 119 | 43.713 | -68.1008 | 122 | 43.499 | -67.9302 | 119 | 43.7138 | -68.1032 |
| 120 | 43.6422 | -68.0447 | 123 | 43.61 | -67.7275 | 120 | 43.6412 | -68.045 |
| 121 | 43.5705 | -67.9862 | 124 | 43.6842 | -67.7827 | 121 | 43.5683 | -67.9882 |
| 122 | 43.4982 | -67.93 | 125 | 43.7532 | -67.8412 | 122 | 43.4953 | -67.9305 |
| 123 | 43.6105 | -67.7252 | 126 | 43.8263 | -67.8987 | 123 | 43.611 | -67.7277 |
| 124 | 43.6818 | -67.784 | 127 | 43.8993 | -67.9565 | 124 | 43.6828 | -67.7858 |
| 125 | 43.7552 | -67.842 | 128 | 43.9703 | -68.015 | 125 | 43.757 | -67.8413 |
| 126 | 43.827 | -67.9002 | 129 | 44.0405 | -68.0752 | 126 | 43.828 | -67.8997 |
| 127 | 43.8993 | -67.9573 | 130 | 44.1113 | -68.133 | 127 | 43.901 | -67.9603 |
| 128 | 43.97 | -68.0148 | 131 | 44.185 | -68.1832 | 128 | 43.9692 | -68.0138 |
| 129 | 44.0408 | -68.074 | 132 | 44.2262 | -68.2187 | 129 | 44.0432 | -68.0728 |
| 130 | 44.1125 | -68.1326 | 133 | 44.3453 | -68.1338 | 130 | 44.1125 | -68.1312 |
| 131 | 44.187 | -68.1852 | 134 | 44.331 | -68.0103 | 131 | 44.1857 | -68.1867 |
| 132 | 44.2268 | -68.2225 | 135 | 44.262 | -67.9523 | 132 | 44.227 | -68.2218 |
| 133 | 44.3485 | -68.1323 | 136 | 44.1893 | -67.8955 | 133 | 44.3468 | -68.1327 |
| 134 | 44.3332 | -68.01 | 137 | 44.1187 | -67.8357 | 134 | 44.3327 | -68.0105 |
| 135 | 44.2608 | -67.9523 | 138 | 44.0442 | -67.7765 | 135 | 44.2607 | -67.9522 |
| 136 | 44.1893 | -67.8948 | 139 | 43.9708 | -67.7213 | 136 | 44.1887 | -67.8947 |
| 137 | 44.1155 | -67.8362 | 140 | 43.8992 | -67.6642 | 137 | 44.1172 | -67.834 |
| 138 | 44.0445 | -67.7798 | 141 | 43.8288 | -67.605 | 138 | 44.0445 | -67.7758 |
| 139 | 43.9723 | -67.7213 | 142 | 43.7568 | -67.5463 | 139 | 43.9747 | -67.7183 |
| 140 | 43.8995 | -67.6622 | 143 | 43.6838 | -67.4895 | 140 | 43.9003 | -67.661 |
| 141 | 43.828 | -67.6032 | 144 | 43.7903 | -67.2947 | 141 | 43.8288 | -67.6043 |
| 142 | 43.7562 | -67.546 | 145 | 43.8625 | -67.3512 | 142 | 43.7565 | -67.5478 |
| 143 | 43.6839 | -67.4887 | 146 | 43.934 | -67.412 | 143 | 43.6837 | -67.4892 |
| 144 | 43.7925 | -67.2922 | 147 | 44.006 | -67.4678 | 144 | 43.7903 | -67.2952 |
| 145 | 43.8645 | -67.3523 | 148 | 44.0798 | -67.527 | 145 | 43.8635 | -67.3535 |
| 146 | 43.935 | -67.4107 | 149 | 44.1513 | -67.5908 | 146 | 43.9313 | -67.4142 |
| 147 | 44.0063 | -67.4682 | 150 | 44.2217 | -67.6425 | 147 | 44.0052 | -67.4693 |
| 148 | 44.0813 | -67.5255 | 151 | 44.2945 | -67.7 | 148 | 44.0798 | -67.5277 |
| 149 | 44.1537 | -67.5853 | 152 | 44.3683 | -67.7578 | 149 | 44.152 | -67.5858 |
| 150 | 44.223 | -67.6422 | 153 | 44.4065 | -67.7923 | 150 | 44.2227 | -67.6415 |
| 151 | 44.2945 | -67.6995 | 154 | 44.4508 | -67.5158 | 151 | 44.2912 | -67.669 |
| 152 | 44.3695 | -67.7605 | 155 | 44.3787 | -67.4638 | 152 | 44.3572 | -67.7207 |

| June 1998 | | | July 1998 | | | August 1998 | | |
|---|---|---|---|---|---|---|---|---|
| 153 | 44.408 | -67.7928 | 156 | 44.3077 | -67.4067 | 153 | 44.407 | -67.7942 |
| 154 | 44.4535 | -67.5197 | 157 | 44.2348 | -67.3467 | 154 | 44.4508 | -67.5215 |
| 155 | 44.3785 | -67.4635 | 158 | 44.1593 | -67.2885 | 155 | 44.3752 | -67.465 |
| 156 | 44.3075 | -67.4043 | 159 | 44.089 | -67.23 | 156 | 44.3058 | -67.4045 |
| 157 | 44.2318 | -67.3432 | 160 | 44.0152 | -67.1698 | 157 | 44.2307 | -67.3435 |
| 158 | 44.1588 | -67.287 | 161 | 43.9442 | -67.1155 | 158 | 44.1597 | -67.2868 |
| 159 | 44.0887 | -67.2305 | 162 | 43.8717 | -67.0578 | 159 | 44.092 | -67.2287 |
| 160 | 44.0167 | -67.1722 | 163 | 43.9612 | -66.8432 | 160 | 44.0173 | -67.1713 |
| 161 | 43.9442 | -67.1165 | 164 | 44.0325 | -66.8997 | 161 | 43.9447 | -67.1147 |
| 162 | 43.8732 | -67.0572 | 165 | 44.104 | -66.9565 | 162 | 43.8738 | -67.0585 |
| 163 | 43.9622 | -66.841 | 166 | 44.1752 | -67.0102 | 163 | 43.9625 | -66.843 |
| 164 | 44.0338 | -66.8983 | 167 | 44.2475 | -67.075 | 164 | 44.032 | -66.8962 |
| 165 | 44.1057 | -66.9558 | 168 | 44.3165 | -67.1308 | 165 | 44.1037 | -66.9575 |
| 166 | 44.1753 | -67.012 | 169 | 44.3933 | -67.1837 | 166 | 44.1732 | -67.015 |
| 167 | 44.2483 | -67.073 | 170 | 44.4668 | -67.2447 | 167 | 44.2477 | -67.0763 |
| 168 | 44.3187 | -67.1323 | 171 | 44.5385 | -67.3003 | 168 | 44.3157 | -67.1333 |
| 169 | 44.3923 | -67.184 | 172 | 44.5765 | -67.3263 | 169 | 44.391 | -67.1888 |
| 170 | 44.4638 | -67.2432 | 173 | 44.6532 | -67.0778 | 170 | 44.4655 | -67.245 |
| 171 | 44.5357 | -67.304 | 174 | 44.6002 | -67.0218 | 171 | 44.5418 | -67.3022 |
| 173 | 44.653 | -67.0778 | 175 | 44.5348 | -66.946 | 172 | 44.6065 | -67.3418 |
| 174 | 44.6018 | -67.0208 | 176 | 44.437 | -66.8422 | 173 | 44.6578 | -67.0752 |
| 175 | 44.5345 | -66.9467 | 177 | 44.3662 | -66.753 | 174 | 44.6018 | -67.0197 |
| 176 | 44.437 | -66.8422 | 178 | 44.3062 | -66.6847 | 175 | 44.5343 | -66.9455 |
| 177 | 44.3665 | -66.7565 | 179 | 44.2625 | -66.627 | 176 | 44.4338 | -66.8432 |
| 178 | 44.3065 | -66.6833 | 180 | 44.2097 | -66.5553 | 177 | 44.366 | -66.7515 |
| 179 | 44.2608 | -66.6235 | 181 | 44.128 | -66.4638 | 178 | 44.3072 | -66.6842 |
| 180 | 44.2105 | -66.5507 | 182 | 44.4485 | -66.233 | 179 | 44.2575 | -66.6248 |
| 181 | 44.105 | -66.4473 | 183 | 44.5132 | -66.3077 | 180 | 44.2043 | -66.5537 |
| 182 | 44.4487 | -66.2338 | 184 | 44.576 | -66.3792 | 182 | 44.4515 | -66.2295 |
| 183 | 44.5142 | -66.3058 | 185 | 44.6433 | -66.4595 | 183 | 44.5157 | -66.3045 |
| 184 | 44.5767 | -66.3807 | 186 | 44.7015 | -66.5285 | 184 | 44.5795 | -66.3772 |
| 185 | 44.641 | -66.4587 | 187 | 44.768 | -66.6087 | 185 | 44.6467 | -66.4565 |
| 186 | 44.7058 | -66.5335 | 188 | 44.8317 | -66.6837 | 186 | 44.7088 | -66.5312 |
| 187 | 44.7715 | -66.606 | 189 | 44.8985 | -66.7538 | 187 | 44.7685 | -66.6102 |
| 188 | 44.8328 | -66.6847 | 190 | 44.959 | -66.8335 | 188 | 44.8318 | -66.6842 |
| 189 | 44.8995 | -66.7558 | 191 | 45.0267 | -66.8845 | 189 | 44.8983 | -66.7582 |
| 190 | 44.964 | -66.8313 | 192 | 45.068 | -66.9813 | 190 | 44.9585 | -66.8328 |
| 193 | 45.0308 | -66.413 | 193 | 45.0323 | -66.4115 | 191 | 45.0212 | -66.8855 |
| 194 | 44.9682 | -66.34 | 194 | 44.9678 | -66.3385 | 193 | 45.0325 | -66.416 |
| 195 | 44.9037 | -66.2638 | 195 | 44.904 | -66.2625 | 194 | 44.9662 | -66.3368 |
| 196 | 44.841 | -66.1887 | 196 | 44.8387 | -66.1893 | 195 | 44.9053 | -66.2607 |
| 197 | 44.7757 | -66.1123 | 197 | 44.774 | -66.111 | 196 | 44.841 | -66.1842 |
| 198 | 44.7113 | -66.0358 | 198 | 44.7113 | -66.0378 | 197 | 44.7745 | -66.1105 |
| 199 | 44.6495 | -65.9625 | 199 | 44.645 | -65.9687 | 198 | 44.712 | -66.0325 |
| 200 | 44.2569 | -66.3539 | 200 | 44.115 | -66.4285 | 199 | 44.6485 | -65.9633 |
| 201 | 43.8643 | -66.7453 | 201 | 43.8642 | -66.743 | 200 | 44.0468 | -66.3672 |
| 202 | 43.7762 | -66.9773 | 202 | 43.776 | -66.9748 | 201 | 43.8643 | -66.7448 |
| 203 | 43.676 | -67.1998 | 203 | 43.6745 | -67.2018 | 202 | 43.7602 | -66.9755 |
| 204 | 43.5845 | -67.4175 | 204 | 43.5835 | -67.4165 | 203 | 43.6757 | -67.2 |
| 205 | 43.4928 | -67.6338 | 205 | 43.491 | -67.6318 | 204 | 43.5845 | -67.4142 |
| 206 | 43.398 | -67.8473 | 206 | 43.398 | -67.8465 | 205 | 43.4923 | -67.6318 |

| June 1998 | | | July 1998 | | | August 1998 | | |
|---|---|---|---|---|---|---|---|---|
| 207 | 43.3172 | -68.0485 | 207 | 43.3163 | -68.0467 | 206 | 43.3962 | -67.8443 |
| 208 | 43.2212 | -68.2675 | 208 | 43.222 | -68.2668 | 207 | 43.3163 | -68.0485 |
| 209 | 43.1328 | -68.4957 | 209 | 43.131 | -68.4947 | 208 | 43.2218 | -68.2698 |
| 210 | 43.0332 | -68.7077 | 210 | 43.0327 | -68.7065 | 209 | 43.1305 | -68.4942 |
| 211 | 42.933 | -68.9492 | 211 | 42.9325 | -68.9452 | 210 | 43.0325 | -68.7075 |
| 212 | 42.8412 | -69.1765 | 212 | 42.8403 | -69.1755 | 211 | 42.9298 | -68.948 |
| 213 | 42.7372 | -69.4122 | 213 | 42.7367 | -69.4118 | 212 | 42.8402 | -69.1763 |
| 214 | 42.6373 | -69.6469 | 214 | 42.6368 | -69.6483 | 213 | 42.7355 | -69.4118 |
| 215 | 42.5411 | -69.8724 | 215 | 42.5417 | -69.8725 | 214 | 42.6368 | -69.6488 |
| | | | | | | 215 | 42.5415 | -69.8723 |

| May 2000 | | | June 2000 | | |
|---|---|---|---|---|---|
| Station # | Latitude | Longitude | Station # | Latitude | Longitude |
| 1 | 43.10 | -70.61 | 1 | 43.651 | -70.142 |
| 2 | 43.05 | -70.56 | 2 | 43.584 | -70.085 |
| 3 | 43.00 | -70.52 | 3 | 43.514 | -70.033 |
| 4 | 42.92 | -70.47 | 4 | 43.451 | -69.981 |
| 5 | 42.85 | -70.41 | 5 | 43.369 | -69.917 |
| 6 | 42.78 | -70.35 | 6 | 43.296 | -69.859 |
| 7 | 42.71 | -70.30 | 7 | 43.221 | -69.796 |
| 8 | 42.64 | -70.23 | 8 | 43.149 | -69.735 |
| 19 | 43.47 | -70.30 | 9 | 43.079 | -69.683 |
| 20 | 43.40 | -70.25 | 10 | 43.004 | -69.634 |
| 21 | 43.33 | -70.19 | 11 | 42.935 | -69.579 |
| 22 | 43.25 | -70.13 | 12 | 42.849 | -69.511 |
| 23 | 43.18 | -70.08 | 13 | 42.752 | -69.443 |
| 24 | 43.11 | -70.02 | 14 | 42.928 | -68.961 |
| 25 | 43.04 | -69.96 | 15 | 43.039 | -69.037 |
| 26 | 42.97 | -69.91 | 16 | 43.122 | -69.104 |
| 27 | 42.90 | -69.85 | 17 | 43.188 | -69.160 |
| 28 | 42.83 | -69.80 | 18 | 43.267 | -69.214 |
| 29 | 42.76 | -69.74 | 19 | 43.341 | -69.276 |
| 42 | 43.72 | -69.91 | 20 | 43.412 | -69.300 |
| 43 | 43.66 | -69.83 | 21 | 43.492 | -69.391 |
| 44 | 43.58 | -69.78 | 22 | 43.562 | -69.446 |
| 45 | 43.51 | -69.72 | 23 | 43.633 | -69.505 |
| 46 | 43.44 | -69.67 | 24 | 43.706 | -69.561 |
| 47 | 43.37 | -69.61 | 25 | 43.766 | -69.555 |
| 48 | 43.30 | -69.56 | 26 | 43.888 | -69.402 |
| 65 | 43.89 | -69.40 | 27 | 43.840 | -69.368 |
| 66 | 43.84 | -69.37 | 28 | 43.790 | -69.315 |
| 67 | 43.79 | -69.32 | 29 | 43.725 | -69.266 |
| 68 | 43.71 | -69.25 | 30 | 43.648 | -69.206 |
| 69 | 43.64 | -69.20 | 31 | 43.575 | -69.145 |
| 70 | 43.56 | -69.14 | 32 | 43.506 | -69.089 |
| 71 | 43.49 | -69.07 | 33 | 43.954 | -69.135 |
| 72 | 43.42 | -69.02 | 34 | 43.885 | -69.083 |
| 73 | 43.35 | -68.96 | 35 | 43.818 | -69.032 |
| 74 | 43.27 | -68.91 | 36 | 43.748 | -68.973 |
| 75 | 43.20 | -68.85 | 37 | 43.672 | -68.912 |
| 76 | 43.13 | -68.80 | 38 | 43.601 | -68.852 |
| 90 | 43.96 | -68.89 | 39 | 43.530 | -68.795 |
| 91 | 43.89 | -68.81 | 40 | 43.456 | -68.736 |
| 92 | 43.82 | -68.75 | 41 | 43.383 | -68.687 |
| 93 | 43.75 | -68.69 | 42 | 43.309 | -68.624 |
| 94 | 43.67 | -68.64 | 43 | 43.234 | -68.565 |
| 95 | 43.60 | -68.58 | 44 | 43.130 | -68.478 |
| 96 | 43.53 | -68.52 | 45 | 43.221 | -68.267 |
| 97 | 43.46 | -68.46 | 46-1 | 43.326 | -68.350 |
| 98 | 43.39 | -68.41 | 46-2 | 43.321 | -68.339 |
| 99 | 43.32 | -68.35 | 46-3 | 43.316 | -68.329 |
| 114 | 44.07 | -68.39 | 46-4 | 43.302 | -68.322 |
| 115 | 44.00 | -68.34 | 46-5 | 43.293 | -68.318 |

| May 2000 | | | June 2000 | | |
|---|---|---|---|---|---|
| Station # | Latitude | Longitude | Station # | Latitude | Longitude |
| 116 | 43.93 | -68.28 | 46-6 | 43.283 | -68.316 |
| 117 | 43.85 | -68.22 | 46-7 | 43.278 | -68.311 |
| 118 | 43.78 | -68.16 | 46-8 | 43.275 | -68.313 |
| 119 | 43.71 | -68.10 | 46-9 | 43.280 | -68.310 |
| 120 | 43.64 | -68.04 | 46-10 | 43.288 | -68.316 |
| 121 | 43.57 | -67.99 | 46-11 | 43.298 | -68.320 |
| 122 | 43.50 | -67.93 | 46-12 | 43.310 | -68.316 |
| 123 | 43.61 | -67.72 | 46-13 | 43.322 | -68.314 |
| 124 | 43.68 | -67.78 | 46-14 | 43.322 | -68.312 |
| 125 | 43.75 | -67.84 | 46-15 | 43.331 | -68.301 |
| 126 | 43.83 | -67.90 | 46-16 | 43.331 | -68.289 |
| 127 | 43.90 | -67.96 | 46-17 | 43.327 | -68.274 |
| 128 | 43.97 | -68.01 | 46-18 | 43.327 | -68.265 |
| 129 | 44.04 | -68.07 | 46-19 | 43.324 | -68.257 |
| 130 | 44.11 | -68.14 | 46-20 | 43.321 | -68.245 |
| 131 | 44.19 | -68.18 | 46-21 | 43.325 | -68.240 |
| 132 | 44.22 | -68.22 | 46-22 | 43.333 | -68.233 |
| 133 | 44.34 | -68.13 | 46-23 | 43.357 | -68.230 |
| 134 | 44.33 | -68.01 | 46-24 | 43.350 | -68.223 |
| 135 | 44.26 | -67.95 | 46-25 | 43.357 | -68.217 |
| 136 | 44.19 | -67.90 | 47 | 43.394 | -68.412 |
| 137 | 44.12 | -67.84 | 48 | 43.470 | -68.463 |
| 138 | 44.04 | -67.78 | 49 | 43.530 | -68.521 |
| 139 | 43.97 | -67.72 | 50 | 43.600 | -68.578 |
| 140 | 43.90 | -67.66 | 51 | 43.657 | -68.629 |
| 141 | 43.83 | -67.60 | 52 | 43.746 | -68.694 |
| 142 | 43.76 | -67.55 | 53 | 43.818 | -68.752 |
| 143 | 43.68 | -67.49 | 54 | 43.893 | -68.809 |
| 144 | 43.79 | -67.29 | 55 | 43.967 | -68.867 |
| 145 | 43.86 | -67.35 | 56 | 44.029 | -68.947 |
| 146 | 43.93 | -67.41 | 57 | 44.109 | -68.983 |
| 147 | 44.01 | -67.47 | 58 | 44.106 | -68.742 |
| 148 | 44.08 | -67.53 | 59 | 44.140 | -68.553 |
| 149 | 44.15 | -67.59 | 60 | 44.073 | -68.396 |
| 150 | 44.22 | -67.64 | 61 | 44.002 | -68.340 |
| 151 | 44.29 | -67.70 | 62 | 43.930 | -68.276 |
| 152 | 44.37 | -67.76 | 63 | 43.857 | -68.217 |
| 153 | 44.41 | -67.79 | 64 | 43.786 | -68.160 |
| 154 | 44.45 | -67.52 | 65 | 43.714 | -68.105 |
| 155 | 44.38 | -67.46 | 66 | 43.643 | -68.045 |
| 156 | 44.31 | -67.41 | 67 | 43.572 | -67.986 |
| 157 | 44.23 | -67.35 | 68 | 43.499 | -67.932 |
| 158 | 44.16 | -67.29 | 69 | 43.398 | -67.849 |
| 159 | 44.09 | -67.23 | 70 | 43.583 | -67.417 |
| 160 | 44.02 | -67.17 | 71 | 43.682 | -67.491 |
| 161 | 43.94 | -67.12 | 72 | 43.755 | -67.551 |
| 162 | 43.87 | -67.06 | 73 | 43.826 | -67.606 |
| 163 | 43.96 | -66.84 | 74 | 43.900 | -67.661 |
| 164 | 44.03 | -66.90 | 75 | 43.976 | -67.725 |
| 165 | 44.11 | -66.96 | 76 | 44.045 | -67.778 |

| May 2000 | | | June 2000 | | |
|---|---|---|---|---|---|
| Station # | Latitude | Longitude | Station # | Latitude | Longitude |
| 166 | 44.18 | -67.01 | 77 | 44.117 | -67.835 |
| 167 | 44.25 | -67.07 | 78 | 44.189 | -67.895 |
| 168 | 44.32 | -67.13 | 79 | 44.261 | -67.952 |
| 169 | 44.39 | -67.18 | 80 | 44.317 | -68.006 |
| 170 | 44.46 | -67.24 | 81 | 44.453 | -67.521 |
| 171 | 44.54 | -67.31 | 82 | 44.379 | -67.467 |
| 172 | 44.61 | -67.34 | 83 | 44.308 | -67.406 |
| 173 | 44.65 | -67.08 | 84 | 44.232 | -67.345 |
| 174 | 44.60 | -67.02 | 85 | 44.159 | -67.289 |
| 175 | 44.53 | -66.95 | 86 | 44.089 | -67.232 |
| 176 | 44.44 | -66.84 | 87 | 44.016 | -67.173 |
| 177 | 44.37 | -66.76 | 88 | 43.945 | -67.115 |
| 178 | 44.31 | -66.68 | 89 | 43.873 | -67.059 |
| 179 | 44.26 | -66.63 | 90 | 43.776 | -66.977 |
| 180 | 44.21 | -66.55 | 91 | 44.132 | -66.466 |
| 181 | 44.11 | -66.45 | 92 | 44.199 | -66.547 |
| 182 | 44.45 | -66.23 | 93 | 44.259 | -66.619 |
| 183 | 44.52 | -66.30 | 94 | 44.316 | -66.686 |
| 184 | 44.58 | -66.38 | 95 | 44.377 | -66.753 |
| 185 | 44.64 | -66.46 | 96 | 44.447 | -66.838 |
| 186 | 44.71 | -66.53 | 97 | 44.540 | -66.945 |
| 187 | 44.77 | -66.61 | 98 | 44.602 | -67.020 |
| 188 | 44.83 | -66.68 | 99 | 44.666 | -67.093 |
| 189 | 44.90 | -66.76 | 101 | 45.026 | -66.884 |
| 190 | 44.96 | -66.83 | 102 | 44.960 | -66.813 |
| 191 | 45.03 | -66.88 | 103 | 44.898 | -66.758 |
| 192 | 45.07 | -66.98 | 104 | 44.833 | -66.685 |
| 193 | 45.03 | -66.41 | 105 | 44.768 | -66.611 |
| 194 | 44.97 | -66.33 | 106 | 44.706 | -66.533 |
| 195 | 44.91 | -66.26 | 107 | 44.644 | -66.459 |
| 196 | 44.84 | -66.19 | 108 | 44.577 | -66.382 |
| 197 | 44.78 | -66.11 | 109 | 44.515 | -66.307 |
| 198 | 44.71 | -66.03 | 110 | 44.449 | -66.234 |
| 199 | 44.65 | -65.96 | 111 | 44.649 | -65.965 |
| 200 | 43.92 | -66.50 | 112 | 44.712 | -66.036 |
| 300 | 43.75 | -66.30 | 113 | 44.776 | -66.113 |
| 301 | 43.71 | -66.41 | 114 | 44.841 | -66.189 |
| 302 | 43.69 | -66.54 | 115 | 44.902 | -66.265 |
| 303 | 43.67 | -66.67 | 116 | 44.969 | -66.341 |
| 304 | 43.65 | -66.81 | 117 | 45.031 | -66.414 |
| 305 | 43.63 | -66.95 | 118 | 44.048 | -66.368 |
| 306 | 43.60 | -67.08 | 119 | 43.881 | -66.368 |
| 307 | 43.58 | -67.21 | 120 | 43.705 | -66.369 |
| 308 | 43.56 | -67.35 | 121 | 43.518 | -66.368 |
| 309 | 43.53 | -67.48 | 122 | 43.335 | -66.368 |
| 310 | 43.52 | -67.60 | 123 | 43.153 | -66.375 |
| 342 | 43.73 | -69.91 | 124 | 44.977 | -66.369 |
| 343 | 43.66 | -69.83 | 125 | 42.800 | -66.367 |
| 344 | 43.58 | -69.78 | 126 | 42.654 | -66.367 |
| 345 | 43.51 | -69.72 | 127 | 42.515 | -66.367 |

| May 2000 | | |
|---|---|---|
| Station # | Latitude | Longitude |
| 346 | 43.44 | -69.67 |
| 347 | 43.37 | -69.61 |
| 348 | 43.30 | -69.56 |
| 349 | 43.23 | -69.50 |
| 350 | 43.16 | -69.44 |
| 351 | 43.09 | -69.39 |
| 352 | 43.01 | -69.33 |
| 353 | 42.94 | -69.27 |

| June 2000 | | |
|---|---|---|
| Station # | Latitude | Longitude |
| 128 | 42.513 | -66.817 |
| 129 | 42.654 | -66.831 |
| 130 | 42.798 | -66.832 |
| 131 | 42.980 | -66.833 |
| 132 | 43.154 | -66.834 |
| 133 | 43.152 | -67.065 |
| 134 | 43.153 | -67.292 |
| 135 | 43.151 | -67.521 |
| 136 | 43.156 | -67.742 |
| 137 | 43.150 | -67.967 |
| 138 | 43.150 | -68.190 |
| 139 | 43.250 | -68.333 |
| 140-1 | 43.328 | -68.456 |
| 140-2 | 43.327 | -68.459 |
| 140-3 | 43.331 | -68.466 |
| 140-4 | 43.335 | -68.467 |
| 140-5 | 43.342 | -68.470 |
| 140-6 | 43.346 | -68.468 |
| 140-7 | 43.351 | -68.470 |
| 140-8 | 43.354 | -68.470 |
| 140-9 | 43.354 | -68.469 |
| 140-10 | 43.347 | -68.457 |
| 140-11 | 43.337 | -68.452 |
| 140-12 | 43.330 | -68.453 |
| 140-13 | 43.324 | -68.456 |
| 140-14 | 43.320 | -68.457 |
| 140-15 | 43.313 | -68.464 |
| 140-16 | 43.317 | -68.460 |
| 140-17 | 43.320 | -68.456 |
| 140-18 | 43.327 | -68.459 |
| 140-19 | 43.332 | -68.462 |
| 140-20 | 43.339 | -68.459 |
| 140-21 | 43.341 | -68.458 |
| 140-22 | 43.339 | -68.458 |
| 140-23 | 43.331 | -68.454 |
| 140-24 | 43.328 | -68.453 |
| 140-25 | 43.320 | -68.459 |
| 946 | 43.319 | -68.352 |
| 947 | 43.394 | -68.411 |

# Appendix B

# AVAILABLE *IN SITU* DATA

| In situ *Parameter Measured* | *Dates of Available Data* |
|---|---|
| Salinity | June 6, 1998 – June 16, 1998<br>July 6, 1998 – July 16, 1998<br>August 4, 1998 – August 16, 1998<br>April 22, 2000 – May 4, 2000<br>June 5, 2000 – June 15, 2000 |
| Temperature (°C) | June 6, 1998 – June 16, 1998<br>July 6, 1998 – July 16, 1998<br>August 4, 1998 – August 16, 1998<br>April 22, 2000 – May 4, 2000<br>June 5, 2000 – June 15, 2000 |
| $\theta_t$ | June 6, 1998 – June 16, 1998<br>July 6, 1998 – July 16, 1998<br>August 4, 1998 – August 16, 1998<br>April 22, 2000 – May 4, 2000<br>June 5, 2000 – June 15, 2000 |
| Depth of Sample Measurement | June 6, 1998 – June 16, 1998<br>July 6, 1998 – July 16, 1998<br>August 4, 1998 – August 16, 1998 |
| Depth of Water Column | April 22, 2000 – May 4, 2000<br>June 5, 2000 – June 15, 2000 |
| Pressure (db) | June 6, 1998 – June 16, 1998<br>July 6, 1998 – July 16, 1998<br>August 4, 1998 – August 16, 1998<br>April 22, 2000 – May 4, 2000<br>June 5, 2000 – June 15, 2000 |
| Fluorescence (v) | June 6, 1998 – June 16, 1998<br>July 6, 1998 – July 16, 1998<br>August 4, 1998 – August 16, 1998<br>April 22, 2000 – May 4, 2000<br>June 5, 2000 – June 15, 2000 |
| Chlorophyll a (μg/L) | June 6, 1998 – June 16, 1998<br>July 6, 1998 – July 16, 1998<br>August 4, 1998 – August 16, 1998<br>April 22, 2000 – May 4, 2000<br>June 5, 2000 – June 15, 2000 |
| Phaeopigments | June 6, 1998 – June 16, 1998<br>July 6, 1998 – July 16, 1998<br>August 4, 1998 – August 16, 1998<br>April 22, 2000 – May 4, 2000<br>June 5, 2000 – June 15, 2000 |

| | |
|---|---|
| $NO_3/N0_2$ (μM) | June 6, 1998 – June 16, 1998<br>July 6, 1998 – July 16, 1998<br>August 4, 1998 – August 16, 1998<br>April 22, 2000 – May 4, 2000<br>June 5, 2000 – June 15, 2000 |
| $SiO_4$ (μM) | June 6, 1998 – June 16, 1998<br>July 6, 1998 – July 16, 1998<br>August 4, 1998 – August 16, 1998<br>April 22, 2000 – May 4, 2000<br>June 5, 2000 – June 15, 2000 |
| $NH_4$ (μM) | June 6, 1998 – June 16, 1998<br>July 6, 1998 – July 16, 1998<br>August 4, 1998 – August 16, 1998<br>April 22, 2000 – May 4, 2000<br>June 5, 2000 – June 15, 2000 |
| $PO_4$ (μM) | June 6, 1998 – June 16, 1998<br>July 6, 1998 – July 16, 1998<br>August 4, 1998 – August 16, 1998<br>April 22, 2000 – May 4, 2000<br>June 5, 2000 – June 15, 2000 |
| *Alexandrium* (cells/L) | June 6, 1998 – June 16, 1998<br>July 6, 1998 – July 16, 1998<br>August 4, 1998 – August 16, 1998<br>April 22, 2000 – May 4, 2000<br>June 5, 2000 – June 15, 2000 |

# Appendix C

# AVAILABLE SATELLITE DATA

## *AVHRR SST*
## June 1998

| | | |
|---|---|---|
| n12.98152.1132.mcsst | n12.98165.2130.mcsst | n14.98159.0811.mcsst |
| n12.98152.2117.mcsst | n12.98166.2109.mcsst | n14.98159.1759.mcsst |
| n12.98152.2257.mcsst | n12.98166.2248.mcsst | n14.98160.0759.mcsst |
| n12.98153.1110.mcsst | n12.98167.1102.mcsst | n14.98161.0748.mcsst |
| n12.98153.2234.mcsst | n12.98167.2225.mcsst | n14.98161.1918.mcsst |
| n12.98154.1048.mcsst | n12.98168.1040.mcsst | n14.98162.0737.mcsst |
| n12.98154.2211.mcsst | n12.98168.2203.mcsst | n14.98162.1906.mcsst |
| n12.98155.1027.mcsst | n12.98169.1019.mcsst | n14.98163.0726.mcsst |
| n12.98155.1208.mcsst | n12.98169.1159.mcsst | n14.98163.1855.mcsst |
| n12.98155.2149.mcsst | n12.98169.2141.mcsst | n14.98164.0716.mcsst |
| n12.98156.1144.mcsst | n12.98170.1136.mcsst | n14.98164.1844.mcsst |
| n12.98156.2128.mcsst | n12.98170.2120.mcsst | n14.98165.0705.mcsst |
| n12.98157.1122.mcsst | n12.98173.2153.mcsst | n14.98165.0846.mcsst |
| n12.98157.2107.mcsst | n12.98174.2131.mcsst | n14.98165.1833.mcsst |
| n12.98157.2246.mcsst | n12.98175.1126.mcsst | n14.98166.0834.mcsst |
| n12.98158.1100.mcsst | n12.98175.2110.mcsst | n14.98166.1822.mcsst |
| n12.98158.2223.mcsst | n12.98175.2250.mcsst | n14.98167.0823.mcsst |
| n12.98159.1038.mcsst | n14.98152.0747.mcsst | n14.98167.1811.mcsst |
| n12.98159.2201.mcsst | n14.98152.1917.mcsst | n14.98168.0812.mcsst |
| n12.98160.1017.mcsst | n14.98153.0736.mcsst | n14.98168.1800.mcsst |
| n12.98160.1157.mcsst | n14.98153.1905.mcsst | n14.98169.0800.mcsst |
| n12.98160.2139.mcsst | n14.98154.0725.mcsst | n14.98169.1750.mcsst |
| n12.98161.1134.mcsst | n14.98154.1854.mcsst | n14.98169.1931.mcsst |
| n12.98161.2118.mcsst | n14.98155.0715.mcsst | n14.98170.0749.mcsst |
| n12.98162.1112.mcsst | n14.98155.1843.mcsst | n14.98170.1919.mcsst |
| n12.98162.2236.mcsst | n14.98156.0704.mcsst | n14.98173.1845.mcsst |
| n12.98163.1050.mcsst | n14.98156.0845.mcsst | n14.98174.1834.mcsst |
| n12.98163.2213.mcsst | n14.98156.1832.mcsst | n14.98175.0657.mcsst |
| n12.98164.1028.mcsst | n14.98157.0833.mcsst | n14.98175.0835.mcsst |
| n12.98164.1210.mcsst | n14.98157.1821.mcsst | n14.98175.1823.mcsst |
| n12.98164.2151.mcsst | n14.98158.0822.mcsst | |
| n12.98165.1146.mcsst | n14.98158.1810.mcsst | |

• filename meaning: sss.yyddd.hhmm.mcsst
s=satellite (i.e. n12, NOAA 12), y=year (i.e. 98, 1998), d=yearday (i.e. 213), h=hour (GMT), m=minute

## *AVHRR SST*
## July 1998

| | | |
|---|---|---|
| n12.98182.1032.mcsst | n12.98198.2244.mcsst | n14.98190.0730.mcsst |
| n12.98182.2155.mcsst | n12.98199.1057.mcsst | n14.98190.1858.mcsst |
| n12.98183.1150.mcsst | n12.98199.2221.mcsst | n14.98191.0719.mcsst |
| n12.98183.2133.mcsst | n12.98200.1035.mcsst | n14.98191.1847.mcsst |
| n12.98184.1127.mcsst | n12.98200.2158.mcsst | n14.98192.0708.mcsst |
| n12.98184.2112.mcsst | n12.98201.1015.mcsst | n14.98192.0849.mcsst |
| n12.98184.2253.mcsst | n12.98201.1154.mcsst | n14.98192.1836.mcsst |
| n12.98185.1105.mcsst | n12.98201.2137.mcsst | n14.98193.0658.mcsst |
| n12.98185.2229.mcsst | n12.98202.1131.mcsst | n14.98193.0837.mcsst |
| n12.98186.1043.mcsst | n12.98202.2115.mcsst | n14.98193.1825.mcsst |
| n12.98186.2207.mcsst | n12.98202.2257.mcsst | n14.98194.0826.mcsst |
| n12.98187.1022.mcsst | n12.98203.1109.mcsst | n14.98194.1814.mcsst |
| n12.98187.1203.mcsst | n12.98203.2233.mcsst | n14.98195.0815.mcsst |
| n12.98187.2145.mcsst | n12.98204.1047.mcsst | n14.98195.1803.mcsst |
| n12.98188.1140.mcsst | n12.98204.2210.mcsst | n14.98196.0804.mcsst |
| n12.98188.2123.mcsst | n12.98205.1026.mcsst | n14.98196.1753.mcsst |
| n12.98189.1117.mcsst | n12.98205.1207.mcsst | n14.98196.1934.mcsst |
| n12.98189.2242.mcsst | n12.98205.2148.mcsst | n14.98197.0752.mcsst |
| n12.98190.1055.mcsst | n14.98182.0718.mcsst | n14.98197.1922.mcsst |
| n12.98190.2219.mcsst | n14.98182.1846.mcsst | n14.98198.0742.mcsst |
| n12.98191.1034.mcsst | n14.98183.0707.mcsst | n14.98199.0731.mcsst |
| n12.98191.2157.mcsst | n14.98183.0848.mcsst | n14.98199.1859.mcsst |
| n12.98192.1152.mcsst | n14.98183.1835.mcsst | n14.98200.0720.mcsst |
| n12.98192.2135.mcsst | n14.98184.0657.mcsst | n14.98200.1848.mcsst |
| n12.98193.1129.mcsst | n14.98184.0836.mcsst | n14.98201.0709.mcsst |
| n12.98193.2114.mcsst | n14.98184.1824.mcsst | n14.98201.0850.mcsst |
| n12.98193.2255.mcsst | n14.98185.0825.mcsst | n14.98201.1837.mcsst |
| n12.98194.1107.mcsst | n14.98185.1813.mcsst | n14.98202.0659.mcsst |
| n12.98194.2231.mcsst | n14.98186.0814.mcsst | n14.98202.0838.mcsst |
| n12.98195.1045.mcsst | n14.98186.1802.mcsst | n14.98202.1826.mcsst |
| n12.98195.2209.mcsst | n14.98187.0802.mcsst | n14.98203.0827.mcsst |
| n12.98196.1024.mcsst | n14.98187.1752.mcsst | n14.98203.1815.mcsst |
| n12.98196.1205.mcsst | n14.98187.1932.mcsst | n14.98204.0816.mcsst |
| n12.98196.2147.mcsst | n14.98188.0751.mcsst | n14.98204.1804.mcsst |
| n12.98197.1142.mcsst | n14.98188.1921.mcsst | n14.98205.0805.mcsst |
| n12.98197.2125.mcsst | n14.98189.0740.mcsst | n14.98205.1754.mcsst |
| n12.98198.1119.mcsst | n14.98189.1909.mcsst | n14.98205.1935.mcsst |

## *AVHRR SST*
## August 1998

| | | |
|---|---|---|
| n12.98213.1049.mcsst | n12.98225.2249.mcsst | n14.98220.1828.mcsst |
| n12.98213.2212.mcsst | n12.98231.2216.mcsst | n14.98221.0829.mcsst |
| n12.98214.1027.mcsst | n12.98232.1031.mcsst | n14.98221.1817.mcsst |
| n12.98214.2150.mcsst | n12.98232.2153.mcsst | n14.98222.0818.mcsst |
| n12.98215.1145.mcsst | n12.98233.1149.mcsst | n14.98222.1806.mcsst |
| n12.98215.2128.mcsst | n12.98233.2132.mcsst | n14.98223.1756.mcsst |
| n12.98216.1123.mcsst | n12.98234.1126.mcsst | n14.98223.1937.mcsst |
| n12.98216.2108.mcsst | n12.98234.2111.mcsst | n14.98224.0755.mcsst |
| n12.98216.2248.mcsst | n12.98234.2251.mcsst | n14.98224.1925.mcsst |
| n12.98217.1100.mcsst | n12.98235.1104.mcsst | n14.98225.0744.mcsst |
| n12.98217.2224.mcsst | n14.98213.0817.mcsst | n14.98225.1913.mcsst |
| n12.98218.1039.mcsst | n14.98213.1805.mcsst | n14.98226.0733.mcsst |
| n12.98218.2202.mcsst | n14.98214.0806.mcsst | n14.98226.1902.mcsst |
| n12.98219.1018.mcsst | n14.98214.1755.mcsst | n14.98227.0723.mcsst |
| n12.98219.1158.mcsst | n14.98214.1936.mcsst | n14.98227.1851.mcsst |
| n12.98219.2140.mcsst | n14.98215.0754.mcsst | n14.98228.0712.mcsst |
| n12.98220.1135.mcsst | n14.98215.1924.mcsst | n14.98228.0853.mcsst |
| n12.98220.2119.mcsst | n14.98216.0744.mcsst | n14.98228.1840.mcsst |
| n12.98221.1112.mcsst | n14.98216.1912.mcsst | n14.98229.0841.mcsst |
| n12.98221.2237.mcsst | n14.98217.0732.mcsst | n14.98229.1829.mcsst |
| n12.98222.1051.mcsst | n14.98217.1901.mcsst | n14.98230.0830.mcsst |
| n12.98222.2214.mcsst | n14.98218.0722.mcsst | n14.98230.1818.mcsst |
| n12.98223.1029.mcsst | n14.98218.1850.mcsst | n14.98231.0819.mcsst |
| n12.98223.2152.mcsst | n14.98219.0711.mcsst | n14.98231.1807.mcsst |
| n12.98224.1147.mcsst | n14.98219.0852.mcsst | n14.98232.1757.mcsst |
| n12.98224.2130.mcsst | n14.98219.1839.mcsst | n14.98233.1926.mcsst |
| n12.98225.1124.mcsst | n14.98220.0701.mcsst | |
| n12.98225.2109.mcsst | n14.98220.0841.mcsst | |

## *AVHRR SST*
## May 2000

| | | |
|---|---|---|
| n12.00108.1042.mcsst | n14.00108.1942.mcsst | n14.00130.0901.mcsst |
| n12.00108.2027.mcsst | n14.00109.0943.mcsst | n15.00108.1237.mcsst |
| n12.00108.2207.mcsst | n14.00109.1930.mcsst | n15.00109.0001.mcsst |
| n12.00109.1020.mcsst | n14.00110.0931.mcsst | n15.00109.1215.mcsst |
| n12.00109.2143.mcsst | n14.00110.1919.mcsst | n15.00109.2338.mcsst |
| n12.00110.0957.mcsst | n14.00111.0920.mcsst | n15.00110.1153.mcsst |
| n12.00110.2120.mcsst | n14.00111.1908.mcsst | n15.00110.2316.mcsst |
| n12.00111.0936.mcsst | n14.00111.2050.mcsst | n15.00111.1310.mcsst |
| n12.00111.1116.mcsst | n14.00112.0908.mcsst | n15.00111.2254.mcsst |
| n12.00111.2058.mcsst | n14.00112.1858.mcsst | n15.00112.1248.mcsst |
| n12.00112.1052.mcsst | n14.00113.0856.mcsst | n15.00112.2233.mcsst |
| n12.00112.2036.mcsst | n14.00113.2025.mcsst | n15.00113.0012.mcsst |
| n12.00113.1029.mcsst | n14.00114.0845.mcsst | n15.00113.1225.mcsst |
| n12.00113.2153.mcsst | n14.00114.2013.mcsst | n15.00113.2349.mcsst |
| n12.00114.1007.mcsst | n14.00115.0834.mcsst | n15.00114.1203.mcsst |
| n12.00114.2130.mcsst | n14.00115.2001.mcsst | n15.00114.2326.mcsst |
| n12.00115.0945.mcsst | n14.00116.0823.mcsst | n15.00115.1143.mcsst |
| n12.00115.2107.mcsst | n14.00116.1950.mcsst | n15.00115.1321.mcsst |
| n12.00116.1102.mcsst | n14.00117.0812.mcsst | n15.00115.2304.mcsst |
| n12.00116.2045.mcsst | n14.00117.0951.mcsst | n15.00116.1258.mcsst |
| n12.00117.1039.mcsst | n14.00117.1938.mcsst | n15.00116.2242.mcsst |
| n12.00117.2024.mcsst | n14.00118.0939.mcsst | n15.00117.1236.mcsst |
| n12.00117.2203.mcsst | n14.00118.1927.mcsst | n15.00118.1213.mcsst |
| n12.00118.1016.mcsst | n14.00119.0928.mcsst | n15.00118.2336.mcsst |
| n12.00118.2139.mcsst | n14.00119.1916.mcsst | n15.00119.1152.mcsst |
| n12.00119.0954.mcsst | n14.00120.0916.mcsst | n15.00119.2314.mcsst |
| n12.00119.2117.mcsst | n14.00120.1905.mcsst | n15.00120.1309.mcsst |
| n12.00120.0933.mcsst | n14.00120.2046.mcsst | n15.00120.2252.mcsst |
| n12.00120.1112.mcsst | n14.00121.0904.mcsst | n15.00121.1246.mcsst |
| n12.00120.2054.mcsst | n14.00121.2033.mcsst | n15.00122.0010.mcsst |
| n12.00121.1048.mcsst | n14.00122.0853.mcsst | n15.00122.1224.mcsst |
| n12.00122.1025.mcsst | n14.00122.2021.mcsst | n15.00122.2347.mcsst |
| n12.00122.2149.mcsst | n14.00123.0841.mcsst | n15.00123.1202.mcsst |
| n12.00123.1003.mcsst | n14.00123.2010.mcsst | n15.00123.2324.mcsst |
| n12.00123.2126.mcsst | n14.00124.0830.mcsst | n15.00124.1320.mcsst |
| n12.00124.0941.mcsst | n14.00124.1958.mcsst | n15.00124.2302.mcsst |
| n12.00124.2103.mcsst | n14.00125.0819.mcsst | n15.00125.1257.mcsst |
| n12.00125.1058.mcsst | n14.00125.1000.mcsst | n15.00125.2241.mcsst |
| n12.00125.2041.mcsst | n14.00125.1946.mcsst | n15.00126.0022.mcsst |
| n12.00126.1035.mcsst | n14.00126.0948.mcsst | n15.00126.1234.mcsst |
| n12.00126.2159.mcsst | n14.00126.1935.mcsst | n15.00126.2358.mcsst |
| n12.00127.1012.mcsst | n14.00127.0936.mcsst | n15.00127.1212.mcsst |
| n12.00127.2136.mcsst | n14.00127.1924.mcsst | n15.00127.2335.mcsst |
| n12.00128.0950.mcsst | n14.00128.0924.mcsst | n15.00128.1150.mcsst |

n12.00128.2113.mcsst
n12.00129.1108.mcsst
n12.00129.2050.mcsst
n12.00130.1044.mcsst
n14.00108.0955.mcsst
n14.00128.1913.mcsst
n14.00128.2055.mcsst
n14.00129.0912.mcsst
n14.00129.1902.mcsst
n14.00129.2042.mcsst
n15.00128.2313.mcsst
n15.00129.1307.mcsst
n15.00129.2251.mcsst
n15.00130.1245.mcsst

***AVHRR SST***
**June 2000**

| | | |
|---|---|---|
| n12.00152.1046.mcsst | n14.00154.2054.mcsst | n15.00154.2330.mcsst |
| n12.00154.2123.mcsst | n14.00155.0912.mcsst | n15.00155.1145.mcsst |
| n12.00155.0938.mcsst | n14.00155.1903.mcsst | n15.00155.1325.mcsst |
| n12.00155.2101.mcsst | n14.00155.2042.mcsst | n15.00155.2307.mcsst |
| n12.00156.1055.mcsst | n14.00156.0901.mcsst | n15.00156.1302.mcsst |
| n12.00156.2039.mcsst | n14.00156.2030.mcsst | n15.00156.2246.mcsst |
| n12.00157.1032.mcsst | n14.00157.0850.mcsst | n15.00157.1239.mcsst |
| n12.00157.2156.mcsst | n14.00157.2018.mcsst | n15.00158.0003.mcsst |
| n12.00158.1009.mcsst | n14.00158.0838.mcsst | n15.00158.1217.mcsst |
| n12.00158.2133.mcsst | n14.00158.2006.mcsst | n15.00158.2340.mcsst |
| n12.00159.0947.mcsst | n14.00159.0827.mcsst | n15.00159.1155.mcsst |
| n12.00159.2110.mcsst | n14.00159.1008.mcsst | n15.00159.2318.mcsst |
| n12.00160.1105.mcsst | n14.00159.1954.mcsst | n15.00160.1312.mcsst |
| n12.00160.2047.mcsst | n14.00160.0956.mcsst | n15.00160.2255.mcsst |
| n12.00161.1041.mcsst | n14.00160.1943.mcsst | n15.00161.1250.mcsst |
| n12.00161.2026.mcsst | n14.00161.0944.mcsst | n15.00161.2234.mcsst |
| n12.00161.2206.mcsst | n14.00161.1932.mcsst | n15.00162.0014.mcsst |
| n12.00162.1019.mcsst | n14.00162.0932.mcsst | n15.00162.1227.mcsst |
| n12.00162.2142.mcsst | n14.00162.1920.mcsst | n15.00162.2350.mcsst |
| n12.00163.0956.mcsst | n14.00163.0920.mcsst | n15.00163.1205.mcsst |
| n12.00163.2119.mcsst | n14.00163.1910.mcsst | n15.00163.2328.mcsst |
| n12.00164.0935.mcsst | n14.00163.2050.mcsst | n15.00164.1144.mcsst |
| n12.00164.1114.mcsst | n14.00164.0909.mcsst | n15.00164.1323.mcsst |
| n12.00164.2057.mcsst | n14.00164.2038.mcsst | n15.00164.2306.mcsst |
| n12.00165.1051.mcsst | n14.00165.0857.mcsst | n15.00165.1300.mcsst |
| n12.00165.2035.mcsst | n14.00165.2026.mcsst | n15.00165.2244.mcsst |
| n12.00166.1028.mcsst | n14.00166.0846.mcsst | n15.00166.1237.mcsst |
| n12.00166.2152.mcsst | n14.00166.2014.mcsst | n15.00167.0001.mcsst |
| n12.00167.1005.mcsst | n14.00167.0834.mcsst | n15.00167.1215.mcsst |
| n12.00167.2128.mcsst | n14.00167.2002.mcsst | n15.00167.2338.mcsst |
| n12.00168.0943.mcsst | n14.00168.0823.mcsst | n15.00168.1153.mcsst |
| n12.00168.2105.mcsst | n14.00168.1004.mcsst | n15.00168.2316.mcsst |
| n12.00169.1100.mcsst | n14.00168.1951.mcsst | n15.00169.1310.mcsst |
| n12.00169.2043.mcsst | n14.00169.1939.mcsst | n15.00169.2254.mcsst |
| n12.00170.1037.mcsst | n14.00170.0940.mcsst | n15.00170.1248.mcsst |
| n12.00170.2022.mcsst | n14.00170.1928.mcsst | n15.00170.2233.mcsst |
| n12.00170.2201.mcsst | n14.00171.0928.mcsst | n15.00171.0012.mcsst |
| n12.00171.1014.mcsst | n14.00171.1917.mcsst | n15.00171.1225.mcsst |
| n12.00171.2138.mcsst | n14.00171.2058.mcsst | n15.00171.2348.mcsst |
| n12.00172.0952.mcsst | n14.00172.0916.mcsst | n15.00172.1203.mcsst |
| n12.00172.2115.mcsst | n14.00172.1906.mcsst | n15.00172.2326.mcsst |
| n14.00152.0948.mcsst | n14.00172.2046.mcsst | |
| n14.00152.1935.mcsst | n15.00152.1251.mcsst | |

***SeaWiFS Chlorophyll***
**June 1998**

| | |
|---|---|
| S1998152170400_remap3.L2_HBIO | S1998165165439_remap3.L2_HNSG |
| S1998153xxxxxx_remap3.L2_MULT | S1998166xxxxxx_remap3.L2_MULT |
| S1998154165446_remap3.L2_HBIO | S1998167164530_remap3.L2_HNSG |
| S1998155xxxxxx_remap3.L2_MULT | S1998168172927_remap3.L2_HNSG |
| S1998156164658_remap3.L2_HNSG | S1998169163628_remap3.L2_HNSG |
| S1998157173108_remap3.L2_HNSG | S1998170172018_remap3.L2_HNSG |
| S1998158163808_remap3.L2_HNSG | S1998171162718_remap3.L2_HNSG |
| S1998159172158_remap3.L2_HNSG | S1998172171058_remap3.L2_HNSG |
| S1998161171249_remap3.L2_HNSG | S1998173xxxxxx_remap3.L2_MULT |
| S1998162xxxxxx_remap3.L2_MULT | S1998174170158_remap3.L2_HNSG |
| S1998163170337_remap3.L2_HNSG | S1998175xxxxxx_remap3.L2_MULT |
| S1998164xxxxxx_remap3.L2_MULT | |

***SeaWiFS Chlorophyll***
**July 1998**

| | |
|---|---|
| S1998182162539_remap3.L2_HNSG | S1998193162358_remap3.L2_HNSG |
| S1998183170918_remap3.L2_HNSG | S1998194170738_remap3.L2_HNSG |
| S1998184xxxxxx_remap3.L2_MULT | S1998195xxxxxx_remap3.L2_MULT |
| S1998185170007_remap3.L2_HNSG | S1998198164918_remap3.L2_HNSG |
| S1998186xxxxxx_remap3.L2_MULT | S1998200164008_remap3.L2_HNSG |
| S1998187165107_remap3.L2_HNSG | S1998201172408_remap3.L2_HNSG |
| S1998188173508_remap3.L2_HNSG | S1998202163118_remap3.L2_HNSG |
| S1998189164158_remap3.L2_HNSG | S1998203171459_remap3.L2_HNSG |
| S1998190172557_remap3.L2_HNSG | S1998204xxxxxx_remap3.L2_MULT |
| S1998192171648_remap3.L2_HNSG | S1998205170547_remap3.L2_HNSG |

***SeaWiFS Chlorophyll***
**August 1998**

| | |
|---|---|
| S1998213162918_remap3.L2_HNSG | S1998225171107_remap3.L2_HNSG |
| S1998214171308_remap3.L2_HNSG | S1998226xxxxxx_remap3.L2_MULT |
| S1998215xxxxxx_remap3.L2_MULT | S1998227170159_remap3.L2_HNSG |
| S1998216170358_remap3.L2_HNSG | S1998228xxxxxx_remap3.L2_MULT |
| S1998217xxxxxx_remap3.L2_MULT | S1998229165258_remap3.L2_HNSG |
| S1998218165437_remap3.L2_HNSG | S1998230xxxxxx_remap3.L2_MULT |
| S1998219xxxxxx_remap3.L2_MULT | S1998231164349_remap3.L2_HNSG |
| S1998220164539_remap3.L2_HNSG | S1998232172739_remap3.L2_HNSG |
| S1998221172938_remap3.L2_HNSG | S1998233163437_remap3.L2_HNSG |
| S1998222163637_remap3.L2_HNSG | S1998234171828_remap3.L2_HNSG |
| S1998223172028_remap3.L2_HNSG | S1998235162538_remap3.L2_HNSG |
| S1998224162728_remap3.L2_HNSG | |

• filename meaning: Syyyydddhhmmss_remaps3.L2_HNSG
y = year (i.e. 1998), d=yearday (i.e. 213), h=hour (GMT), m=minute, s=seconds, L2= level 2 data

***SeaWiFS Chlorophyll***
**May 2000**

| | |
|---|---|
| S2000108xxxxxx_remap3.L2_MULT | S2000120165259_remap3.L2_HNSG |
| S2000109170449_remap3.L2_HNSG | S2000121173609_remap3.L2_HNSG |
| S2000110174810_remap3.L2_HNSG | S2000122164209_remap3.L2_HNSG |
| S2000111165350_remap3.L2_HNSG | S2000123172459_remap3.L2_HNSG |
| S2000112173701_remap3.L2_HNSG | S2000124163059_remap3.L2_HNSG |
| S2000114172559_remap3.L2_HNSG | S2000125171359_remap3.L2_HNSG |
| S2000115163210_remap3.L2_HNSG | S2000126xxxxxx_remap3.L2_MULT |
| S2000116171459_remap3.L2_HNSG | S2000127170259_remap3.L2_HNSG |
| S2000117xxxxxx_remap3.L2_MULT | S2000128xxxxxx_remap3.L2_MULT |
| S2000118170358_remap3.L2_HNSG | S2000129165158_remap3.L2_HNSG |
| S2000119xxxxxx_remap3.L2_MULT | S2000130173459_remap3.L2_HNSG |

***SeaWiFS Chlorophyll***
**June 2000**

| | |
|---|---|
| S2000152170939_remap3.L2_HNSG | S2000163165649_remap3.L2_HNSG |
| S2000153xxxxxx_remap3.L2_MULT | S2000164xxxxxx_remap3.L2_MULT |
| S2000154165839_remap3.L2_HNSG | S2000165164539_remap3.L2_HNSG |
| S2000155xxxxxx_remap3.L2_MULT | S2000166172839_remap3.L2_HNSG |
| S2000156164729_remap3.L2_HNSG | S2000167163439_remap3.L2_HNSG |
| S2000157173030_remap3.L2_HNSG | S2000168171729_remap3.L2_HNSG |
| S2000158163619_remap3.L2_HNSG | S2000169162339_remap3.L2_HNSG |
| S2000159171919_remap3.L2_HNSG | S2000170170620_remap3.L2_HNSG |
| S2000160162519_remap3.L2_HNSG | S2000171xxxxxx_remap3.L2_MULT |
| S2000161170810_remap3.L2_HNSG | S2000172165500_remap3.L2_HNSG |
| S2000162xxxxxx_remap3.L2_MULT | |

# Appendix D

# AVAILABLE PATHFINDER AVHRR DATA

March 30-April 6 (yeardays 89-96)
April 7-14 (yeardays 97-104)
April 15-22 (yeardays 105-112)
April 23-30 (yeardays 113-120)
May 1-8 (yeardays 121-128)
May 9-16 (yeardays 129-136)
May 17-24 (yeardays 137-144)
May 25-June1 (yeardays 145-152)
June 2-9 (yeardays 153-160)
June 10-17 (yeardays 161-168)
June 18-25 (yeardays 169-176)
June 26-July 3 (yeardays 177-184)
July 4-11 (yeardays 185-192)
July 12-19 (yeardays 193-200)
July 20-27 (yeardays 201-208)
July 28-August 4 (yeardays 209-216)

# Appendix E

# SAMPLING STATIONS IN GOM DATA SUBSETS

***All 1998 Subsets:***

| *Subset* | *Stations included* |
|---|---|
| Eastern Maine | 1-99, 208-215 |
| Western Maine | 100-207 |
| EMCC | 169-176, 152-154, 129-132, 134-136, 114-117, 104-107 |
| WMCC | 85-87, 63-67, 44, 43, 40, 39, 17-20, 1-8, 90-92 |
| Jordan Basin | 156-162, 138-149, 119-127, 202-207, 100-102 |
| Wilkinson Basin | 93-99, 208-215, 68-84, 45-62, 21-38, 9-16 |
| Bay of Fundy | 183-188, 194-198 |
| Scotian Shelf | 178-180, 163, 164, 200, 201 |

***May 2000 Subsets:***

| *Subset* | *Stations included* |
|---|---|
| Eastern Maine | 114-200, 300-310 |
| Western Maine | 1-8, 19-29, 42-48, 65-76, 90-99, 342-353 |
| EMCC | 114, 115, 130-132, 134-136, 151-153, 170-176 |
| WMCC | 1-8, 19-21, 43, 44, 65-67, 90-92, 342-344 |
| Jordan Basin | 118-127, 138-149, 156-162 |
| Wilkinson Basin | 22-29, 45-48, 68-76, 93-99, 344-353 |
| Bay of Fundy | 183-188, 194-198 |
| Scotian Shelf | 163, 164, 177-181, 200, 300-303 |

***June 2000 Subsets:***

| *Subset* | *Stations included* |
|---|---|
| Eastern Maine | 58-137 |
| Western Maine | 1-57, 138-140 |
| EMCC | 60-62, 78-80, 81, 82, 96-99 |
| WMCC | 2, 3, 25, 24, 26-29, 33-36, 53-56 |
| Jordan Basin | 65-69, 70-76, 83-90, 133-137 |
| Wilkinson Basin | 4-23, 30-32, 37-52, 138-140 |
| Bay of Fundy | 104-110, 112-116 |
| Scotian Shelf | 91, 92, 118-123 |

# Appendix F

## CORRELATION RESULTS OF LINEAR REGRESSION ANALYSES

| Year | Month | Area | X | LOG? | Y | Y-intercept | Slope | r-value | N |
|---|---|---|---|---|---|---|---|---|---|
| 1998 | June | All GOM | AVHRR | yes | *Alexandrium* | 3.87348 | -0.22567 | -0.476528 | 153 |
| 1998 | June | All GOM | AVHRR | no | *Alexandrium* | 767.132 | -54.9817 | -0.178849 | 236 |
| 1998 | June | WM | AVHRR | yes | *Alexandrium* | 6.80974 | -0.510667 | -0.670645 | 65 |
| 1998 | June | EM | AVHRR | yes | *Alexandrium* | 3.33439 | -0.154831 | -0.247133 | 87 |
| 1998 | July | All GOM | AVHRR | yes | *Alexandrium* | 3.90386 | -0.187262 | -0.565019 | 140 |
| 1998 | July | All GOM | AVHRR | no | *Alexandrium* | 1249.98 | -75.9977 | -0.250198 | 218 |
| 1998 | July | WM | AVHRR | yes | *Alexandrium* | 1.93706 | -0.0674101 | -0.3158 | 50 |
| 1998 | July | EM | AVHRR | yes | *Alexandrium* | 3.8464 | -0.177545 | -0.337766 | 90 |
| 1998 | August | All GOM | AVHRR | yes | *Alexandrium* | 4.77747 | -0.225342 | -0.592013 | 132 |
| 1998 | August | All GOM | AVHRR | no | *Alexandrium* | 1190.48 | -60.985 | -0.153492 | 204 |
| 1998 | August | WM | AVHRR | yes | *Alexandrium* | 1.53217 | -0.0467997 | -0.236055 | 41 |
| 1998 | August | EM | AVHRR | yes | *Alexandrium* | 3.91283 | -0.156799 | -0.341829 | 91 |
| 2000 | May | All GOM | AVHRR | yes | *Alexandrium* | 0.550715 | 0.099204 | 0.147208 | 119 |
| 2000 | May | All GOM | AVHRR | no | *Alexandrium* | -15.1976 | 7.12095 | 0.137873 | 164 |
| 2000 | May | EM | AVHRR | yes | *Alexandrium* | 0.605583 | 3.49971 | 0.131167 | 77 |
| 2000 | June | All GOM | AVHRR | yes | *Alexandrium* | 1.40294 | 0.0778236 | 0.138734 | 160 |
| 2000 | June | All GOM | AVHRR | no | *Alexandrium* | -7.70742 | 42.3237 | 0.100029 | 130 |
| 1998 | June | All GOM | SeaWifs | yes | *Alexandrium* | 1.78238 | 0.270937 | 0.146174 | 153 |
| 1998 | June | All GOM | SeaWifs | no | *Alexandrium* | 264.459 | -4.29423 | -0.0092728 | 228 |
| 1998 | June | WM | SeaWifs | yes | *Alexandrium* | 1.46879 | 0.150606 | 0.0664906 | 65 |
| 1998 | June | EM | SeaWifs | yes | *Alexandrium* | 2.01443 | 0.327873 | 0.228194 | 88 |
| 1998 | July | All GOM | SeaWifs | yes | *Alexandrium* | 1.5591 | 0.0778775 | 0.0401115 | 140 |
| 1998 | August | All GOM | SeaWifs | yes | *Alexandrium* | 1.56139 | 0.379432 | 0.20331 | 132 |
| 2000 | May | All GOM | SeaWifs | yes | *Alexandrium* | 1.16271 | -0.00649899 | -0.00293767 | 48 |
| 2000 | June | All GOM | SeaWifs | yes | *Alexandrium* | 2.64255 | -0.667496 | -0.203542 | 55 |
| 1998 | June | All GOM | AVHRR | yes | nitrate | 0.298798 | -0.0404045 | -0.157014 | 177 |
| 1998 | June | All GOM | AVHRR | no | nitrate | 3.84029 | -0.255022 | -0.355757 | 177 |
| 1998 | July | All GOM | AVHRR | yes | nitrate | 2.23585 | -0.218694 | -0.586268 | 69 |
| 1998 | July | All GOM | AVHRR | no | nitrate | 8.56347 | -0.599744 | -0.560743 | 69 |
| 1998 | August | All GOM | AVHRR | yes | nitrate | 2.43177 | -0.206115 | -0.650912 | 152 |
| 1998 | August | All GOM | AVHRR | no | nitrate | 7.91008 | -0.475168 | -0.668751 | 152 |

| Year | Month | Area | X | LOG? | Y | Y-intercept | Slope | r-value | N |
|---|---|---|---|---|---|---|---|---|---|
| 2000 | May | All GOM | AVHRR | yes | nitrate | 1.47119 | -0.13472 | -0.50652 | 158 |
| 2000 | May | All GOM | AVHRR | no | nitrate | 13.6588 | -1.42859 | -0.513606 | 158 |
| 2000 | June | All GOM | AVHRR | yes | nitrate | 0.970542 | -0.161484 | -0.29964 | 210 |
| 2000 | June | All GOM | AVHRR | no | nitrate | 5.24186 | -0.407493 | -0.510839 | 210 |
| 1998 | June | All GOM | SeaWifs | yes | nitrate | -0.0961816 | 0.175676 | 0.133345 | 262 |
| 1998 | June | All GOM | SeaWifs | no | nitrate | 0.9441877 | 0.319912 | 0.217112 | 280 |
| 1998 | June | WM | SeaWifs | yes | nitrate | -0.16884 | -0.139891 | -0.0824112 | 94 |
| 1998 | June | EM | SeaWifs | yes | nitrate | -0.0321849 | 0.51617 | 0.334349 | 84 |
| 1998 | June | WMCC | SeaWifs | yes | nitrate | 0.0476534 | -0.210015 | -0.186181 | 19 |
| 1998 | June | WB | SeaWifs | yes | nitrate | -0.221277 | 0.099212 | 0.0158154 | 71 |
| 1998 | June | EMCC | SeaWifs | yes | nitrate | 0.358535 | 0.224971 | 0.25066 | 21 |
| 1998 | June | JB | SeaWifs | yes | nitrate | -0.284547 | 2.30948 | 0.563258 | 26 |
| 1998 | June | BF | SeaWifs | yes | nitrate | 0.361681 | -1.49671 | -0.574544 | 11 |
| 1998 | June | SS | SeaWifs | yes | nitrate | -0.155246 | -0.04548 | -0.129649 | 7 |
| 1998 | July | All GOM | SeaWifs | yes | nitrate | -0.136592 | 0.3003 | 0.24282 | 78 |
| 1998 | July | All GOM | SeaWifs | no | nitrate | 1.95099 | 0.0453615 | 0.0295008 | 98 |
| 1998 | July | WM | SeaWifs | yes | nitrate | -1.08543 | 0.934425 | 0.903355 | 11 |
| 1998 | July | EM | SeaWifs | yes | nitrate | -0.254503 | 0.524704 | 0.236234 | 58 |
| 1998 | July | WMCC | SeaWifs | yes | nitrate | -1.1998 | 1.00977 | 0.959353 | 3 |
| 1998 | July | EMCC | SeaWifs | yes | nitrate | 0.00708763 | 0.790181 | 0.298926 | 18 |
| 1998 | July | JB | SeaWifs | yes | nitrate | -0.907787 | 4.85895 | 0.8121 | 11 |
| 1998 | July | BF | SeaWifs | yes | nitrate | -1.21507 | 4.00242 | 0.709735 | 7 |
| 1998 | July | SS | SeaWifs | yes | nitrate | -1.37086 | 7.76404 | 0.99513 | 3 |
| 1998 | August | All GOM | SeaWifs | yes | nitrate | -0.572874 | -0.00843593 | -0.00561541 | 236 |
| 1998 | August | All GOM | SeaWifs | no | nitrate | 1.02577 | -0.0230198 | -0.0260882 | 258 |
| 1998 | August | WM | SeaWifs | yes | nitrate | -1.00021 | 0.349524 | 0.220703 | 63 |
| 1998 | August | EM | SeaWifs | yes | nitrate | -0.450042 | 0.192856 | 0.0825746 | 89 |
| 1998 | August | WMCC | SeaWifs | yes | nitrate | -1.02241 | 0.148899 | 0.11814 | 20 |
| 1998 | August | WB | SeaWifs | yes | nitrate | -1.1643 | 1.76714 | 0.380035 | 39 |
| 1998 | August | EMCC | SeaWifs | yes | nitrate | -0.324691 | -0.16576 | -0.084452 | 25 |
| 1998 | August | JB | SeaWifs | yes | nitrate | -0.817649 | 0.813373 | 0.174561 | 28 |
| 1998 | August | BF | SeaWifs | yes | nitrate | -0.34935 | 1.03274 | 0.281852 | 5 |

| Year | Month | Area | X | LOG? | Y | Y-intercept | Slope | r-value | N |
|---|---|---|---|---|---|---|---|---|---|
| 1998 | August | SS | SeaWifs | yes | nitrate | 0.304767 | -3.39624 | -0.180362 | 6 |
| 2000 | May | All GOM | SeaWifs | yes | nitrate | 0.637104 | 0.0285144 | 0.064382 | 228 |
| 2000 | May | All GOM | SeaWifs | no | nitrate | 3.98213 | 0.46537 | 0.348962 | 242 |
| 2000 | June | All GOM | SeaWifs | yes | nitrate | -0.908552 | 0.102518 | 0.0411867 | 114 |
| 2000 | June | WM | SeaWifs | yes | nitrate | -0.916015 | -0.0500041 | -0.0203197 | 135 |
| 2000 | June | EM | SeaWifs | yes | nitrate | -0.852803 | 0.261805 | 0.102434 | 48 |
| 1998 | June | All GOM | AVHRR | yes | SeaWifs | 0.551191 | -0.0545542 | -0.240174 | 198 |
| 1998 | June | All GOM | AVHRR | no | SeaWifs | 2.65216 | -0.133814 | -0.217325 | 198 |
| 1998 | July | All GOM | AVHRR | yes | SeaWifs | 0.097637 | -0.00384233 | -0.0241521 | 212 |
| 1998 | July | All GOM | AVHRR | no | SeaWifs | 1.18738 | 0.0305795 | 0.0955155 | 212 |
| 1998 | August | All GOM | AVHRR | yes | SeaWifs | 0.460048 | -0.0235758 | -0.135665 | 213 |
| 1998 | August | All GOM | AVHRR | no | SeaWifs | 3.51744 | -0.115476 | -0.179935 | 213 |
| 1998 | June | All GOM | nitrate | yes | *Alexandrium* | 1.81204 | 0.0822375 | 0.0513484 | |
| 1998 | July | All GOM | nitrate | yes | *Alexandrium* | 2.001321 | 0.394569 | 0.38216 | |
| 1998 | August | All GOM | nitrate | yes | *Alexandrium* | 1.7347 | 0.46674 | 0.432192 | |
| 2000 | May | All GOM | nitrate | yes | *Alexandrium* | 0.699917 | -0.000993411 | -0.201738 | |
| 2000 | June | All GOM | nitrate | yes | *Alexandrium* | -0.76283 | -0.000271224 | -0.183375 | |
| 1998 | June | All GOM | chlorophyll | yes | *Alexandrium* | -0.20822 | 0.108279 | 0.244867 | 199 |
| 1998 | June | All GOM | chlorophyll | no | *Alexandrium* | 1.34985 | 0.000121769 | 0.0472745 | 199 |
| 1998 | June | WM | chlorophyll | yes | *Alexandrium* | -0.213439 | 0.0572264 | 0.140784 | 65 |
| 1998 | June | EM | chlorophyll | yes | *Alexandrium* | -0.153374 | 0.0956224 | 0.19181 | 88 |
| 1998 | July | All GOM | chlorophyll | yes | *Alexandrium* | -0.429695 | 0.190262 | 0.407584 | 212 |
| 1998 | July | WM | chlorophyll | yes | *Alexandrium* | -0.275339 | 0.0644045 | 0.0893329 | 50 |
| 1998 | July | EM | chlorophyll | yes | *Alexandrium* | -0.538323 | 0.23705 | 0.466973 | 89 |
| 1998 | August | All GOM | chlorophyll | yes | *Alexandrium* | -0.237467 | 0.240872 | 0.504058 | 213 |
| 1998 | August | WM | chlorophyll | yes | *Alexandrium* | -0.465438 | 0.485342 | 0.48914 | 41 |
| 1998 | August | EM | chlorophyll | yes | *Alexandrium* | 0.129401 | 0.190262 | 0.417464 | 89 |
| 1998 | June | All GOM | temperature | yes | nitrate | 0.863438 | -0.998165 | -0.307286 | |
| 1998 | June | WM | temperature | yes | nitrate | -0.598183 | 0.0411124 | 0.122097 | |
| 1998 | June | EM | temperature | yes | nitrate | 2.28185 | -0.251579 | -0.694547 | |

| Year | Month | Area | X | LOG? | Y | Y-intercept | Slope | r-value | N |
|---|---|---|---|---|---|---|---|---|---|
| 1998 | June | JB | temperature | yes | nitrate | 2.42346 | -0.274466 | -0.720471 | |
| 1998 | June | BF | temperature | yes | nitrate | 5.2185 | -0.585638 | -0.798275 | |
| 1998 | June | SS | temperature | yes | nitrate | 2.71785 | -0.321521 | -0.844164 | |
| 1998 | July | All GOM | temperature | yes | nitrate | 1.71793 | -0.174954 | -0.685182 | |
| 1998 | July | WM | temperature | yes | nitrate | -1.36814 | 0.0205105 | 0.175801 | |
| 1998 | July | EM | temperature | yes | nitrate | 2.94631 | -0.293335 | -0.759986 | |
| 1998 | July | WMCC | temperature | yes | nitrate | -5.1998 | 0.307948 | 0.832517 | |
| 1998 | July | WB | temperature | yes | nitrate | -1.10963 | 0.00362825 | 0.0756908 | |
| 1998 | July | EMCC | temperature | yes | nitrate | 6.8545 | -0.730334 | -0.841736 | |
| 1998 | July | JB | temperature | yes | nitrate | 2.52263 | -0.257805 | -0.823084 | |
| 1998 | July | BF | temperature | yes | nitrate | 3.36879 | -0.310679 | -0.508852 | |
| 1998 | July | SS | temperature | yes | nitrate | 2.1868 | -0.243894 | -0.928681 | |
| 1998 | August | All GOM | temperature | yes | nitrate | 1.60315 | -0.154299 | -0.665058 | |
| 1998 | August | WM | temperature | yes | nitrate | 1.04458 | -0.117157 | -0.549677 | |
| 1998 | August | EM | temperature | yes | nitrate | 2.25549 | -0.209461 | -0.644509 | |
| 1998 | August | WMCC | temperature | yes | nitrate | 0.608258 | -0.0985045 | -0.459982 | |
| 1998 | August | WB | temperature | yes | nitrate | 1.17396 | -0.120731 | -0.537346 | |
| 1998 | August | EMCC | temperature | yes | nitrate | 7.40931 | -0.676667 | -0.865325 | |
| 1998 | August | JB | temperature | yes | nitrate | 1.36965 | -0.139249 | -0.646089 | |
| 1998 | August | BF | temperature | yes | nitrate | 3.52722 | -0.297246 | -0.440974 | |
| 1998 | August | SS | temperature | yes | nitrate | 7.22407 | -0.673931 | -0.947707 | |
| 1998 | June | All GOM | salinity | yes | chlorophyll | -1.53244 | 0.0466118 | 0.0705857 | |
| 1998 | June | WM | salinity | yes | chlorophyll | -1.57056 | 0.0442985 | 0.0519858 | |
| 1998 | June | EM | salinity | yes | chlorophyll | 14.3229 | -0.451193 | 0.53699 | |
| 1998 | June | WMCC | salinity | yes | chlorophyll | -16.5241 | 0.538696 | 0.45879 | |
| 1998 | June | WB | salinity | yes | chlorophyll | -6.61262 | 0.203606 | 0.381856 | |
| 1998 | June | EMCC | salinity | yes | chlorophyll | 14.5664 | -0.456471 | -0.276934 | |
| 1998 | June | JB | salinity | yes | chlorophyll | 14.1042 | -0.450104 | -0.359535 | |
| 1998 | June | BF | salinity | yes | chlorophyll | -1.37903 | 0.0537791 | 0.213008 | |
| 1998 | June | SS | salinity | yes | chlorophyll | 1.7871 | -0.364026 | -0.292308 | |
| 1998 | July | All GOM | salinity | yes | chlorophyll | 1.78761 | -0.0637963 | -0.250229 | 212 |
| 1998 | July | EM | salinity | yes | chlorophyll | 9.64793 | -0.308765 | -0.328848 | 107 |

| Year | Month | Area | X | LOG? | Y | Y-intercept | Slope | r-value | N |
|---|---|---|---|---|---|---|---|---|---|
| 1998 | July | WM | salinity | yes | chlorophyll | 3.60973 | -0.128614 | -0.69347 | 104 |
| 1998 | August | All GOM | salinity | yes | chlorophyll | -8.16531 | 0.259289 | 0.372977 | 213 |
| 1998 | August | EM | salinity | yes | chlorophyll | 12.1862 | -0.374784 | -0.243095 | 101 |
| 1998 | August | WM | salinity | yes | chlorophyll | -2.58553 | 764100 | 0.102277 | 103 |
| 1998 | June | All GOM | salinity | yes | *Alexandrium* | -15.3966 | 0.548088 | 0.349522 | 199 |
| 1998 | July | All GOM | salinity | yes | *Alexandrium* | -6.3527 | 0.253367 | 0.368964 | |
| 1998 | July | WM | salinity | yes | *Alexandrium* | -0.456611 | 0.0462526 | 0.16178 | |
| 1998 | July | EM | salinity | yes | *Alexandrium* | -4.31262 | 0.194888 | 0.0763555 | |
| 1998 | July | WMCC | salinity | yes | *Alexandrium* | 0.194948 | 0.029106 | 0.153048 | |
| 1998 | July | WB | salinity | yes | *Alexandrium* | -3.7653 | 0.152734 | 0.48248 | |
| 1998 | July | EMCC | salinity | yes | *Alexandrium* | -21.2945 | 0.741904 | 0.212932 | |
| 1998 | July | JB | salinity | yes | *Alexandrium* | -68.3992 | 2.19402 | 0.381439 | |
| 1998 | July | BF | salinity | yes | *Alexandrium* | -28.9473 | 1.01153 | 0.509795 | |
| 1998 | July | SS | salinity | yes | *Alexandrium* | 26.0987 | -0.780171 | -0.571325 | |
| 1998 | August | All GOM | salinity | yes | *Alexandrium* | -27.1832 | 0.906324 | 0.539376 | 213 |
| 1998 | June | All GOM | nitrate | yes | silicate | 0.0775838 | 0.411593 | 0.473702 | 199 |
| 1998 | June | All GOM | nitrate | no | silicate | 0.858908 | 0.559473 | 0.581156 | 199 |
| 1998 | June | All GOM | nitrate | yes | chlorophyll | -0.0923008 | 0.00635256 | 0.00898169 | |
| 1998 | June | WM | nitrate | yes | chlorophyll | -0.216986 | -0.102883 | -0.149725 | |
| 1998 | June | EM | nitrate | yes | chlorophyll | 0.0475443 | 0.0244371 | 0.0374211 | |
| 1998 | June | WMCC | nitrate | yes | chlorophyll | 0.0602097 | -0.444433 | -0.481418 | |
| 1998 | June | WB | nitrate | yes | chlorophyll | -0.332158 | -0.113255 | -0.276304 | |
| 1998 | June | EMCC | nitrate | yes | chlorophyll | 0.412693 | -0.828512 | -0.745098 | |
| 1998 | June | JB | nitrate | yes | chlorophyll | -0.0880582 | 0.28135 | 0.616876 | |
| 1998 | June | BF | nitrate | yes | chlorophyll | 0.289958 | -0.117419 | -0.458669 | |
| 1998 | June | SS | nitrate | yes | chlorophyll | 0.276307 | 0.605344 | 0.920984 | |
| 1998 | June | All GOM | temperature | no | phosphate | 1.25735 | -0.0851075 | -0.560587 | |
| 1998 | June | WM | temperature | | phosphate | 0.923165 | -0.0585178 | -0.423792 | |
| 1998 | June | EM | temperature | | phosphate | 1.20092 | -0.0725929 | -0.476706 | |

| Year | Month | Area | X | LOG? | Y | Y-intercept | Slope | r-value | N |
|---|---|---|---|---|---|---|---|---|---|
| 1998 | June | WMCC | temperature | | phosphate | 0.757002 | -0.0458112 | -0.465099 | |
| 1998 | June | WB | temperature | | phosphate | 1.10046 | -0.0743835 | -0.511245 | |
| 1998 | June | EMCC | temperature | | phosphate | 1.68229 | -0.127166 | -0.599708 | |
| 1998 | June | JB | temperature | | phosphate | 1.15189 | -0.0627349 | -0.323828 | |
| 1998 | June | BF | temperature | | phosphate | 1.85682 | -0.159468 | -0.834671 | |
| 1998 | June | SS | temperature | | phosphate | 0.606825 | -0.0118599 | -0.33519 | |
| 1998 | July | All GOM | temperature | | phosphate | 0.888901 | -0.0466011 | -0.847575 | 212 |
| 1998 | August | All GOM | temperature | | phosphate | 0.813381 | -0.0363382 | -0.65328 | 213 |
| 1998 | June | All GOM | sigma-t | no | temperature | 53.2805 | -1.80844 | -0.70025 | |
| | | | | | | | | | |
| 1998 | June | All GOM | fluorescence | no | chlorophyll | -3.38785 | 26.0728 | 0.805886 | |
| 1998 | June | All GOM | fluorescence | yes | chlorophyll | 2.3875 | 3.23437 | 0.826499 | |
| 1998 | July | All GOM | fluorescence | yes | chlorophyll | 0.923548 | 1.13501 | 0.831789 | |
| 1998 | July | All GOM | fluorescence | no | chlorophyll | -0.273773 | 9.70491 | 0.830926 | |
| 1998 | August | All GOM | fluorescence | yes | chlorophyll | 0.0161993 | 1.15516 | 0.926183 | |
| 1998 | August | All GOM | fluorescence | no | chlorophyll | -0.147971 | 1.31964 | 0.940772 | |
| 1998 | June | All GOM | phosphate | no | AVHRR | 12.1753 | -5.30809 | -0.627876 | 318 |
| 1998 | July | All GOM | phosphate | | AVHRR | 16.8438 | -13.2817 | -0.773517 | 348 |
| 1998 | August | All GOM | phosphate | | AVHRR | 16.8807 | -6.61271 | -0.48555 | 364 |
| 1998 | May | All GOM | phosphate | | AVHRR | 6.5163 | -0.346781 | -0.0599345 | 242 |
| 1998 | June | All GOM | phosphate | | AVHRR | 12.071 | -1.80103 | -0.264175 | 206 |
| 1998 | June | All GOM | temperature | no | AVHRR | 1.08769 | 0.894008 | 0.580424 | 199 |
| 1998 | June | WM | temperature | no | AVHRR | 5.28819 | 0.569836 | 0.592194 | 90 |
| 1998 | June | EM | temperature | no | AVHRR | 4.25113 | 0.500113 | 0.613602 | 87 |
| 1998 | June | WMCC | temperature | no | AVHRR | 6.58979 | 0.448584 | 0.737087 | 15 |
| 1998 | June | WB | temperature | no | AVHRR | 4.51496 | 0.639739 | 0.57508 | 73 |
| 1998 | June | EMCC | temperature | no | AVHRR | 5.11746 | 0.37471 | 0.462409 | 16 |
| 1998 | June | JB | temperature | no | AVHRR | 4.36071 | 0.47762 | 0.520086 | 33 |
| 1998 | June | BF | temperature | no | AVHRR | 4.64007 | 0.502229 | 0.517853 | 10 |
| 1998 | June | SS | temperature | no | AVHRR | -0.0616891 | 0.998777 | 0.877036 | 7 |

| Year | Month | Area | X | LOG? | Y | Y-intercept | Slope | r-value | N |
|---|---|---|---|---|---|---|---|---|---|
| 1998 | July | All GOM | temperature | no | AVHRR | 2.23116 | 1.19459 | 0.578253 | 306 |
| 1998 | August | All GOM | temperature | no | AVHRR | 5.08677 | 0.684202 | 0.890042 | 354 |
| 2000 | May | All GOM | temperature | no | AVHRR | 4.36736 | 0.337379 | 0.163122 | 262 |
| 2000 | June | All GOM | temperature | no | AVHRR | 3.84571 | 0.81854 | 0.70077 | 278 |
| 1998 | June | All GOM | SeaWiFS | yes | chlorophyll | -0.0784696 | 0.151435 | 0.0801181 | 199 |
| 1998 | June | All GOM | SeaWiFS | no | chlorophyll | 0.751996 | 0.339044 | 0.273512 | 320 |
| 1998 | June | WM | SeaWiFS | yes | chlorophyll | -0.225644 | -0.449747 | 0.20338 | 99 |
| 1998 | June | EM | SeaWiFS | yes | chlorophyll | 0.0348888 | 0.232379 | 0.144808 | 100 |
| 1998 | June | WMCC | SeaWiFS | yes | chlorophyll | 0.0521883 | -0.702058 | -0.368161 | 21 |
| 1998 | June | WB | SeaWiFS | yes | chlorophyll | -0.351755 | -0.607253 | -0.372681 | 74 |
| 1998 | June | EMCC | SeaWiFS | yes | chlorophyll | 0.0359472 | 0.364365 | 0.26789 | 24 |
| 1998 | June | JB | SeaWiFS | yes | chlorophyll | -0.212851 | 0.261372 | 0.252916 | 34 |
| 1998 | June | BF | SeaWiFS | yes | chlorophyll | 0.288237 | -1.52096 | -0.609912 | 11 |
| 1998 | June | SS | SeaWiFS | yes | chlorophyll | 0.190817 | -1.94742 | -0.388209 | 7 |
| 1998 | July | All GOM | SeaWiFS | no | chlorophyll | 0.691202 | 0.234914 | 0.244994 | 360 |
| 1998 | August | All GOM | SeaWiFS | no | chlorophyll | 0.784794 | 0.528756 | 0.468884 | 362 |
| 2000 | May | All GOM | SeaWiFS | no | chlorophyll | 1.17323 | -0.0410191 | -0.113785 | 242 |
| 2000 | June | All GOM | SeaWiFS | no | chlorophyll | 2.14989 | 0.931911 | 0.287776 | 218 |
| 2000 | June | All GOM | temperature | yes | *Alexandrium* | 3.70352 | -0.204135 | -0.334631 | |
| 2000 | June | WM | temperature | yes | *Alexandrium* | 2.65223 | -0.119 | -0.184324 | |
| 2000 | June | EM | temperature | yes | *Alexandrium* | 3.64005 | -0.179827 | -0.308672 | |
| 2000 | June | WMCC | temperature | yes | *Alexandrium* | -0.14044 | 0.158771 | 0.359479 | |
| 2000 | June | WB | temperature | yes | *Alexandrium* | 4.22551 | -0.260758 | -0.347609 | |
| 2000 | June | EMCC | temperature | yes | *Alexandrium* | 0.456696 | 0.212936 | 0.29133 | |
| 2000 | June | JB | temperature | yes | *Alexandrium* | 5.94542 | -0.425413 | -0.695998 | |
| 2000 | June | BF | temperature | yes | *Alexandrium* | -0.367326 | 0.0752527 | 0.480273 | |
| 2000 | June | SS | temperature | yes | *Alexandrium* | -2.46364 | 0.473257 | 0.771807 | |
| 1998 | June | All GOM | temperature | yes | chlorophyll | 1.2653 | -0.136765 | -0.543394 | |
| 1998 | June | WM | temperature | yes | chlorophyll | 1.0471 | -0.120326 | -0.51577 | |
| 1998 | June | EM | temperature | yes | chlorophyll | 1.14057 | -0.117777 | -0.409644 | |

| Year | Month | Area | X | LOG? | Y | Y-intercept | Slope | r-value | N |
|---|---|---|---|---|---|---|---|---|---|
| 1998 | June | WMCC | temperature | yes | chlorophyll | 1.2149 | -0.121746 | -0.541819 | |
| 1998 | June | WB | temperature | yes | chlorophyll | 0.267699 | -0.0544657 | -0.338443 | |
| 1998 | June | EMCC | temperature | yes | chlorophyll | -0.486386 | 0.0759103 | 0.185278 | |
| 1998 | June | JB | temperature | yes | chlorophyll | 1.1792 | -0.136845 | -0.750578 | |
| 1998 | June | BF | temperature | yes | chlorophyll | -0.367326 | 0.0752527 | 0.480273 | |
| 1998 | June | SS | temperature | yes | chlorophyll | 2.29591 | -0.236757 | -0.945737 | |
| 1998 | July | All GOM | temperature | yes | chlorophyll | 0.420041 | -0.0425367 | -0.351829 | |
| 1998 | July | WM | temperature | yes | chlorophyll | -0.029839 | -0.0114727 | -0.0780203 | |
| 1998 | July | EM | temperature | yes | chlorophyll | 1.19054 | -0.113164 | -0.571623 | |
| 1998 | July | WMCC | temperature | yes | chlorophyll | 1.10136 | -0.0654386 | -0.458338 | |
| 1998 | July | WB | temperature | yes | chlorophyll | -0.717419 | 0.023516 | 0.269674 | |
| 1998 | July | EMCC | temperature | yes | chlorophyll | -0.592197 | 0.0791556 | 0.260353 | |
| 1998 | July | JB | temperature | yes | chlorophyll | 1.14087 | -0.120197 | -0.94059 | |
| 1998 | July | BF | temperature | yes | chlorophyll | 1.25541 | -0.114429 | -0.604854 | |
| 1998 | July | SS | temperature | yes | chlorophyll | 1.34199 | -0.133412 | -0.901284 | |
| 1998 | August | All GOM | temperature | yes | chlorophyll | 1.50457 | -0.098898 | -0.747669 | |
| 1998 | August | WM | temperature | yes | chlorophyll | 2.10743 | -0.131324 | -0.744037 | |
| 1998 | August | EM | temperature | yes | chlorophyll | 1.49259 | -0.100229 | -0.590081 | |
| 1998 | August | WMCC | temperature | yes | chlorophyll | 2.91132 | -0.171841 | -0.81792 | |
| 1998 | August | WB | temperature | yes | chlorophyll | 0.95464 | -0.0718367 | -0.576488 | |
| 1998 | August | EMCC | temperature | yes | chlorophyll | -1.19137 | 0.141858 | 0.509051 | |
| 1998 | August | JB | temperature | yes | chlorophyll | 1.52942 | -0.111539 | -0.888276 | |
| 1998 | August | BF | temperature | yes | chlorophyll | 0.379608 | 0.00382064 | 0.0138905 | |
| 1998 | August | SS | temperature | yes | chlorophyll | -1.16017 | 0.115017 | 0.442269 | |
| 1998 | June | All GOM | temperature | yes | fluorescence | -0.493382 | -0.0273587 | -0.425405 | |
| 1998 | June | WM | temperature | yes | fluorescence | -0.530641 | -0.024078 | -0.403801 | |
| 1998 | June | EM | temperature | yes | fluorescence | -0.47538 | -0.0289502 | -0.361649 | |
| 1998 | June | WMCC | temperature | yes | fluorescence | -0.557443 | -0.0175623 | -0.340263 | |
| 1998 | June | WB | temperature | yes | fluorescence | -0.697993 | -0.0101896 | -0.219669 | |
| 1998 | June | EMCC | temperature | yes | fluorescence | -0.705359 | -0.00342148 | -0.0365574 | |
| 1998 | June | JB | temperature | yes | fluorescence | -0.470074 | -0.034108 | -0.559821 | |
| 1998 | June | BF | temperature | yes | fluorescence | -1.06248 | 0.0474146 | 0.759279 | |

| Year | Month | Area | X | LOG? | Y | Y-intercept | Slope | r-value | N |
|---|---|---|---|---|---|---|---|---|---|
| 1998 | June | SS | temperature | yes | fluorescence | -0.356878 | -0.0406263 | -0.674872 | |

# Appendix G

## *ALEXANDRIUM* AND THE EMCC RESULTS

June 1998

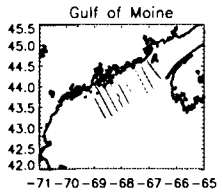


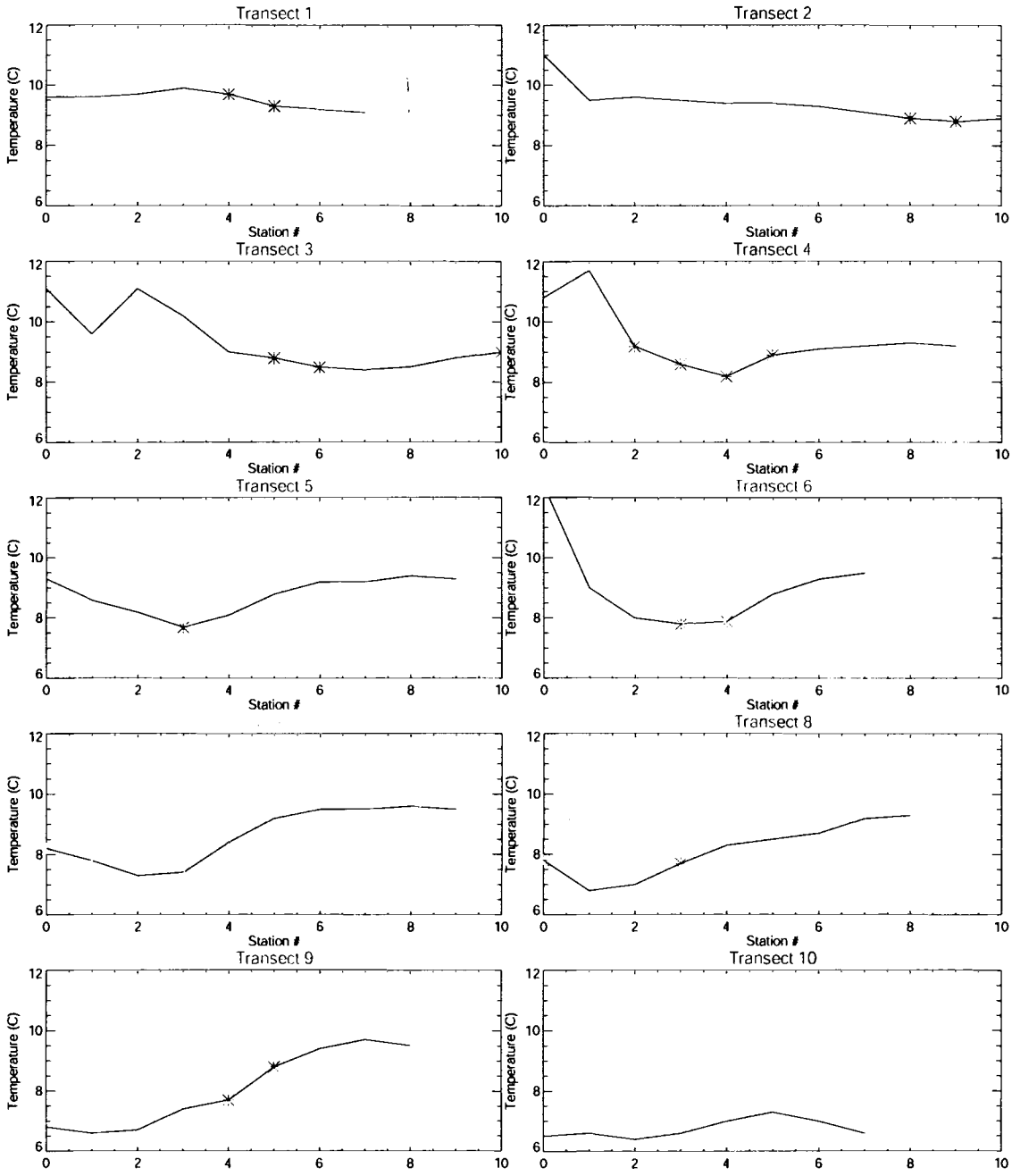


Asterisk (*) = station with *Alexandrium* concentration > 200.000 cells/L

# July 1998

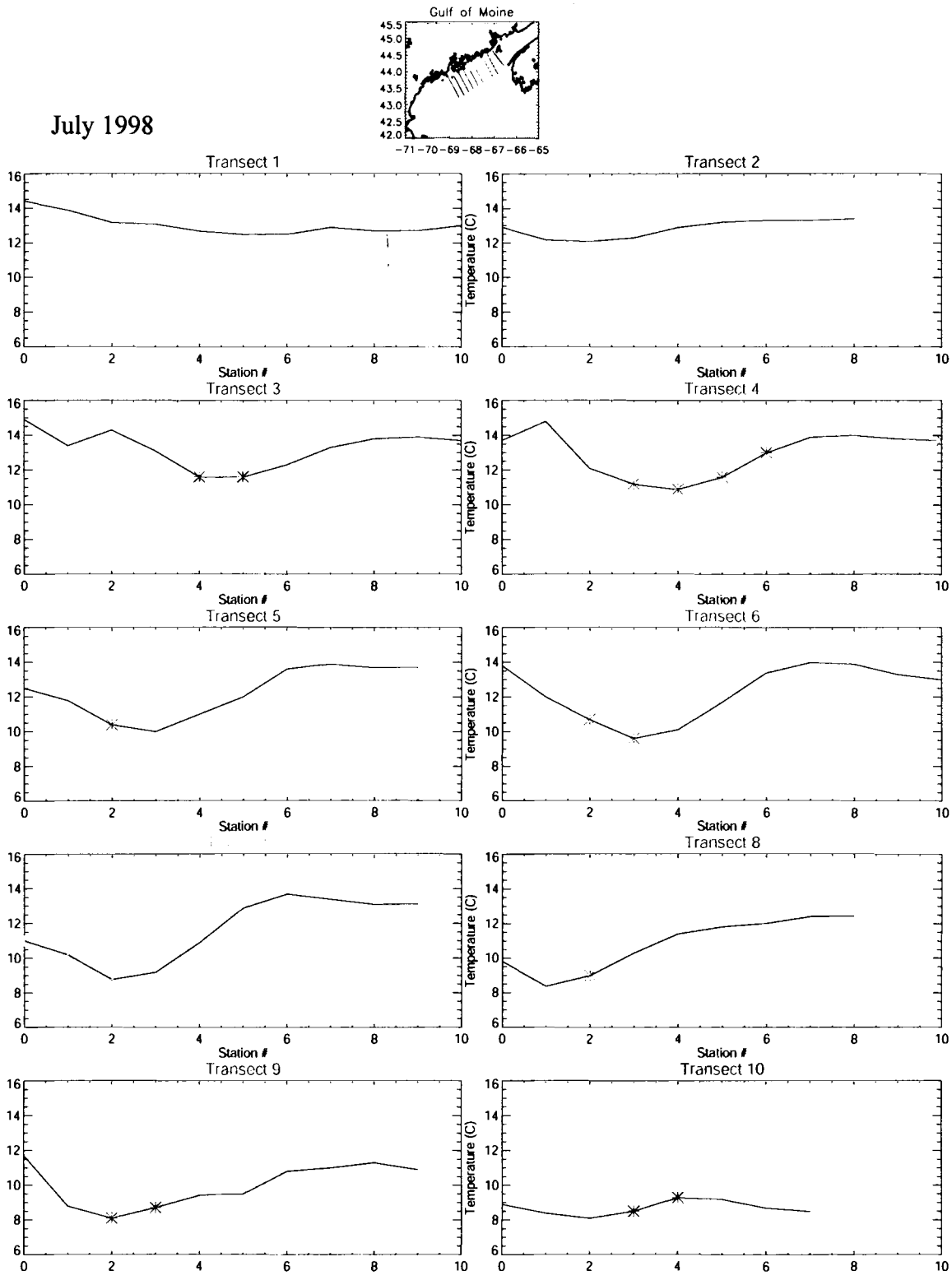


Asterisk (*) = station with *Alexandrium* concentration > 200.000 cells/L

# August 1998

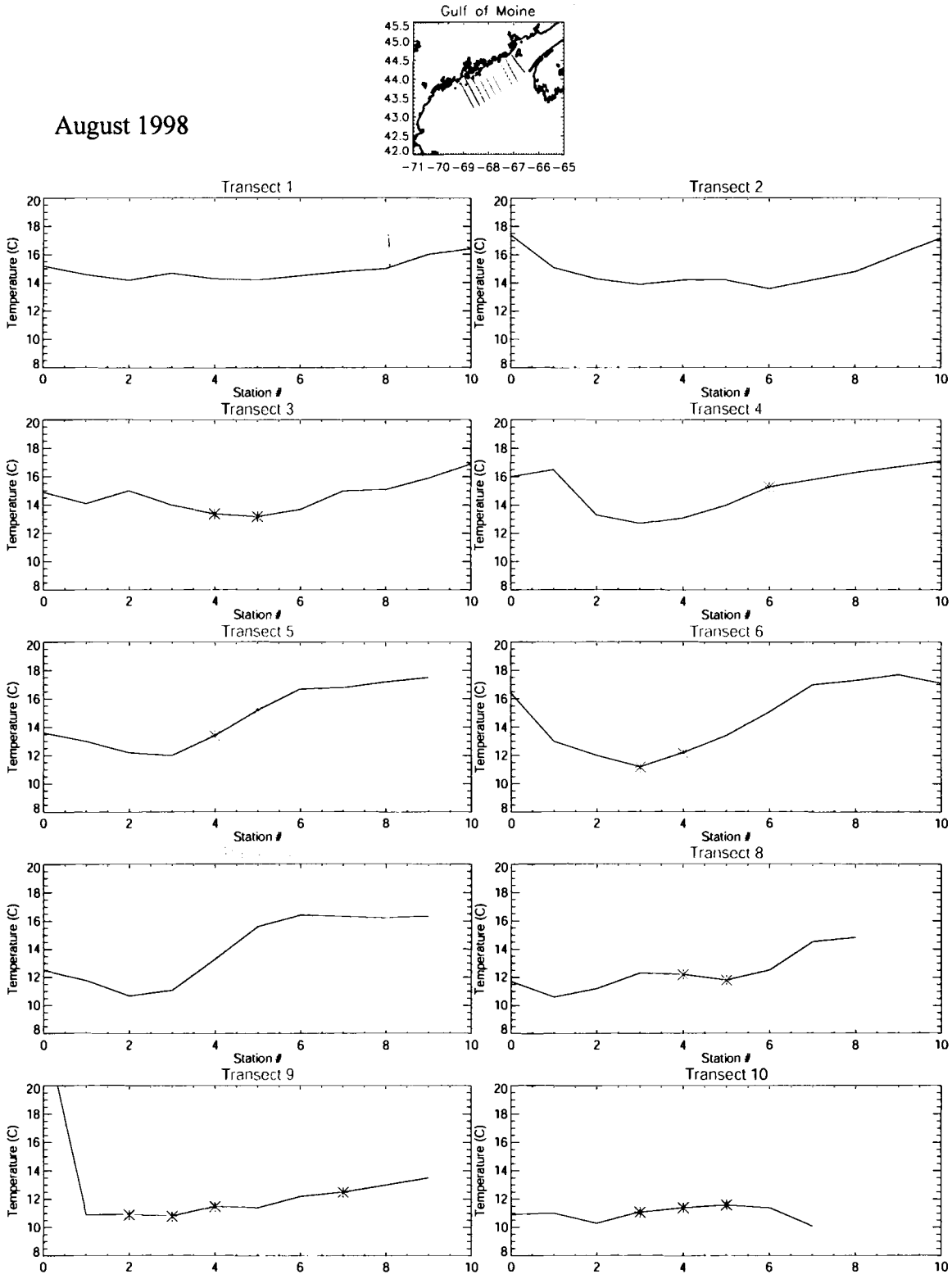


Asterisk (*) = station with *Alexandrium* concentration > 200.000 cells/L

May 2000

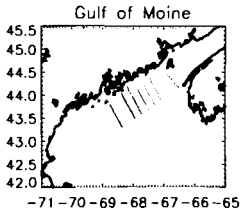


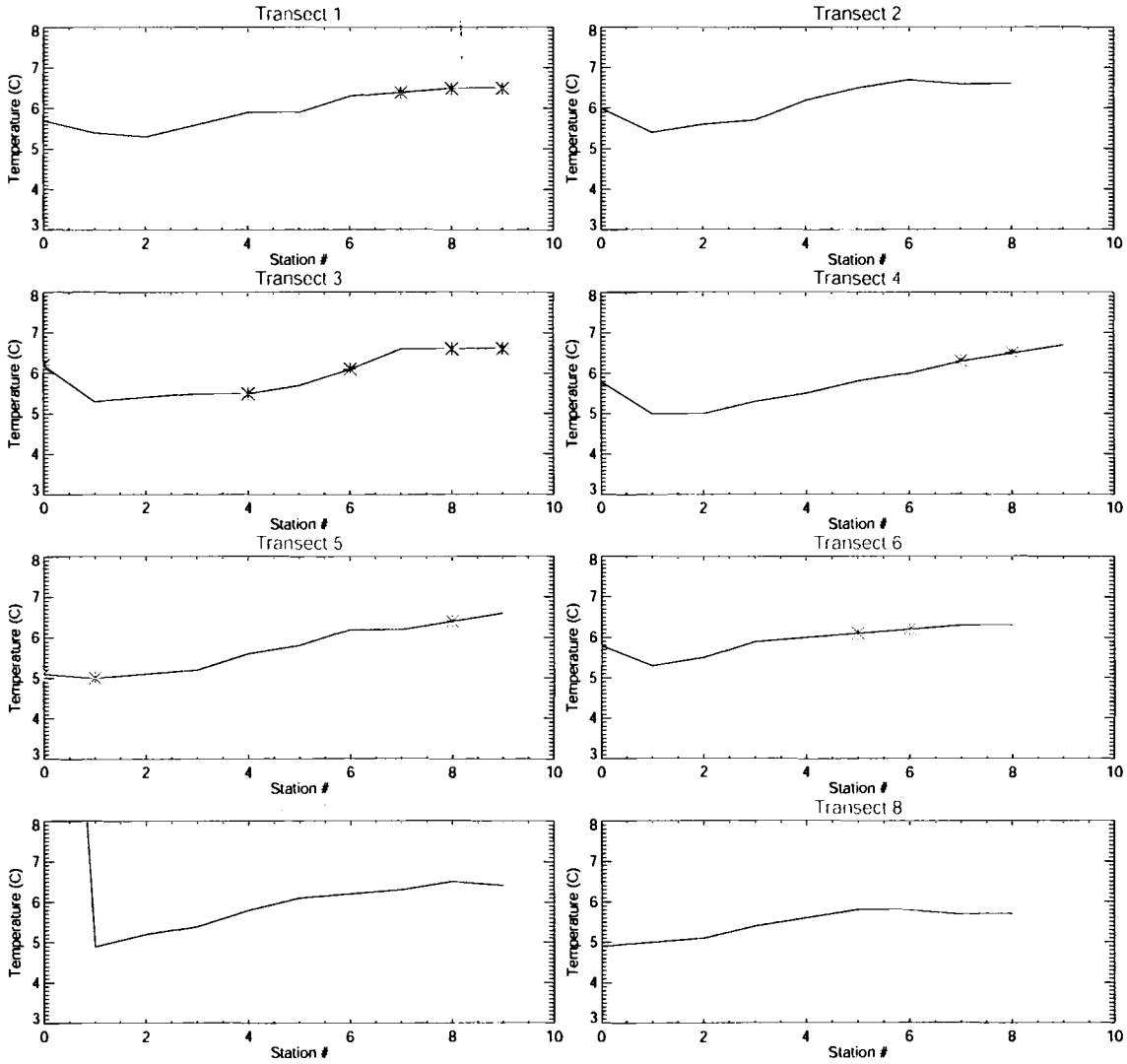


Asterisk (*) = station with *Alexandrium* concentration > 30.000 cells/L

June 2000

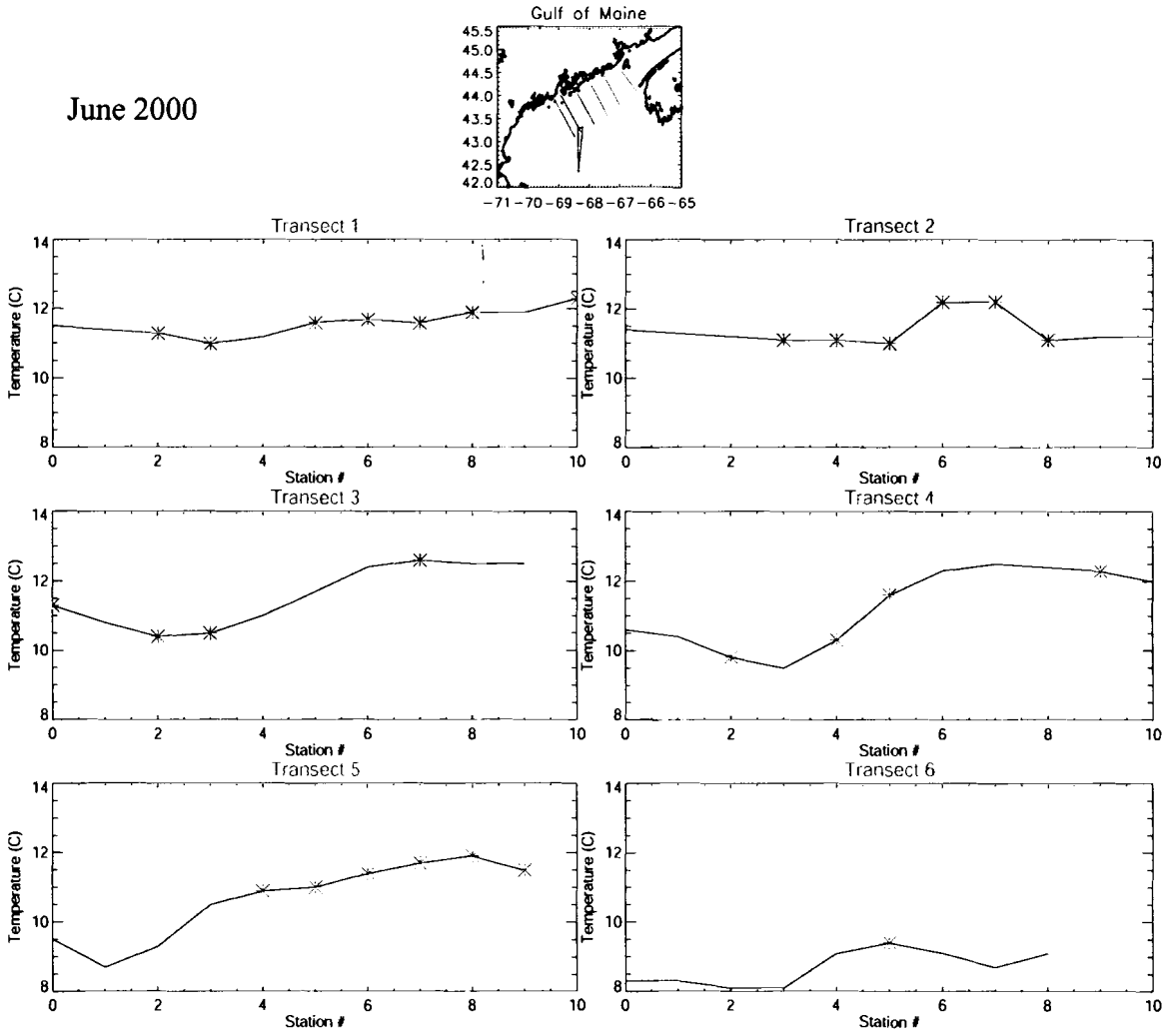


Asterisk (*) = station with *Alexandrium* concentration > 200.000 cells/L

## BIOGRAPHY OF THE AUTHOR

Remy Luerssen was born in Salem, Massachusetts on November 27, 1977. She was raised in Marblehead, Massachusetts and moved to Ipswich, Massachusetts in 1989 and graduated from Ipswich High School in 1995. She attended James Madison University and graduated in May 1999 magna cum laude with a Bachelor's degree in Integrated Science and Technology with a concentration in Environmental Studies. She returned to New England in the fall of 1999 when she entered the Oceanography graduate program at The University of Maine.

After receiving her degree, she will be moving to the coast of Maine to work at the Darling Marine Center with Dr. Mary Jane Perry on Bio-optical research. Remy is a candidate for the Master of Science degree in Oceanography from The University of Maine in December, 2001.